Kairos Power

KP-NRC-2006-005

June 30, 2020

Project No. 99902069

US Nuclear Regulatory Commission
ATTN: Document Control Desk
Washington, DC 20555-0001

Subject: Kairos Power LLC
Topical Report Submittal
KP-FHR Mechanistic Source Term Methodology Topical Report

This letter submits the subject topical report which provides the methodology to evaluate the mechanistic source term for the Kairos Power Fluoride Salt-Cooled, High Temperature Reactor (KP-FHR). This topical report is provided for NRC review and approval and is expected to be referenced by future license applicants using the KP-FHR. The scope and schedule for submittal of this report was discussed in a closed meeting with NRC staff May 28, 2020. Kairos Power respectfully requests an NRC acceptance review be completed and a review schedule be provided within 60 days of the receipt of this letter. In recognition of an aggressive deployment schedule and substantial pre-application engagement, Kairos Power has established a generic assumption of a 12-month review for topical reports.

Portions of the attached report are considered proprietary, and Kairos Power requests it be withheld from public disclosure in accordance with the provisions of 10 CFR 2.390. Enclosure 1 provides the proprietary version of the report and Enclosure 2 provides the non-proprietary report. An affidavit supporting the withholding request is provided in Enclosure 3.

Additionally, the information indicated as proprietary has also been determined to contain Export Controlled Information. This information must be protected from disclosure pursuant to the requirements of 10 CFR 810.

If you have any questions or need any additional information, please contact Drew Peebles at peebles@kairospower.com or (704) 275-5388, or Darrell Gardner at gardner@kairospower.com or (704) 769-1226.

Sincerely,

Peter Hastings, PE
Vice President, Regulatory Affairs and Quality

Enclosures:

1) KP-FHR Mechanistic Source Term Methodology (Proprietary)
2) KP-FHR Mechanistic Source Term Methodology (Non-Proprietary)
3) Affidavit Supporting Request for Withholding from Public Disclosure (10 CFR 2.390)

xc (w/enclosure):

Benjamin Beasley, Chief, Advanced Reactor Licensing Branch, USNRC
Stewart Magruder, Project Manager, Advanced Reactor Licensing Branch, USNRC
JoAnne Hanners, Contracting Officer, USDOE
Andrew Ford, Contract Specialist, USDOE

Enclosure 2
KP-FHR Mechanistic Source Term Methodology Topical Report

(Non-Proprietary)

KP-TR-012-NP

Kairos Power LLC
707 W. Tower Ave
Alameda, CA 94501

KP-FHR Mechanistic Source Term Methodology

Revision No. 0
Document Date: June 2020

Non-Proprietary

© 2020 Kairos Power LLC

Acknowledgement of Federal Support and Disclaimer

This material is based upon work supported by the Department of Energy under Award Number DE-NE0008862.

This report was prepared as an account of work sponsored by an agency of the United States Government. Neither the United States Government nor any agency thereof, nor any of their employees, makes any warranty, express or implied, or assumes any legal liability or responsibility for the accuracy, completeness, or usefulness of any information, apparatus, product, or process disclosed, or represents that its use would not infringe privately owned rights. Reference herein to any specific commercial product, process, or service by trade name, trademark, manufacturer, or otherwise does not necessarily constitute or imply its endorsement, recommendation, or favoring by the United States Government or any agency thereof. The views and opinions of authors expressed herein do not necessarily state or reflect those of the United States Government or any agency thereof.

COPYRIGHT Notice

This document is the property of Kairos Power LLC (Kairos Power) and was prepared in support of the development of the KP Fluoride Salt Cooled High Temperature Reactor (KP-FHR) design. Other than by the NRC and its contractors as part of regulatory reviews of the KP-FHR design, the content herein may not be reproduced, disclosed, or used, without prior written approval of Kairos Power.

Rev	Description of Change	Date
0	Initial Issuance	June 2020

© 2020 Kairos Power LLC

Executive Summary

Kairos Power is pursuing the design, licensing, and deployment of a Fluoride Salt Cooled, High Temperature Reactor (KP-FHR). To enable these objectives, the development of a technology-specific source term evaluation methodology is required. This report has been prepared to document the methodology for evaluation of the KP-FHR mechanistic source term to be used to calculate radiological source terms for anticipated operational occurrences (AOOs), design basis events (DBEs), and design basis accidents (DBAs).

KP-FHR technology is fundamentally different from the existing light water reactor (LWR) technologies because the fully-ceramic Tri-Structural Isotropic (TRISO) fuel used in KP-FHRs has large thermal margins to damage, and the KP-FHR coolant is operated at low pressures, has high chemical stability, and the capability to immobilize solid fission products. These characteristics make the safety case of the KP-FHR technology fundamentally different from LWRs. Due to these inherent safety features of the KP-FHR, the design relies on a functional containment approach to retain radioactive materials. The functional containment approach is further simplified because the majority of the radioactive material at risk for release (MAR) is retained within the TRISO fuel used in the KP-FHR. During normal operation, the small fraction of fission products that are released from the TRISO fuel will diffuse into the molten fluoride salt reactor coolant (Flibe) or are released into the gas space of the reactor vessel or the pebble handling and storage system, depending on the location of the fuel pebbles. There will also be activation products (including tritium) that will be created as a result of normal operation. This report provides the methodology to calculate the source term for licensing basis events (excluding beyond design basis events) based on the fission products and activation products generated from normal operation of a KP-FHR.

The source term methodology is event-specific because it depends on the amount of MAR and conditions of the MAR in the locations affected by the licensing basis event. The normal operation conditions provide an initial amount of MAR, that is used to calculate the source term for licensing basis event conditions. Due to the robust TRISO fuel design, there is not expected to be any significant incremental fuel failure due to a design basis event. The evaluation of design basis events is outside the scope of this report and are provided as part of licensing application safety analysis reports for a KP-FHR.

The source term evaluation method for AOOs and DBEs uses a more mechanistic or realistic accounting of radionuclide barriers consistent with the methodology for licensing basis events. The source term evaluation method for the DBAs is deterministic and only credits the properties of the TRISO fuel and the Flibe coolant for retention of radionuclides in the KP-FHR.

The sample calculations included in this appendix are provided to illustrate how the methodology is used and do not represent final design information. Kairos Power is not asking for NRC review and approval of these sample calculations in a safety evaluation report.

Kairos Power is requesting NRC approval of the source term methodology presented in this report as an appropriate means to calculate source terms to evaluate consequences of AOOs and DBEs for frequency-consequence targets and quantitative health objectives (QHOs), and source terms to evaluate DBA consequences to ensure that the KP-FHR meets the dose limits in 10 CFR 50.34.

© 2020 Kairos Power LLC

Table of Contents

KP-FHR Mechanistic Source Term Methodology 1
1 Introduction 13
1.1 Historical Perspective 13
1.2 Design Features 13
1.2.1 Design Background 13
1.2.2 Key Design Features of the KP-FHR 14
1.3 Regulatory Background 15
1.3.1 Requirements 15
2 KP-FHR Mechanistic Source Term Evaluation Approach 18
2.1 Material at Risk and Release Fraction Definitions 18
2.2 Sources of Material at Risk in the KP-FHR 20
2.3 KP-FHR Source Term Evaluation 20
2.3.1 Identification of MAR and Affected Barriers 20
2.3.2 Qualitative Evaluation 21
2.3.3 Quantitative Evaluation 21
2.3.4 Additional Design Information Used in the Methodology 23
2.4 Phenomena Identification and Ranking Tables 24
2.5 Software Used In KP-FHR Source Term Evaluation 26
2.5.1 SERPENT2 26
2.5.2 KP-Bison 26
2.5.3 KP-SAM 27
2.5.4 ARCON96 27
2.5.5 RADTRAD 27
3 Evaluating Fuel Retention of Radionuclides 70
3.1 Important Source Term Phenomena Identified for Fuel 70
3.2 Sources of Radionuclides in Fuel 71
3.2.1 Manufacturing Defects 71
3.2.2 Heavy Metal Contamination 71
3.2.3 In-service Failures 72
3.2.4 Release from Intact Particles 72
3.2.5 Tritium 72
3.3 Radionuclide BeHavior and Retention Properties of Fuel 73
3.3.1 Radionuclide Behavior in Fuel 74
3.3.2 Selection of Radionuclides 74
3.4 Radionuclide Transport in Fuel 75
3.4.1 Radionuclide Transport Groups in Fuel 76
3.4.2 KP-Bison Diffusion Model 76
3.5 Retention of Tritium in the Graphite Pebble 78
4 Evaluating Flibe Retention of Radionculides 91
4.1 Important Source Term Phenomena Identified for Flibe 91
4.1.1 Phenomena for Flibe with Intact Reactor Coolant Boundary 91
4.1.2 Phenomena for Flibe with Compromised Reactor Coolant Boundary 92
4.2 Sources of radionuclides in Flibe 93
4.3 Radionuclide Transport in Flibe 94
4.3.1 Radionuclides Transport Groups in Flibe 94

© 2020 Kairos Power LLC

4.3.2 Quantification of Release Fractions for Flibe 100
5 Evaluating Radionuclide Retention in Graphite Structures 112
5.1 Radionuclide Retention Phenomena Identified for Graphite Structures 112
5.1.1 Phenomenon Associated with Events Involving an Intact Reactor Coolant Boundary 112
5.1.2 Phenomenon Associated with Events Involving a Compromised Reactor Coolant Boundary. 112
5.2 Sources of Radionuclides in Graphite Structures 112
5.3 Radionuclide Transport in Graphite Structures 112
5.3.1 Tritium Speciation 113
5.3.2 Tritium Retention and Permeation 114
6 Other Sources of MAR 115
6.1 Important Source Term Phenomena Identified for Other Sources of MAR 115
6.2 Sources of RAdionuclides in the PHSS, chemistry control, and heat transport systems 116
6.2.1 Graphite Dust 116
6.2.2 Vapor and Off-Gas in PHTS and CCS 116
6.2.3 Cold Trap and Filters in the CCS 117
6.3 Model Interfaces 117
6.4 Radionuclides present in Other sources of MAR 118
6.4.1 Radionuclides Born in Other Sources of MAR 118
6.4.2 Radionuclides Transfer 118
6.4.3 Radionuclides Escaped or Transferred 120
6.4.4 Impact of Degraded Barriers on Retention of Radionuclides 121
6.4.5 Radionuclide Transfer During AOOs or DBEs 121
6.4.6 Radionuclides Transferred During DBAs 122
7 Evaluating Radionuclide Transport in the Gas Space and Atmospheric Transport 123
7.1 Important Source Term Phenomena Associated with Gas Space Transport 123
7.1.1 Phenomena for Gas Space with Intact Reactor Coolant Boundary 123
7.1.2 Phenomena for Gas Space with Compromised Reactor Coolant Boundary 123
7.2 Radionuclide Groups 124
7.3 Characterizing Aerosols 124
7.3.1 Material at Risk During a Pipe Break 124
7.3.2 Pipe Break Airborne Release Fraction Approach 131
7.3.3 Material at Risk in the Pebble Handling and Storage System 131
7.3.4 Airborne Releases for Material at Risk in the Pebble Handling and Storage System 132
7.4 Building Transport Models 133
7.4.1 RADTRAD Model Structure 134
7.4.2 Release Models 134
7.5 Building Transport Inputs 136
7.5.1 Activities of Radionuclide Sources 136
7.5.2 Volumetric Flow Rates 137
7.5.3 Aerosol Formation Heights 138
7.5.4 Aerosol Particle Density 139
7.5.5 Atmospheric Dispersion Ratios 139
7.6 Building Transport Outputs 139
7.6.1 Worst Two-Hour Dose 139
7.6.2 Cumulative 30-day dose 139

© 2020 Kairos Power LLC

7.6.3 Release Fractions 139
7.7 Atmospheric Dispersion Models 140
7.7.1 Selecting the Conservative Release Distance 140
7.7.2 Calculation of the Time Averaged Percentile χQ Values 140
7.7.3 Selecting the Conservative Release Wind Direction 141
7.8 Atmospheric Dispersion Inputs 141
7.8.1 Release Inputs 141
7.8.2 Receptor Data 142
7.8.3 Meteorological Data 142
7.9 Dispersion Outputs 144
7.9.1 Pre-calculated 95th percentile 144
7.9.2 Complimentary Cumulative Distribution Functions 144
8 CONCLUSIONS and Limitations 159
8.1 Conclusions 159
8.2 Limitations 159
9 REFERENCES 160
Appendix A. Sample Source Term Calculation: Anticipated Operational Occurrence 164
A.1 Sample Calculation 164
A.2 Event Description 164
A.3 Source Term Evaluation 165
A.4 Conclusions: 168
Appendix B. Sample Source Term Calculation: Design Basis Accident 177
B.1 Sample Calculation 177
B.2 Event Description 177
B.3 Source Term Evalaution 178
B.4 Conclusions 180

Figures

Figure 2-1 Steady State Material at Risk Accumulation in the Heat Transport and Cover Gas Systems 68
Figure 2-2 Steady State Material At Risk Accumulation in the Pebble Handling and Storage System 69
Figure 3-1 Representation for T_2 Mass Transfer From Flibe to Graphite Pebble. 89
Figure 3-2 Notation for Tritium Gains and Losses Between Nodes 90
Figure 4-1 Schematic Depiction of Grouping of Radionuclides in Flibe Barrier[a] 109
Figure 4-2 Log Vapor Pressure Equilibrium Constants 110
Figure 4-3 Vapor Pressure Equilibrium Constants (K) for the Indicated Liquid-to-Gas Phase Change Reactions 111
Figure 7-1 Airborne Release Fraction and Sauter Mean Diameter as a Function of Pipe Pressure 149
Figure 7-2 Initial and Impact Velocity of the Salt Given a One Meter Drop as a Function of Pressure 150
Figure 7-3 The Froude Number and the Gas Entrainment Rate as a Function of Pressure 151
Figure 7-4 Entrainment Coefficient for Bubble Burst Aerosols from Ginsberg 152
Figure 7-5 Airborne Release Fractions for a One Meter Drop Height as a Function of Pressure 153
Figure 7-6 A SNAP graphical schematic of a single source RADTRAD model 154
Figure 7-7 A SNAP Graphical Schematic of a Multiple Source RADTRAD model 155
Figure 7-8 Notation for Tritium Flows in One Node of the Downcomer Region 156
Figure 7-9 Raw Complementary Cumulative Distribution Produced by the SAMPLE problem in ARCON96 157
Figure 7-10 Complementary Cumulative Distribution Produced by SAMPLE Problem in ARCON95 With Counts Converted to Percentiles 158
Figure A-1 Mass of Aerosol Generated from the Leak as a Function of Time 176
Figure B-1 Cumulative Release of Salt Soluble Fluoride and Elements Dependent on Redox from Flibe 186
Figure B-2 Cumulative Release of Noble Metals from Flibe 187
Figure B-3 Cumulative Release of Oxides from Flibe 188
Figure B-4 Thirty Day Doses at the EAB 189
Figure B-5 Thirty Day Doses at the LPZ 190

© 2020 Kairos Power LLC

Tables

Table 2-1 Fuel Phenomena for Accidents Involving Both Intact and Compromised Reactor Coolant Boundaries 29
Table 2-2 Coolant Phenomena for Accidents Involving Intact Reactor Coolant Boundaries 32
Table 2-3 Coolant Phenomena for Accidents Involving Compromised Reactor Coolant Boundaries 36
Table 2-4 Graphite Structure Phenomenon for Accidents Involving Intact Reactor Coolant Boundaries . 50
Table 2-5 Graphite Structure Phenomenon for Accidents Involving Compromised Reactor Coolant Boundaries 51
Table 2-6 Phenomena for Accidents Involving Radioactive Waste 52
Table 2-7 Phenomena for Accidents Involving the Pebble Handling and Storage System 58
Table 2-8 Gas Space Phenomena for Accidents Involving an Intact Reactor Coolant Boundary 64
Table 2-9 Gas Space Phenomena for Accidents Involving a Compromised Reactor Coolant Boundary 66
Table 3-1 Functional Containment of TRISO Outer Coating Layers With Qualitative Impact on Fission Product Release 84
Table 3-2 Periodic Table of Chemical Groups, Valence Electron Orbital Shell, and Elements 85
Table 3-3 Notational Fission Product and Actinide Inventory List of Elements 86
Table 3-4 AGR In-Service Failure Fractions 87
Table 3-5 Diffusion Coefficients for Selected Radionuclides 88
Table 4-1 Bounding Conditions of Reactor Coolant Redox Potential, E_{salt}, at 650 °C. 107
Table 4-2 Radionuclide Groups for Transport Analysis in Flibe 108
Table 7-1 KP-FHR Radionuclide Groups and Representative Elements and Compounds for Gas Space Transport 145
Table 7-2 Pipe Break Assumptions in Aerosol Characterization Methodology Demonstration 146
Table 7-3 Summary of the 95th Percentile ARF from NUREG/CR-6410 147
Table 7-4 Determination of B 148
Table A-1 Tritium Distribution in Primary System with no Permeation Barrier Coatings at 4.75 Years ... 170
Table A-2 Summary of the Activity Transmission from Flibe to Gas Space 171
Table A-3 Radionuclides for AOO Leakage Conditions that Produce a Thirty Day TEDE Above 2.5E-05 rem 172
Table A-4 Radionuclides for No Holdup Leakage Conditions that Produce a 30 Day TEDE Above 2.5E-05 rem 173
Table A-5 Source Term Inventory Calculation Parameters 174
Table A-6 Summary of Release Fraction Values for Various Radionuclide Groups Across Various Barriers 175
Table B-1 Tritium Distribution in the Primary System with no Permeation Barrier Coatings at 4.75 years 181
Table B-2 Flibe Source Term Inventory Calculation Inputs 182
Table B-3 Release Fractions of Radionuclide Groups in Flibe 183
Table B-4 Cumulative Attenuation Factor of Flibe Radionuclide Groups 184
Table B-5 EAB TEDE Dose Results 185

© 2020 Kairos Power LLC

Abbreviation or Acronym	Definition
AOO	Anticipated Operational Occurrence
ARF	Airborne Release Fraction
BDBE	Beyond Design Basis Event
CCS	Chemistry Control System
CFR	Code of Federal Regulation
DBA	Design Basis Accident
DBE	Design Basis Event
DOE	Department of Energy
EAB	Exclusion Area Boundary
FHR	Fluoride-Salt Cooled High Temperature Reactor
FP	Fission Product
HALEU	High Assay Low Enriched Uranium
HM	Heavy Metal
HVAC	Heating Ventilation and Air Conditioning
IHTS	Intermediate Heat Transfer System
IHX	Intermediate Heat Exchanger
IPyC	Inner Pyrolytic Carbon
IRP	Integrated Research Projects
KP	Kairos Power
LPF	Leak Path Factor
LPZ	Low Population Zone
LWR	Light Water Reactor
MAR	Material at Risk
MHTGR	Modular High Temperature Gas-Cooled Reactor
MSRE	Molten Salt Reactor Experiment
NRC	Nuclear Regulatory Commission
OPyC	Outer Pyrolytic Carbon
ORNL	Oak Ridge National Laboratory
PHSS	Pebble Handling and Storage System
PHTS	Primary Heat Transfer System
PIRT	Phenomena Identification and Ranking Tables
PNNL	Pacific Northwest National Laboratory
PRA	Probabilistic Risk Assessment
PSD	Particle Size Distribution
QHO	Qualitative Health Objectives

© 2020 Kairos Power LLC

Abbreviation or Acronym	Definition
RCB	Reactor Coolant Boundary
RF	Release Fraction
RG	Regulatory Guide
RN	Radionuclides
RVACS	Reactor Vessel Auxiliary Cooling System
SAM	System Analysis Module
SSC	Structures Systems and Components
TEDE	Total Effective Dose Equivalent
TRISO	Tri-Structural Isotopic
UCO	Uranium Oxicarbide

© 2020 Kairos Power LLC

1 INTRODUCTION

Kairos Power is pursuing the design, licensing, and deployment of a Fluoride Salt Cooled, High Temperature Reactor (KP-FHR). To enable these objectives, the development of a technology-specific source term evaluation methodology is required. This report has been prepared to document the methodology for evaluation of the KP-FHR mechanistic source term to be used for radiological source terms for anticipated operational occurrences (AOOs), design basis events (DBEs), and design basis accidents (DBAs). Kairos is requesting NRC approval of this methodology as an appropriate means to calculate: consequences of AOOs and DBEs for the evaluation of frequency-consequence targets and quantitative health objectives; and DBA consequences to ensure that the KP-FHR meets the dose limits in 10 CFR 50.34.

1.1 HISTORICAL PERSPECTIVE

The KP-FHR source term methodology takes advantage of the inherent safety features of the KP-FHR design. Historically, the nuclear accidents that resulted in a radioactive release involved the melting of a large fraction of the reactor fuel. These accidents reached temperatures where most of the volatile fission products were vaporized and released from the fuel. The molten fuel materials reached sufficiently high temperatures that only non-volatile elements were retained in the frozen ceramic material (corium) that remained. The most important volatile fission products that were released in these earlier severe accidents were radioiodine and radiocesium. These accidents also resulted in the generation of combustible hydrogen and high-pressure steam, providing a significant driving force to release the volatile fission products.

KP-FHR technology is fundamentally different from these earlier reactor technologies because the fully ceramic Tri-Structural Isotropic (TRISO) fuel used in KP-FHRs has very large thermal margins to damage. The coolant used in KP-FHRs has a relatively low pressure, high chemical stability, and the capability to immobilize solid fission products. These characteristics make the safety strategy of KP-FHR technology fundamentally different from light water reactor (LWR) technologies.

While the KP-FHR LBEs will not result in the mobilization of radioiodine and radiocesium in amounts comparable to the releases that have occurred in historical light water reactor severe accidents, the capability to predict inventories of radioactive materials at risk (MAR) and their transport remains central to effective design, analysis, and licensing of advanced reactors. This topical report provides a detailed description of these predictive methods for KP-FHRs.

1.2 DESIGN FEATURES

1.2.1 Design Background

To facilitate NRC review and approval of this report for use by future applicants, key design features are provided in this section which are considered inherent to the KP-FHR technology. These features are not expected to change during the design development by Kairos Power and provide the basis to support the safety review. Should fundamental changes occur to these key design features or revised regulations be promulgated that affect the source term methodology for the KP-FHR, such changes would be reconciled and addressed in future license application submittals.

© 2020 Kairos Power LLC

The KP-FHR is a U.S.-developed Generation IV advanced reactor technology. In the last decade, U.S. national laboratories and universities have developed pre-conceptual Fluoride Salt-Cooled High Temperature Reactor (FHR) designs with different fuel geometries, core configurations, heat transport system configurations, power cycles, and power levels. More recently, University of California at Berkeley developed the Mark 1 pebble-bed FHR, incorporating lessons learned from the previous decade of FHR pre-conceptual designs. Kairos Power has built on the foundation laid by Department of Energy (DOE)-sponsored university Integrated Research Projects (IRPs) to develop the KP-FHR.

Although not intended to support the findings necessary to approve the applicability of regulations provided in this report, additional design description information is provided in the "Design Overview of the Kairos Power Fluoride Salt-Cooled, High Temperature Reactor (KP-FHR)" Technical Report (Reference 1) and the "Testing and Development Program Overview for the Kairos Power Fluoride Salt Cooled, High Temperature Reactor" Technical Report (Reference 2).

1.2.2 Key Design Features of the KP-FHR

The KP-FHR is a high-temperature, packed pebble-bed reactor with molten fluoride salt coolant operating at near-atmospheric pressure. The fuel in the KP-FHR is based on the Tri-Structural Isotropic (TRISO) high-temperature, carbonaceous-matrix coated particle fuel developed for high-temperature gas-cooled reactors in a pebble fuel element. Coatings on the particle fuel provide retention of fission products. The KP-FHR fuel is slightly buoyant with respect to the reactor coolant. The reactor coolant is a chemically stable molten fluoride salt mixture, $2\cdot^{7}LiF:BeF_2$ [[ ]] which also provides retention of fission products that escape from any fuel defects. A primary coolant loop circulates the reactor coolant using pumps and transfers the heat to an intermediate coolant loop via a heat exchanger. The pumped-flow intermediate coolant loop utilizes a nitrate salt, compatible with the reactor coolant, and transfers heat from the reactor coolant to the power conversion system through a steam generator. A pebble handling and storage system connected directly to the reactor vessel head permits the continuous extraction and insertion of fuel pebbles during operations. Pebbles are examined for burnup and damage and are either returned to the vessel or directed to storage. The upper portion of the reactor vessel, including pebble extraction and insertion penetrations, are maintained with an inert cover gas above the Flibe coolant. The design includes two decay heat removal systems: a normal decay heat removal system, which is used following normal shutdowns and anticipated operational occurrences; and a separate passive decay heat removal system which, along with natural circulation in the reactor vessel, removes decay heat in response to a design basis accident and does not rely on electrical power.

The KP-FHR design relies on a functional containment approach similar to the Modular High Temperature Gas-Cooled Reactor (MHTGR) and to hot cell facilities used to handle radiological materials, instead of the typical light water reactor (LWR) low-leakage, pressure-retaining containment structure. The KP-FHR functional containment safety design objective is to meet 10 CFR 50.34 (10 CFR 52.79) offsite dose requirements at the plant's exclusion area boundary (EAB) with margin. A functional containment is defined in Regulatory Guide (RG) 1.232 as a "barrier, or set of barriers taken together, that effectively limit the physical transport and release of radionuclides to the environment across a full range of normal operating conditions, anticipated operational occurrences, and accident conditions." RG 1.232 includes an example design criterion for the functional containment (MHTGR Criterion 16). As also stated in RG 1.232, the NRC has reviewed the functional containment concept and found it "generally acceptable," provided that "appropriate performance requirements and criteria" are developed. The NRC staff has

© 2020 Kairos Power LLC

developed a proposed methodology for establishing functional containment performance criteria for non-LWRs, which is presented in SECY-18-0096. This SECY document has been approved by the Commission.

The functional containment approach for the KP-FHR is to control radionuclides primarily at their source within the coated fuel particle under normal operations and accident conditions without requiring active design features or operator actions. The KP-FHR design relies primarily on the multiple barriers within the TRISO fuel particles and fuel pebble to ensure that the dose at the site boundary as a consequence of postulated accidents meets regulatory limits. However, in the KP-FHR as opposed to the MHTGR, the molten salt coolant serves as a distinct barrier providing retention of solid fission products that escape the fuel particle and fuel pebble barriers. This additional retention is a key feature of the enhanced safety and reduced source term in the KP-FHR.

1.3 REGULATORY BACKGROUND

1.3.1 Requirements

Applicants will pursue licensing for the KP-FHR under Title 10 of the Code of Federal Regulations (10 CFR) using a licensing pathway provided in Part 50 or Part 52. Regardless of the licensing path, there are associated regulatory requirements to evaluate the potential dose consequences of the design. 10 CFR 50.2, Definitions, provides the following general definition of source term:

> *Source term refers to the magnitude and mix of the radionuclides released from the fuel, expressed as fractions of the fission product inventory in the fuel, as well as their physical and chemical form, and the timing of their release.*

The regulation in 10 CFR 50.34(a)(1)(D) provides the requirement for an applicant submitting a preliminary safety analysis report to document the following:

> *The safety features that are to be engineered into the facility and those barriers that must be breached as a result of an accident before a release of radioactive material to the environment can occur. Special attention must be directed to plant design features intended to mitigate the radiological consequences of accidents. In performing this assessment, an applicant shall assume a fission product release* [Footnote 6] *from the core into the containment assuming that the facility is operated at the ultimate power level contemplated. The applicant shall perform an evaluation and analysis of the postulated fission product release, using the expected demonstrable containment leak rate and any fission product cleanup systems intended to mitigate the consequences of the accidents, together with applicable site characteristics, including site meteorology, to evaluate the offsite radiological consequences.* [emphasis added]. *Site characteristics must comply with part 100 of this chapter. The evaluation must determine that:*
>
> *(1) An individual located at any point on the boundary of the exclusion area for any 2 hour period following the onset of the postulated fission product release, would not receive a radiation dose in excess of 25 rem* [Footnote 7] *total effective dose equivalent (TEDE).*
>
> *(2) An individual located at any point on the outer boundary of the low population zone, who is exposed to the radioactive cloud resulting from the postulated fission product release (during the entire period of its passage) would not receive a radiation dose in excess of 25 rem total TEDE.*

© 2020 Kairos Power LLC

This requirement is echoed for the final safety analysis report (FSAR) in 10 CFR 50.34(b)(1) and for Part 52 licensing paths in 10 CFR 52.47(a)(2)(iv), 10 CFR 52.79(a)(1)(vi), 10 CFR 52.137(a)(2)(iv), 10 CFR 52.157(d). Footnote 6 cited in the above regulation is provided below:

> [Footnote 6] *The fission product release assumed for this evaluation should be based upon a major accident, hypothesized for purposes of site analysis or postulated from considerations of possible accidental events. Such accidents have generally been assumed to result in substantial meltdown of the core with subsequent release into the containment of appreciable quantities of fission products* [emphasis added].

The regulations cited above require an applicant to consider a fission product release from the core to evaluate dose. However, the regulations do not require a specific type of accident or source term to be evaluated. Footnote 6 states that core meltdown accidents have generally been assumed but stops short of requiring that an applicant postulate such an accident.

The NRC recognizes the need for mechanistic source term evaluations to satisfy the above regulations for advanced reactor designs and has released several SECY papers that provide guidance relevant to mechanistic source terms. Two of these SECY papers were approved by the Commission in respective Staff Requirements Memoranda (SRMs), and present a pathway for the NRC staff to review and approve mechanistic source term results relying on a functional containment approach:

- SECY-93-092 provides staff positions on several issues pertaining to the advanced reactors that were in preapplication engagement at the time (PRISM, MHTGR, and PIUS) as well as the CANDU 3 design. In this SECY, the NRC staff recommended that source terms for advanced reactor types base source term analyses upon a mechanistic analysis permitting, data exists on the reactor and fuel performance through research, development, and testing programs to provide confidence in such an approach. The transport of fission products would also need to model all barriers and pathways to the environs, including specific considerations of containment designs. NRC staff recommended that these calculations be as realistic as possible so that the values and limitations of any mechanism or barrier are not obscured and the events considered in the analysis to develop the set of source terms for each design are selected to bound severe accidents and design-dependent uncertainties. The Commission approved the staff's recommendations in SRM-SECY-93-092.
- SECY-18-0096 defines a functional containment as a "barrier, or set of barriers taken together, that effectively limit the physical transport of radioactive material to the environment. The staff recommends a technology inclusive, risk informed, and performance-based method for evaluating the adequacy of an applicant's functional containment design. The Commission approved the staff's recommendations in SRM-SECY-18-0096.

The NRC has various regulatory guidance documents that pertain to LWR source term methodologies. While many of the guidance documents pertaining to the source term modeling within the plant do not apply to the KP-FHR mechanistic source term methodology, the guidance available for atmospheric transport and dispersion of radionuclides is either applicable or relevant. Specifically, the gas transport methodology section of this report cites atmospheric transport guidance in Regulatory Guides 1.23, 1.145, and 1.183. See Section 7 for areas where this guidance is utilized.

© 2020 Kairos Power LLC

This report has been prepared to document and request NRC approval of the source term methodology to be used for evaluating the consequences of anticipated operational occurrences (AOOs), design basis events (DBEs), and design basis accidents (DBAs) consistent with the requirements in 10 CFR 50.34(a)(1)(D), 10 CFR 50.34(b)(1), 10 CFR 52.47(a)(2)(iv), 10 CFR 52.79(a)(1)(vi), 10 CFR 52.137(a)(2)(iv), 10 CFR 52.157(d). Specific evaluations of consequences using this methodology will be provided as part of license applications submitted under 10 CFR 50 or 10 CFR 52.

© 2020 Kairos Power LLC

2 KP-FHR MECHANISTIC SOURCE TERM EVALUATION APPROACH

The evaluation of the source term associated with licensing basis events is a key aspect of the KP-FHR safety case. The source term represents the amount, timing, and nature of the radioactive material available for release to the environment following an off normal event. The source term methodology accounts for accident source term phenomena that are unique to the KP-FHR. The KP-FHR design relies on a functional containment approach, described in Section 1.1.2 of this report, to meet 10 CFR 50.34 offsite dose requirements at the plant's EAB with margin. As discussed in Section 1.3.1 of this report, Regulatory Guide 1.232 defines functional containment as a "barrier, or set of barriers taken together, that effectively limit the physical transport and release of radionuclides to the environment across a full range of normal operating conditions, AOOs, and accident conditions." The KP-FHR source term is evaluated using a mechanistic approach, consistent with the NRC staff position on mechanistic source terms approved by the Commission in SRM-SECY-93-092.

2.1 MATERIAL AT RISK AND RELEASE FRACTION DEFINITIONS

The mechanistic source term for the KP-FHR is evaluated by decomposing the system into a series of sources of radioactive material at risk for release (MAR) and release fractions (RFs) for each barrier that holds up the MAR. To simplify terminology, this report refers to 'barriers' as any radionuclide transport medium between the MAR generator and the receptor for which an RF can be assessed. Radionuclides are divided and grouped into various classes of chemically similar isotopes to evaluate RFs which can be used to derive the MARs contained within those barriers. For a given radionuclide group, the time dependent source term at the receptor is:

$$ST^i(t) = \sum_{j=1}^{J} MAR_j^i(t) \prod_{j}^{J} RF_j^i(t) \qquad \text{Equation 1}$$

Note that the final source term in Equation 1 is a linear combination of multiple sources of MAR in the plant thus allowing the analyst to determine the relative fraction of each source of MAR that contributed to the overall source term. While some non-linearities exist in the models used in this methodology (e.g., aerosol deposition with the Henry correlation), these non-linearities typically increase the expected RF within a barrier thus making a linear combination conservative.

For non-gas space barriers, $RF_j^i(t)$is a ratio of the quantity of material that leaves a barrier to what is contained in the barrier, as shown in:

$$RF_j^i(t) = \frac{\sum_{k=1}^{K} N_{j\to k}^i(t)}{N_j^i(t)} \qquad \text{Equation 2}$$

The RF is calculated by the ratio the radionuclide group's mass or activity before and after the barrier.

For the gas space barrier, the process is different than that used for non-gas space barriers. Limitations in RADTRAD make its use impractical. For instance, RADTRAD's plot file only plots doses to the receptor and will not report activity quantities elsewhere in the model (such as within the reactor building). RADTRAD does report activities in output file, however it only reports these for major time steps

© 2020 Kairos Power LLC

which are typically hours apart. Radioactive decay, which is not explicitly evaluated in other barriers, is evaluated by RADTRAD from the beginning of the accident. RADTRAD only reports activities, such that providing an appropriate activity ratio that impacts the dose calculation is impractical.

Time-averaged χ changes as a function of time after the initiator. As a result, a given quantity of isotopes released in the first few hours will have a greater impact on offsite dose than that same quantity of isotopes released long after the initiating event.

As such, the RF of the gas space is calculated via the following formula:

$$RF_{GS} = \frac{D_{LBE\ Holdup}}{D_{No\ Holdup}} \qquad \text{Equation 3}$$

where:

RF_{GS} = the release fraction for the gas space

$D_{LBE\ Holdup}$ = the dose over the relevant time period assuming whatever LBE building holdup conditions are used

$D_{No\ Holdup}$ = the dose over the relevant time period assuming no holdup

In Equation 4, RF is a function of the mechanical and thermal loadings applied to the barrier at a given time. Conversely, MAR is an integral quantity that is impacted by generation (*S*), decay (λ) into and out of the group, and attenuation of radionuclides across barriers:

$$MAR_j^i(t_0) = \int_0^{t_0} S_j^i(t) + \sum_{k\neq j}^{J} MAR_k^i(t)\, RF_{k\to j}^i(t) - MAR_j^i(t) RF_j^i(t) + \sum_{l\neq i}^{I} \lambda_j^{l\to i}(t) - \lambda_j^i(t) MAR_j^i(t) dt \qquad \text{Equation 4}$$

From a physical perspective, MAR will be generated and then move through and held up within various barriers during normal operations. This held-up MAR may be mobilized during AOOs, DBEs, and DBAs. In modeling space, once event sequence modeling begins (t_o), MAR generation stops (the integrated generation of MAR is negligible compared to the quantity of MAR generated during normal operations.) Thus, for the event sequence analysis, Equation 4 simplifies to Equation 5 for most barriers and to Equation 6 for building transport:

$$MAR_j^i(T) = MAR_j^i(t_0) + \int_{t0}^{T} \sum_{k\neq j}^{J} MAR_k^i(t)\, RF_{k\to j}^i(t) - MAR_j^i(t) RF_j^i(t) - \lambda_j^i(t) MAR_j^i(t) dt \qquad \text{Equation 5}$$

$$MAR_j^i(T) = MAR_j^i(t_0) + \int_{t0}^{T} \sum_{k \neq j}^{J} MAR_k^i(t)\, RF_{k \to j}^i(t) - MAR_j^i(t) RF_j^i(t) + \sum_{l \neq i}^{I} \lambda_j^{l \to i}(t) - \lambda_j^i(t) MAR_j^i(t) dt \quad \text{Equation 6}$$

As part of the analysis of each barrier, radionuclides are grouped together and transported at the rate of a representative element.

2.2 SOURCES OF MATERIAL AT RISK IN THE KP-FHR

The sources of MAR in the KP-FHR are fission products and activation products (including tritium). The primary locations for MAR-holdup in the KP-FHR include:

- Fuel and Graphite Pebble
- Flibe (circulating in the reactor vessel and primary heat transport system)
- Graphite Structures (reflector)
- Other sources of MAR (e.g., graphite dust, filters, cold traps)
- Cover gas

These sources of steady state MAR are represented graphically in Figure 2-1 for the heat transport and cover gas systems and in Figure 2-2 for the pebble handling and storage system. The steady state distribution of MAR throughout the plant is the initial condition for MAR that can be mobilized in a transient. Migration of MAR in steady state and transient conditions is discussed in more detail in subsequent sections of this topical report.

2.3 KP-FHR SOURCE TERM EVALUATION

The radiological source term analysis for AOOs, DBEs, and DBAs is performed in a linear workflow fashion. Additional details about the barrier methodologies that support these steps is provided in subsequent sections of this topical report. The workflow includes the following steps:

1. Identify the MAR and barriers affected by the transient,
2. Qualitatively evaluate each barrier affected by the transient, and
3. Quantitatively evaluate the RFs for each barrier and provide the resultant site boundary dose evaluation.

2.3.1 Identification of MAR and Affected Barriers

The first step in the source term evaluation is to determine the scope for the event being analyzed. The source term analysis for the AOO, DBE, or DBA identifies:

1. The primary sources of MAR affected by an event sequence.
2. Barriers to radionuclide release separating each source of MAR from the EAB for an event sequence.

The sources of MAR and their associated barriers are discussed in Section 2.2, with further detail provided in subsequent sections of this topical report. The characterization of specific KP-FHR licensing

© 2020 Kairos Power LLC

basis events will be included in safety analysis reports associated with licensing application submittals. However, expected KP-FHR design aspects are provided in Section 2.3.4 to inform which licensing basis events are covered by the source term methodology.

2.3.2 Qualitative Evaluation

The second step in the source term evaluation is to conduct a qualitative evaluation for each barrier identified in Section 2.3.1 Item #2. This step will refine the information related to MAR, barriers, and structures, systems, and components (SSCs) that will be used in the quantitative evaluation.

1. MAR originating in the barrier at the start of the event sequence and the corresponding radionuclide groups used to calculate attenuation through the barrier.
2. Neighboring barrier effects:
    a) MAR from neighboring barriers that can attenuate into the current barrier during the event sequence.
    b) Neighboring barriers into which MAR can move, from the current barrier.
3. Barrier performance models:
    a) The baseline RF assessment models for the barrier for the given AOO, DBE, or DBA.
    b) If the performance of the barrier (e.g., RF) requires thermal fluid analysis (e.g., System Analysis Module (KP-SAM) calculation) for the given AOO, DBE, or DBA.
    c) Input parameters that drive the barrier performance. The selection of conservative estimates, best estimate values, or uncertainty distributions should be justified for each input parameter identified.
4. SSC performance, either passive or active, that will be included in the AOO, DBE, or DBA analysis.
5. Sources of model uncertainty and related assumptions: This includes consideration of uncertainties associated with the first of a kind design and would affect the results of the source term analysis. Uncertainties will be identified and assessed per the requirements in ASME/ANS RA-S-1.4-2020, “Probabilistic Risk Assessment Standard for Advanced Non-Light Water Reactor Nuclear Power Plants,” using an approach similar to that outlined in NUREG-1855 Revision 1, “Guidance on the Treatment of Uncertainties Associated with PRAs in Risk-Informed Decision Making.”

2.3.3 Quantitative Evaluation

The final step in the source term evaluation is to conduct a quantitative analysis for each barrier by modeling:

1. Thermal fluid evolutions of the reactor system if it was determined to be needed in Section 2.3.2 Item #3(b).
2. Attenuate screened sources (see de minimis threshold discussion below) of MAR using demonstrably conservative inputs for the timing and/or the magnitude of the release. Screened MAR are not removed from the model or the simulation results. Instead, screened MAR are identified as unable to challenge the dose figures of merit and thus are conservatively treated so as to focus the analysis on sources of MAR that cannot be conservatively bounded in a simplified analysis.

    A pathway is considered de minimis (i.e., negligible or screened), thus only subject to either conservative quantitative assessments or qualitative evaluations on the dose if either:

© 2020 Kairos Power LLC

a. Absolute: [[

]]

b. Relative: [[

]]

3. Attenuation of MAR which originated in the current barrier (i.e., identified in Section 2.3.2 Item #1) as function of time. Identify any release pathways which meets the de minimis thresholds to justify not transferring this MAR to the next barrier.
4. Attenuation of MAR within the current barrier which transports into the current barrier from another barrier as a function of time.

The radionuclide release figures of merit are assessed as follows:

1. Quantify the integral RF for the barrier on a radionuclide class or isotopic basis over the entire transient. For RADTRAD simulations, the RF for key isotopes will be calculated instead of an RF for radionuclide classes if the explicit radionuclide decay modeling results in various radionuclides within a radionuclide class having different RFs depending on their ingrowth and decay rates.
2. Calculate either:
    a. DBAs: The worst two-hour EAB and thirty-day low population zone (LPZ) doses and specify the key isotopes, sources of MAR, and any SSC performance that drove the release for DBAs or
    b. AOOs or DBEs: A probabilistic representation of thirty-day doses at the site boundary and quantify the corresponding 95th percentile:
        i. Include a horsetail representation of the time histories of releases.
        ii. Specify the key isotopes, sources of MAR, and SSC performance, if any, that drove the release.
3. Evaluate the effects of the demonstrably conservative inputs associated with screened MAR on the timing and magnitude of the radionuclide release figures of merit.
4. Assess the effects of model uncertainty, reasonable alternatives and assumptions made due to the lack of as-built and as-operated details on the figures of merit via either qualitative descriptions or sensitivity studies.

© 2020 Kairos Power LLC

2.3.4 Additional Design Information Used in the Methodology

Section 1.2.2 provides fundamental design information about a KP-FHR that defines the technology. This section provides a list of additional KP-FHR design information (including some expected LBE characteristics) that is used in the KP-FHR mechanistic source term methodology. The characterization of specific KP-FHR licensing basis events will be provided in safety analysis reports associated with future licensing application submittals, therefore, the design information provided in this section is necessary to determine which source term phenomena are within the KP-FHR design basis. This design information is described below:

1. Beryllium is a constituent of the reactor coolant (Flibe) and requires control for personnel protection. This methodology assumes that such controls will include a beryllium confinement area within building enclosures that is designed to operate at a negative pressure induced by the heating, ventilation, and air conditioning (HVAC) system during normal operation. This enclosure or structure is assumed to be non-safety related from a confinement perspective.
2. Where the potential for internal flooding exists, it is assumed that flood barriers will be erected to preclude Flibe-water interactions. Significant Flibe-water interactions are assumed to be beyond design basis conditions.
3. The portions of the reactor vessel that ensure the pebbles are covered with Flibe are assumed to be safety-related. The design of vessel penetrations and pump operation are assumed to preclude fuel uncovery in the active region of the core. Therefore, reactor vessel failure, leakage from the reactor vessel, and fuel uncovery in the active region of the core are assumed to be beyond design basis conditions.
4. The reactor vessel head is assumed to be a nonsafety-related portion of the reactor coolant boundary that retains cover gas in AOO, DBE, and DBA conditions. Under these conditions, the vessel head is assumed to be transparent to radionuclides while retaining cover gas and preventing air ingress. Significant air ingress in terms of oxidation co-incident with AOO, DBE, and DBA unrelated to vessel head performance is assumed to be a beyond design basis scenario.
5. The KP-FHR design is assumed to preclude reactions of reactor coolant with large quantities of chemical reactants that would result in the salt deviating from the range of redox potentials in Table 4-1 Such reactions are assumed to be beyond design basis conditions.
6. Concrete surfaces upon which Flibe can be sprayed, splashed, or as a result of leaks or breaks in the reactor coolant boundary will either be protected, shown to be non-reactive, or incorporate other design solutions to ensure that chemical reactions with concrete only mobilize a de minimis quantity of radionuclides (defined as less than five percent of any given radionuclide group released by the spray). Therefore, excessive Flibe concrete reactions are assumed to be beyond design basis conditions.
7. The design of the primary system is assumed to preclude:
    - Syphoning of Flibe outside of the vessel
    - Chemical reactions between reactor coolant and gasket materials
    - The cessation of natural circulation to cool the core
    - Two phase flow of cover-gas and Flibe out of the pipe break
8. It is assumed that flood barriers, catch trays, and/or other design features will preclude leaked Flibe from pooling in an area where it either cannot cool and solidify or where it will be exposed to quantities of water which can change the chemical potential of the Flibe beyond those supported in this topical report.

© 2020 Kairos Power LLC

9. Long-term evaporation of Flibe remaining in the primary system is assumed to be negligible compared to other aerosol formation mechanisms because this would be governed by counter-current exchange flow which is assumed to be precluded by design. The methodology also assumes no evaporation from the Flibe pool surface in the confinement during and after the spill due to the high freezing point of Flibe.
10. The pebble handling and storage system (PHSS) and its surroundings are assumed to be designed such that pebbles cannot form a critical geometry. Therefore, criticality of spilled pebbles will be considered a beyond design basis scenario.
11. The pebble handling system and pebble storage systems are assumed to be designed such that TRISO kernel temperatures will remain below TRISO failure limits of approximately 1600 °C under loss of forced circulation conditions.
12. Cover gas activity is assumed to be monitored and detection of high activity would result in stopping the movement of pebbles through the PHSS. Therefore, excessive mechanical grinding of pebbles due to forced pebble circulation through the PHSS is assumed to be a beyond design basis condition.
13. The KP-FHR design is assumed to result in oxidation levels that should preclude the formation of a quantity of carbon monoxide that can support combustion. Therefore, combustion of carbon monoxide is assumed to be a beyond design basis condition.
14. All circulating graphite dust is assumed to have the radionuclide activity density corresponding to the highest graphite matrix activity of a fuel pebble.
15. The design of the PHSS is expected to prevent graphite oxidation during an air ingress event.
16. In the evaluation of MAR in other locations than the fuel and Flibe, it is assumed that mechanical damage to the fuel is restricted to gradual generation of particulate matter. Bulk mechanical damage that compromises the layers of the TRISO particle is not considered.
17. The steady state rate of radionuclides evaporation into the headspace gas is assumed to be much lower than the rate of argon sweep gas through the system. As a result, these radionuclides will be collected in the vapor and off gas cleanup systems at the rate at which they escape the Flibe. Therefore, the MAR in the cover gas is assumed to be minimal.
18. The KP-FHR design basis is assumed to preclude the possibility of new MAR being generated in quantities above the de minimis screening detailed in Section 2.3.3 after the initiation of a transient.
19. The KP-FHR design limits on the quantities of MAR in the intermediate system (see limitations in Section 8.2) will prevent safety-significant quantities of radionuclide accumulation.

2.4 PHENOMENA IDENTIFICATION AND RANKING TABLES

Phenomena identification and ranking tables (PIRTs) are an important step in the evaluation model development and assessment process detailed by the NRC in Regulatory Guide 1.203. PIRTs rely on analysis, scaling, and expert judgment to identify and rank key phenomenology in an evaluation model. KP-FHR PIRTs were initiated early in the KP-FHR design process to aid in system design and evaluation model development. The mechanistic source term methodology is informed by a KP-FHR radiological source term PIRT.

The KP-FHR radiological source term PIRT covers phenomena associated with normal operations, transients with intact reactor coolant boundary, leak or rupture of the external reactor coolant boundary (a “compromised” reactor coolant boundary) with or without water, pebble handling and/or cleaning,

© 2020 Kairos Power LLC

radioactive waste accidents, nitrate/graphite/Flibe reaction, and vessel failure. Some of the phenomena identified during the PIRT process apply to scenarios that will be beyond the design basis of the KP-FHR, which will be addressed in future licensing submittals. Since the PIRTs were performed prior to the formalization of KP-FHR event classifications, phenomena associated with the assumed BDBE conditions are not addressed in this topical report.

The KP-FHR radiological source term PIRT combines rankings of importance and knowledge level of the phenomena identified by the PIRT panel. The importance ranking is based on influence of the phenomenon on safety, using the following scale:

- High (H): phenomenon has critical influence on evaluation criteria
- Medium (M): phenomenon has moderate influence on evaluation criteria
- Low (L): phenomenon has minimal influence on evaluation criteria

The evaluation criteria or figures of merit for judging the relative importance of phenomena relevant to safety and reliability are:

- Top level: dose at site boundary due to fission and activation product releases. This regulatory criterion, directly tied to source term analysis, will be common to all KP-FHR PIRTs.
- Second level: releases of radioactivity that impact worker dose. This criterion will also be common to all KP-FHR PIRTs.
- Lower level criteria for KP-FHR PIRTs are derived from top level regulatory criteria and from reliability and investment protection criteria.

Knowledge level ranking is based on level of understanding of phenomena through existing experimental data using the following scale:

- High (H): knowledge base is adequate for modeling, analysis, or decision making (approximately 70-100% of complete knowledge and understanding)
- Medium (M): knowledge base is incomplete for modeling, analysis, or decision making (30-70% of complete knowledge and understanding)
- Low (L): knowledge base is sparse for modeling, analysis, or decision making (0-30% of complete knowledge and understanding)

The combined rankings form a doublet (Importance, Knowledge) prioritized as follows:

- (H, L) and (H, M): Top priority tier. Merits further investigation and consideration of design to eliminate/mitigate the phenomenon,
- (M, M) and (M, L): Second priority tier. Lower priority at the present time, use judgement, and
- Others: Lowest priority tier. No efforts beyond existing tools and data due to low ranking.

The source term methodology presented in this report addresses the design basis phenomena identified in the top priority tier and second priority tier. The phenomena relevant to the source term methodology presented in this report and the associated ranking for each phenomenon is provided in the following tables:

© 2020 Kairos Power LLC

- Table 2-1 Fuel Phenomena for Accidents Involving Both Intact and Compromised Reactor Coolant Boundaries
- Table 2-2 Coolant Phenomena for Accidents Involving Intact Reactor Coolant Boundaries
- Table 2-3 Coolant Phenomena for Accidents Involving Compromised Reactor Coolant Boundaries
- Table 2-4 Graphite Structure Phenomenon for Accidents Involving Intact Reactor Coolant Boundaries
- Table 2-5 Graphite Structure Phenomenon for Accidents Involving Compromised Reactor Coolant Boundaries
- Table 2-6 Phenomena for Accidents Involving Radioactive Waste
- Table 2-7 Phenomena for Accidents Involving the Pebble Handling and Storage System
- Table 2-8 Gas Space Phenomena for Accidents Involving an Intact Reactor Coolant Boundary
- Table 2-9 Gas Space Phenomena for Accidents Involving a Compromised Reactor Coolant Boundary

Each barrier discussion in subsequent sections of this topical report disposition the high, high-to-medium and medium importance phenomena identified in the PIRTs.

2.5 SOFTWARE USED IN KP-FHR SOURCE TERM EVALUATION

2.5.1 SERPENT2

SERPENT2 (Reference 3) is a multi-purpose three-dimensional continuous-energy Monte Carlo particle transport code, developed at VTT Technical Research Centre of Finland, Ltd. The applications of SERPENT2 can be divided into three main categories:

1. Traditional reactor physics applications, including spatial homogenization, criticality calculations, depletion analysis, fuel cycle studies,
2. Multi -physics simulations, i.e. coupled calculations with thermal hydraulics, computational fluid dynamics and fuel performance codes, and
3. Neutron and photon transport simulations for radiation dose rate calculations and shielding analysis.

The KP-FHR source term methodology includes the use of SERPENT2 to provide core inventory information as an input to other models. However, SERPENT2 will be verified and validated as part of the KP-FHR core design and analysis methodology, which will be provided in a future licensing submittal.

2.5.2 KP-Bison

BISON has been selected as the platform to develop the KP-FHR fuel performance code. BISON is a finite element-based nuclear fuel performance code applicable to a variety of fuel forms including TRISO particle fuel (Reference 6). KP-Bison will model and simulate nuclear fuel behavior in the KP-FHR during normal operating conditions and licensing basis event conditions. The latter include anticipated operational occurrences, design basis accidents, and the early stages of beyond design basis accidents. The KP-FHR source term methodology includes the use of KP-Bison to assess the mechanical integrity of the TRISO-coated particles and the retention of fission products by intact or potentially failed particles. KP-Bison will be verified and validated as part of the KP-FHR fuel performance methodology, which is presented in Reference 4.

© 2020 Kairos Power LLC

2.5.3 KP-SAM

The System Analysis Module (SAM) has been selected as the basis to develop the KP-FHR systems code, KP-SAM. SAM is a modern system analysis code being developed at Argonne National Laboratory under the DOE Nuclear Energy Advanced Modeling and Simulation program (Reference 5). SAM focuses on modeling advanced reactor designs, including SFRs (sodium fast reactors), MSRs (molten salt reactors), and FHRs (fluoride-salt-cooled, high-temperature reactors). These designs use single-phase, low-pressure, and high-temperature liquid coolants. The KP-FHR source term methodology includes the use of KP-SAM to provide event-specific thermal fluid conditions for an LBE source term evaluation. KP-SAM will be verified and validated as part of the KP-FHR transient methodology, which will be provided in a future licensing submittal.

2.5.4 ARCON96

ARCON96 (Reference 9) is a near-field atmospheric dispersion tool designed to provide directional source strength (Q) values for control room dose estimates consistent with guidance from Regulatory Guide 1.194. ARCON96 directly reports the directionally dependent 95th percentile atmospheric dispersion factor ($\frac{\chi}{Q}$) time averaged values appropriate for control room habitability analysis.

The KP-FHR source term methodology is intended to evaluate EAB dispersion distances around 400 meters from the reactor building, the ARCON96 models are more appropriate for KP-FHR applications than the PAVAN models. PAVAN is an atmospheric dispersion tool that is used in LWR applications that evaluate EABs that are typically over 1000 meters from the reactor building. This application of ARCON96 is consistent with the approach implemented by NuScale, which the NRC deemed acceptable in the Safety Evaluation for NuScale Power, LLC Topical Report, TR-0915-17565, "Accident Source Term Methodology" which states:

> *"ARCON96 is a general code for assessing atmospheric relative concentrations in building wakes under a wide range of situations and was approved by the NRC staff in RG 1.194 for use in performing control room atmospheric dispersion calculations. The ARCON96 dispersion algorithms are based on field measurements taken out to distances of 1,200 meters."*

While ARCON96 does not directly report 99.5th percentile directionally dependent, time averaged $\frac{\chi}{Q}$s, ARCON96 does report the cumulative distribution functions for directionally dependent $\frac{\chi}{Q}$s at 1, 2, 4, 8, 12, 24, 48, 96, 168, 360, and 720 hours. From these outputs, the following quantities can be calculated:

- Directionally independent 95th percentile $\frac{\chi}{Q}$s
- Directionally dependent 99.5th percentile $\frac{\chi}{Q}$s

2.5.5 RADTRAD

RADTRAD (Reference 10) is a control volume radionuclide gas transport code supported by the NRC that evaluates design basis source term consequences for light water reactors (LWRs). While some models are LWR-specific, the computational framework of RADTRAD has the flexibility to support KP-FHR source term analysis. However, the non-applicable LWR models within RADTRAD will not be used for the KP-FHR source term analysis. The key outputs of RADTRAD are:

© 2020 Kairos Power LLC

- Worst two-hour dose (for DBAs)
- Thirty-day dose (for Licensing Basis Events (LBEs) that are AOOs or DBEs)

RADTRAD does not include thermal fluid models and cannot calculate natural convection or forced circulation flows.

© 2020 Kairos Power LLC

Table 2-1 Fuel Phenomena for Accidents Involving Both Intact and Compromised Reactor Coolant Boundaries

Index	Relevant System	Phenomenon	Imp.	Imp. Rationale	K.L.	K.L. Rationale
[[						
						]]

Index	Relevant System	Phenomenon	Imp.	Imp. Rationale	K.L.	K.L. Rationale
[[						
						]]

Index	Relevant System	Phenomenon	Imp.	Imp. Rationale	K.L.	K.L. Rationale
[[						
						]]

Table 2-2 Coolant Phenomena for Accidents Involving Intact Reactor Coolant Boundaries

Index	Relevant System	Phenomenon	Imp.	Imp. Rationale	K.L.	K.L. Rationale
[[						
						]]

Index	Relevant System	Phenomenon	Imp.	Imp. Rationale	K.L.	K.L. Rationale
[[						
						]]

Index	Relevant System	Phenomenon	Imp.	Imp. Rationale	K.L.	K.L. Rationale
[[						
						]]

Index	Relevant System	Phenomenon	Imp.	Imp. Rationale	K.L.	K.L. Rationale
[[						]]

Table 2-3 Coolant Phenomena for Accidents Involving Compromised Reactor Coolant Boundaries

Index	Relevant System	Phenomenon	Imp.	Imp. Rationale	K.L.	K.L. Rationale
[[						
						]]

Index	Relevant System	Phenomenon	Imp.	Imp. Rationale	K.L.	K.L. Rationale
[[						
						]]

Index	Relevant System	Phenomenon	Imp.	Imp. Rationale	K.L.	K.L. Rationale
[[						
						]]

Index	Relevant System	Phenomenon	Imp.	Imp. Rationale	K.L.	K.L. Rationale
[[						
						]]

Index	Relevant System	Phenomenon	Imp.	Imp. Rationale	K.L.	K.L. Rationale
[[						
						]]

Index	Relevant System	Phenomenon	Imp.	Imp. Rationale	K.L.	K.L. Rationale
[[						
						]]

Index	Relevant System	Phenomenon	Imp.	Imp. Rationale	K.L.	K.L. Rationale
[[						
						]]

Index	Relevant System	Phenomenon	Imp.	Imp. Rationale	K.L.	K.L. Rationale
[[						
						]]

Index	Relevant System	Phenomenon	Imp.	Imp. Rationale	K.L.	K.L. Rationale
[[						
						]]

Index	Relevant System	Phenomenon	Imp.	Imp. Rationale	K.L.	K.L. Rationale
[[						
						]]

Index	Relevant System	Phenomenon	Imp.	Imp. Rationale	K.L.	K.L. Rationale
[[						
						]]

Index	Relevant System	Phenomenon	Imp.	Imp. Rationale	K.L.	K.L. Rationale
[[						
						]]

Index	Relevant System	Phenomenon	Imp.	Imp. Rationale	K.L.	K.L. Rationale
[[						
						]]

Index	Relevant System	Phenomenon	Imp.	Imp. Rationale	K.L.	K.L. Rationale
[[						
						]]

Table 2-4 Graphite Structure Phenomenon for Accidents Involving Intact Reactor Coolant Boundaries

Index	Relevant System	Phenomenon	Imp.	Imp. Rationale	K.L.	K.L. Rationale
[[						]]

Table 2-5 Graphite Structure Phenomenon for Accidents Involving Compromised Reactor Coolant Boundaries

Index	Relevant System	Phenomenon	Imp.	Imp. Rationale	K.L.	K.L. Rationale
[[						]]

Table 2-6 Phenomena for Accidents Involving Radioactive Waste

Index	Relevant System	Phenomenon	Imp.	Imp. Rationale	K.L.	K.L. Rationale
[[						
						]]

Index	Relevant System	Phenomenon	Imp.	Imp. Rationale	K.L.	K.L. Rationale
[[						
						]]

Index	Relevant System	Phenomenon	Imp.	Imp. Rationale	K.L.	K.L. Rationale
[[						
						]]

Index	Relevant System	Phenomenon	Imp.	Imp. Rationale	K.L.	K.L. Rationale
[[						
						]]

Index	Relevant System	Phenomenon	Imp.	Imp. Rationale	K.L.	K.L. Rationale
[[						
						]]

Index	Relevant System	Phenomenon	Imp.	Imp. Rationale	K.L.	K.L. Rationale
[[						
						]]

Table 2-7 Phenomena for Accidents Involving the Pebble Handling and Storage System

Index	Relevant System	Phenomenon	Imp.	Imp. Rationale	K.L.	K.L. Rationale
[[						
						]]

Index	Relevant System	Phenomenon	Imp.	Imp. Rationale	K.L.	K.L. Rationale
[[						
						]]

Index	Relevant System	Phenomenon	Imp.	Imp. Rationale	K.L.	K.L. Rationale
[[						
						]]

Index	Relevant System	Phenomenon	Imp.	Imp. Rationale	K.L.	K.L. Rationale
[[						
						]]

Index	Relevant System	Phenomenon	Imp.	Imp. Rationale	K.L.	K.L. Rationale
[[						
						]]

Index	Relevant System	Phenomenon	Imp.	Imp. Rationale	K.L.	K.L. Rationale
[[						
						]]

Table 2-8 Gas Space Phenomena for Accidents Involving an Intact Reactor Coolant Boundary

Index	Relevant System	Phenomenon	Imp.	Imp. Rationale	K.L.	K.L. Rationale
[[						
						]]

Index	Relevant System	Phenomenon	Imp.	Imp. Rationale	K.L.	K.L. Rationale
[[						]]

Table 2-9 Gas Space Phenomena for Accidents Involving a Compromised Reactor Coolant Boundary

Index	Relevant System	Phenomena	Imp.	Imp. Rationale	K.L.	K.L. Rationale
[[						
						]]

Index	Relevant System	Phenomena	Imp.	Imp. Rationale	K.L.	K.L. Rationale
[[						
						]]

Figure 2-1 Steady State Material at Risk Accumulation in the Heat Transport and Cover Gas Systems

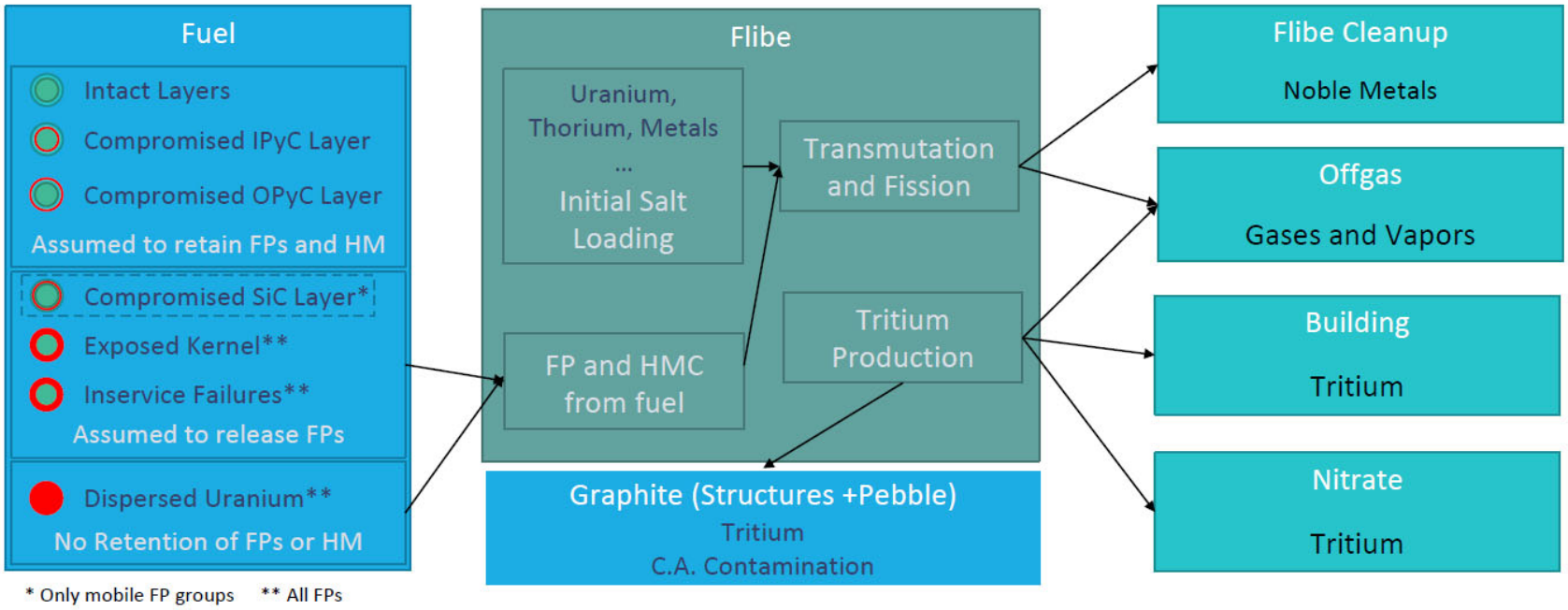

(C.A. = Circulating Activity)

© 2020 Kairos Power LLC

Figure 2-2 Steady State Material At Risk Accumulation in the Pebble Handling and Storage System

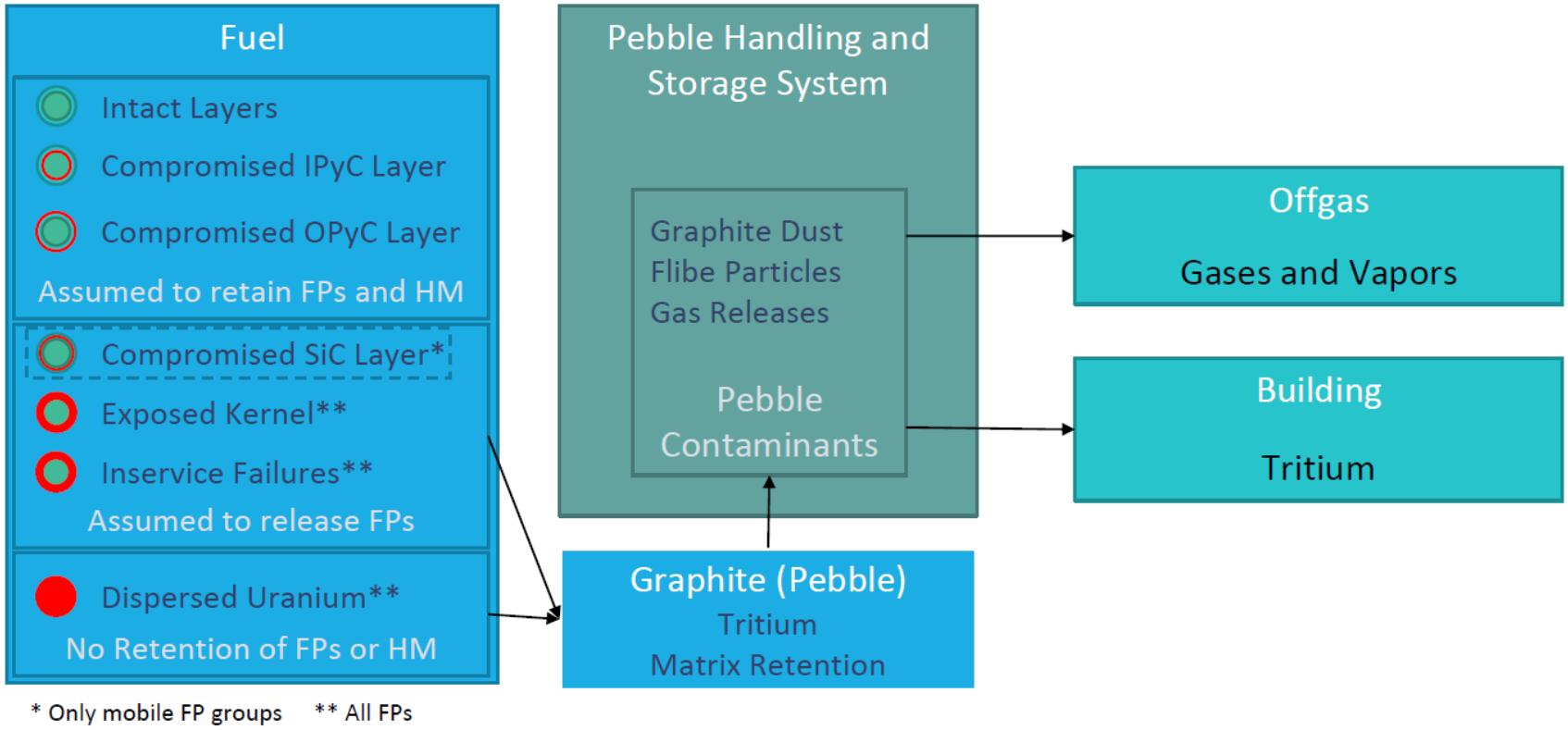

3 EVALUATING FUEL RETENTION OF RADIONUCLIDES

The KP-FHR fuel pebble is a carbon matrix sphere containing three regions: a low-density carbon core, a fuel region containing carbon matrix material embedded with TRISO coated particles, and a fuel-free carbon outer shell. The TRISO particles contain high assay low enriched uranium (HALEU) fuel kernels in the form of uranium oxycarbide (UCO). The particle includes the UCO kernel, a porous carbon buffer layer, an inner pyrolytic carbon (IPyC) layer, a silicon carbide (SiC) layer, and an outer pyrolytic carbon (OPyC) layer. The TRISO IPyC, SiC, and OPyC barriers are part of the KP-FHR functional containment strategy.

TRISO fuel particles have been irradiated in a series of Advanced Gas Reactor (AGR) test campaigns. The AGR-1 and AGR-2 campaigns conducted safety testing and post-irradiation examinations to support understanding of in-service failures, manufacturing defects, and the behavior of radionuclides (i.e., mobility and retention) in the TRISO particle. The information from the AGR program was reviewed in Kairos Power's evaluation of fuel source term. The fuel specification is described in the KP-FHR Fuel Qualification Topical Report (Reference 8).

3.1 IMPORTANT SOURCE TERM PHENOMENA IDENTIFIED FOR FUEL

The radiological source term PIRT described in Section 2.4 above considered fuel related phenomena for transients in which the Reactor Coolant Boundary (RCB) integrity is maintained, thus excluding Flibe leaks and nitrate salt ingress as well as fuel related phenomenon in which the RCB was compromised. In both cases, intact and compromised RCB, the PIRT results identify five phenomena related to fuel and that have a high importance to safety. [[

]]

No fuel related phenomena were identified in the PIRT with a high-to-medium importance to safety for event sequences involving an intact or compromised reactor coolant boundary. Table 2-1 also summarizes phenomena which are listed as having a medium importance to safety relative to the fuel for accidents involving an intact or compromised RCB. These phenomena are grouped into one category discussed below.

[[

]]

3.2 SOURCES OF RADIONUCLIDES IN FUEL

The sources of radionuclides from the fuel include the release of fission products from manufacturing defects, heavy metal contamination, in-service failures, and releases from intact TRISO fuel particles. The evaluation of fuel performance, including fuel particle failure, is performed using the methodology described in KP-FHR topical report KP-TR-010-P (Reference 4). These sources of fission products are described below.

3.2.1 Manufacturing Defects

A manufacturing defect can lead to fission product release from the beginning of service life or lead to a premature failure due to an in-service failure mechanism. Potential manufacturing defects include malformed kernels, coating anomalies, defective SiC layer, carbon matrix impurity, IPyC defects, and uranium dispersion. [[

]] Manufacturing defects, as a source of fission product release during normal and accident conditions, can be minimized or reduced in frequency during manufacturing through process design, process specifications, and quality control inspections to align with the fuel specification requirements.

3.2.2 Heavy Metal Contamination

Uranium, transuranic elements produced under a neutron flux, and elements that are present as natural contaminants in materials used to fabricate TRISO particles and pebbles not contained within a gas-tight, intact dense pyrocarbon or silicon carbide layer are considered to represent heavy-metal contamination. The two types of heavy-metal contamination are exposed kernels and dispersed uranium.

The radionuclide release fraction from exposed kernels can be higher than that from particles with cracked coatings; the release fraction from all exposed kernels is reduced relative to dispersed uranium by retention within the kernel. Retention within the kernel is a function of temperature as well as the radionuclide of interest. The release fraction of dispersed uranium (i.e., uranium on or near the surface of the OPyC layer and impurities within the matrix) is higher than that of exposed kernels. In the case of dispersed uranium, retention is a function of temperature as well as the half-life and diffusion characteristics of the radionuclide of interest.

© 2020 Kairos Power LLC

3.2.3 In-service Failures

TRISO particles can fail in-service during normal operation, and such failures historically consist of two types of mechanisms: mechanical failure mechanisms and thermo-chemical failure mechanisms. Mechanical failure mechanisms include over pressurization (i.e., in particles without manufacturing defects), irradiation-induced failure of the OPyC coating, debonding between the IPyC and SiC layers, and irradiation-induced cracking of the IPyC layer leading to potential SiC failure. Thermo-chemical failure mechanisms include failure of the SiC coating due to kernel migration in the presence of a temperature gradient, heavy metal dispersion in the IPyC coating, thermal decomposition (SiC →Si+C) and fission product/SiC interactions.

The usage of UCO fuel at KP-FHR operating and accident temperatures limit the number of potential failure mechanisms that need to be considered in source term analysis. Details about the applicable failure mechanisms is given in Reference 4.

3.2.4 Release from Intact Particles

After the fuel kernel, the physical barriers against release are the outer coating layers (i.e., IPyC, SiC, and OPyC) that surround the kernel and the buffer layer. These three coating layers act as a functional containment to prevent or impede fission products from leaving the kernel and buffer layers. Table 3-1 provides a list of various barrier conditions and a qualitative assessment of fission products based upon the state of each of the coating layers. When the SiC layer remains intact, there is a marginal release of historically observed fission products such as cerium, cesium, europium, and strontium.

3.2.5 Tritium

Tritium in the KP-FHR is primarily generated through neutron reactions with the Flibe. Each component of Flibe has some contribution to total tritium generation, as shown in the reactions in Equation 7 to Equation 12. The beryllium reaction in Equation 11 does not produce tritium directly but produces lithium-6 through Equation 12. Therefore, an equilibrium tritium production rate in Flibe will be reached once the depletion rate of lithium-6 matches the production rate from the reaction with beryllium.

$$^{6}Li + n \rightarrow {}^{4}He + {}^{3}H \qquad \text{Equation 7}$$

$$^{7}Li + n \rightarrow {}^{4}He + {}^{3}H + n' \qquad \text{Equation 8}$$

$$^{9}Be + n \rightarrow {}^{7}Li + {}^{3}H \qquad \text{Equation 9}$$

$$^{19}F + n \rightarrow {}^{17}O + {}^{3}H \qquad \text{Equation 10}$$

$$^{9}Be + n \rightarrow {}^{6}He + {}^{4}He \qquad \text{Equation 11}$$

$$^{6}He \rightarrow {}^{6}Li + \beta + \bar{\nu}_e \quad (t_{1/2} = 0.8\ \text{s}) \qquad \text{Equation 12}$$

Tritium production is calculated from the reactions in Equation 7 and Equation 8 since these reactions account for the majority of tritium generation in the KP-FHR. All isotopic concentrations are

assumed to be steady with time except for Lithium-6, which changes in time based on the differential equation shown in Equation 13.

$$\frac{dN_{Li-6}}{dt} = \phi N_{Be-9}\sigma_{Be-9}^{n,\alpha}V_{Core}/V_{Loop} - \phi N_{Li-6}\sigma_{Li-6}^{n,abs}V_{Core}/V_{Loop} \quad \text{Equation 13}$$

where:

$\phi =$ Average neutron flux [n/cm^2-s]

$\sigma_{Li-7}^{n,n'} =$ Lithium-7 tritium production microscopic cross section [barn]

$N_{Li-7=}$ Lithium-7 atomic number density [atoms/cm^3]

$\sigma_{Li-6}^{n,t} =$ Lithium-6 tritium production microscopic cross section [barn]

$N_{Li-6}^{o} =$ Lithium-6 initial (time=0) number density [atoms/cm^3]

$V_{Core} =$ Volume of Flibe in the core [m^3]

$V_{Loop} =$ Total volume of Flibe in the primary loop [m^3]

$\sigma_{Li-6}^{n,abs} =$ Lithium-6 total neutron absorption microscopic cross section [barn]

$\sigma_{Be-9}^{n,\alpha} =$ Beryllium-9 n,α reaction microscopic cross section [barn]

The volumetric tritium production rate as a function of time can then be calculated according to Equation 14.

$$G'''(t) = \phi\sigma_{Li-7}^{n,n'}N_{Li-7} + \phi\sigma_{Li-6}^{n,t}\left(N_{Li-6}^{o}\exp\left(-\frac{V_{Core}}{V_{Loop}}\phi\sigma_{Li-6}^{n,abs}t\right) + \frac{\phi\sigma_{Be-9}^{n,\alpha}N_{Be-9}}{\phi\sigma_{Li-6}^{n,abs}}\left(1-\exp\left(-\frac{V_{Core}}{V_{Loop}}\phi\sigma_{Li-6}^{n,abs}t\right)\right)\right) \quad \text{Equation 14}$$

The equation requires that accurate 1-group cross sections have been generated, which depend on the average neutron energy spectrum in the core.

3.3 RADIONUCLIDE BEHAVIOR AND RETENTION PROPERTIES OF FUEL

The fuel pebble has three physical barriers to radionuclide release: the TRISO particle fuel kernel, the particle's outer coating layers (i.e., IPyC, SiC, and OPyC), and the fuel pebble carbon matrix. The

TRISO particle is the primary retention medium for fission products in the KP-FHR and the MAR in the fuel particle is held up by the fuel kernel and the three outer coating layers. These layers have varying manufacturing defects and in-service failure fractions that impact their radionuclide retention functions during steady state operations. Table 3-1 provides a list of radionuclides qualitatively assumed to be retained within a TRISO fuel particle under various barrier conditions. The radionuclides that are retained within the TRISO fuel particle will determine the amount of MAR contained in fuel pebbles in lieu of being captured by the Flibe as described in Section 2.3.2.

The fuel particles are divided into three groups for retention or release of radionuclides. The first group includes TRISO particles with intact coating layers that are expected to retain fission products during normal operations. The second group includes TRISO fuel particles where some of the coating layers have failed. If only the IPyC and OPyC layers have failed, most of the fission products will be retained by the remaining intact SiC layer. If the SiC fails and the PyC layers are intact, then mobile metallic fission products will be increasingly released while gaseous fission products will be retained. The third and final group includes TRISO particles where all coating layers have failed. [[

]]

3.3.1 Radionuclide Behavior in Fuel

The chemical form of fission products is important to determining their mobility when a pathway is present for release from the fuel particle. Fission products generated in the fuel kernel react with free carbon and oxygen from the UCO mixture of UO_2 and UC_X (where UC_x can be UC, UC_2 or a mixture of both depending on carbon content and temperature) when uranium fissions. If the kernel has a lack of free oxygen and carbon, then metallic fission products are more likely to be present. If a stable oxide or carbide compound is formed, the diffusion of the fission product can be limited especially at lower operating temperatures. Due to their higher mobility, the volatile fission products are most likely to be released from the TRISO fuel particle when the coating layers are damaged or failed. Fission products have been observed to follow similar trends based on the chemical group in the periodic table due to the valence electron orbital shell. The chemical groups and common group names for elements found in the periodic table are in Table 3-2. These groups are based on valence electrons being partial or filled s, p, d, or f orbital shells. In the periodic table, blocks of elements correspond to these electron shells as noted in Table 3-2.

Thermodynamic calculations were performed for KP-FHR fuel elements to determine the tendency of fission products to take a chemical form at relevant conditions. [[

]]

3.3.2 Selection of Radionuclides

Radionuclides of interest may be produced directly as fission products, indirectly as part of a fission product decay chain, or as activation products. The characteristics that affect the relative importance of radioisotopes and their selection as part of the source term are fission yield or activation cross section, half-life, and mobility.

© 2020 Kairos Power LLC

3.3.2.1 Fission Product Yield Criteria

For fission products, the fission yield directly affects the rate of production within the fuel. For decay chain radioisotopes, the fission yield of the originating fission product and the branching and half-lives along its decay chain affect the production rate. For HALEU fuel the fission yields vary significantly with burnup due to the depletion of U-235 and increasing concentrations of Pu-239 and Pu-241. [[

]]

3.3.2.2 Half Life

Radionuclides with very short half-lives (i.e., seconds to minutes) will decay before they can be transported from their point of origin to a location of concern relative to occupational dose or public safety. Conversely, radionuclides with very long half-lives will have relatively low specific activities and thus may be of lesser radiological importance. However, they could also be released from the fuel element and potentially compete with radioactive elements or precipitate in the salt coolant.

Historically codes used for source term analysis have considered half-life. [[

]]

3.3.2.3 Mobility

Mobility is the ability of a radionuclide to escape the kernel and diffuse through the intact coating layers and the surrounding matrix. The mobility of a radionuclide is affected by its inherent characteristics as well as the physical and chemical form. The mobility of fission products is described by diffusion models of an element through the fuel kernel, coating layers, and matrix.

Radionuclides can remain in elemental form or form chemical compounds, significantly affecting their mobility within the kernel and coating layers. The formation of chemical compounds within the kernels is affected by the thermochemical environment, which varies with burnup in a UCO kernel due to the buildup of fission and decay products and the depletion of oxygen. Gaseous and volatile fission products will most significantly be released from fuel particles with failed coating layers. Fission products that have limited or complete solubility in the fuel crystal lattice or form metallic or oxide precipitates can diffuse through the fuel kernel and be released from failed fuel particles.

3.4 RADIONUCLIDE TRANSPORT IN FUEL

Most radioisotopes significant to source term are produced in the kernels of the coated TRISO particles. Exceptions include recoil fission fragments near the kernel surface that are deposited in the

© 2020 Kairos Power LLC

buffer layer and fission product decay or activation products that may be transported out of the kernel before decaying or being activated by neutron flux. Radioisotopes could also be produced by the fission of dispersed uranium on the OPyC surface and in the carbon matrix.

Transport mechanisms for a given radioisotope are dependent upon the isotope's properties and location of origin. Location could range from near the center of the kernel of an intact TRISO fuel particle to the carbon matrix near the surface of the pebble.

The release fraction of a radioisotope, which is obtained by normalizing its calculated release from the pebble to its calculated inventory, can be affected by decay during transport within the pebble. Therefore, short half-life radioisotopes (i.e., minutes, and seconds) will be eliminated, while the release of intermediate half-life radioisotopes (i.e., hours, and days) will be reduced. Kairos Power uses KP-Bison (described in Reference 4) to model the transport of mobile fission products through a TRISO particle.

3.4.1 Radionuclide Transport Groups in Fuel

Complete sets of diffusivities (i.e., diffusivities in the kernel, coating layers, and matrix) are currently available for four elements (Cs, Sr, Ag, Kr). These elements were the most volatile of the quantifiable elements observed from the fuel in the AGR campaigns. Elements of a class with a representative element are, therefore assumed to be released at the same release fraction as the representative element for that class, as shown in Table 3-3. Several classes of elements do not have representative elements for their diffusion behavior and, as such, are represented by one of the four existing models or are assumed to be completely retained within the TRISO particle or completely released from the particle depending on the element class. For instance, release of iodine and xenon has been historically observed with a behavior similar to krypton. Krypton is therefore representative of iodine and xenon as shown in Table 3-3.

3.4.2 KP-Bison Diffusion Model

In KP-Bison, fission product transport is calculated successively through the TRISO particles and through the fuel element matrix the particles are embedded in. First, transport is calculated for individual fuel particles, assessing diffusion through each coating layer and subsequent potential release into the surrounding matrix in the fuel element. Individual releases then serve as time- and position-dependent fission product sources for fission product transport analysis in the fuel element. [[

]]

[[

]]

In addition to the release from intact or failed (in-service) TRISO particles, the model also includes potential release from as-fabricated defective particles (e.g., exposed kernels or particles with defective coating layers) and from dispersed uranium. [[

]]

[[

]]

3.5 RETENTION OF TRITIUM IN THE GRAPHITE PEBBLE

Tritium contained in the fuel pebbles is expected to be a low off-site dose contributor and thus the release rates may be treated conservatively in analyses to demonstrate minimal contributions to dose. Release rates using structural temperatures from the primary system will be used to estimate the depletion of tritium from pebbles after shutdown by using Equation 18.

$$\frac{T_{2,Surf}}{K_{H,T_2}} = \left(\frac{T_{d,g(R_{pebble})}}{K_{S,g}}\right)^2 \qquad \text{Equation 18}$$

where, $T_{2,Surf}$ is the Flibe tritium concentration at the surface of the pebble, K_{H,T_2} is the Henry's law coefficient for T_2 in Flibe, $T_{d,g(R_{pebble})}$ is the graphite tritium concentration at the surface of the pebble, and $K_{S,g}$ is the tritium solubility in graphite. These methods calculate holdup and release of tritium in graphite pebbles.

The time-dependent uptake of tritium into the reactor vessel reflector graphite and graphite moderator pebbles in the core accounts for pebble recirculation. In the model there is no distinction between a fuel pebble and a moderator pebble, and all graphite is considered to be IG-110 grade material. Measurements applicable to the KP-FHR graphite grade are being made under NSUF RTE Project 2840. The concentration of tritium fluoride (TF) and T_2 is determined for each "node" in the reactor loop where the first node is the inlet of the reactor core. Concentrations are then updated for each time step in the simulation. Inside of the core, tritium concentration in the salt increases based on the tritium generation in each node and decreases according to a calculation for tritium retention in graphite.

The tritium retention calculation first requires a mass transfer coefficient to represent tritium transit from the salt bulk to the graphite pebble surface. The mass transfer coefficient is based primarily on the Reynolds (Re) and Schmidt (Sc) non-dimensional numbers in the core. As shown in Equation 19, the Reynolds number for a random packed bed of uniform spheres depends on the pebble diameter d_{pebble} and packing fraction PF, as well as the density and viscosity of the salt – ρ and μ, respectively. The Reynolds number also uses the superficial velocity of salt flow in the core as defined in Equation 20, where $\dot{V}$ is the total volumetric flow rate of salt through the core and $A_{CX,Core}$ is the cross-sectional area available flow through the pebble bed. In Equation 21, the Schmidt number is defined based on the ratio of salt viscosity to the product of density and diffusivity of T_2 in Flibe. The Reynolds and Schmidt numbers are converted to a Sherwood number in Equation 22, which is a correlation for a packed bed of uniform spheres valid for Reynolds numbers between 22 and 8000. Equation 22 was originally

reported as a heat transfer coefficient for a packed bed (Reference 20), but is converted to a mass transfer correlation here assuming that the Sherwood number is analogous to the Nusselt and the Schmidt number is similar to the Prandtl number. The resulting Sherwood number is converted to the mass transfer coefficient for tritium retention in pebbles, $k_{T2,Core}$, as shown in Equation 23. Since the Reynolds and Schmidt numbers have temperature-dependent properties as inputs, the numbers are calculated at each node to account for temperature changes around the reactor loop.

$$Re_{Core} = \frac{\rho v_s d_{pebble}}{\mu PF} \quad \text{Equation 19}$$

$$v_s = \dot{V}/A_{CX,Core} \quad \text{Equation 20}$$

$$Sc_{Core} = \frac{\mu}{\rho D_{T_2}} \quad \text{Equation 21}$$

$$Sh_{Core} = \left(0.5Re^{1/2} + 0.2Re^{2/3}\right)Sc^{1/3} \quad \text{Equation 22}$$

$$k_{T2,Core} = Sh_{Core} D_{T2}/d_{pebble} \quad \text{Equation 23}$$

Tritium uptake in graphite is only calculated for T_2 in the salt. Any TF present in the core is assumed to have no interaction with graphite. This assumption is based on tritium chemical analysis from graphite samples tested in the Massachusetts Institute of Technology (MIT) fluoride salt irradiation experiments, which found only about 2% of total tritium retained in graphite samples was soluble in water, which could be explained by either TF or HTO (Reference 21). With reducing salt conditions, the majority of tritium is present as T_2 and thus neglecting interactions between TF and graphite does not have a significant impact on the tritium distribution in the reactor.

With a mass transfer coefficient determined, the flux of T_2 to the graphite pebbles, $j_{Core,T2}$, can be calculated according to Equation 24. The resulting flux depends on the difference between the T_2 concentration in the bulk fluid and the T_2 concentration in contact with the graphite surface, $T_{2,Core}$ and $T_{2,Surf}$, respectively. At the interface, the salt and graphite are both exposed to the same partial pressure of T_2 and each material surface is assumed to be at an equilibrium condition. For the salt surface, Henry's law applies and thus the concentration can be related to the T_2 partial pressure according to Equation 65. Solubility of hydrogen in graphite has been observed to follow Sievert's law, where the equilibrium concentration in graphite depends on the square root of the charging gas pressure (Reference 26 and Reference 27). Sievert's law is shown in Equation 25, where c_T is the concentration of tritium in graphite, K_S is the Sievert's law coefficient, and p_{T2} is the partial pressure of tritium in the gas phase. By rearranging Equation 65 and Equation 25 to solve for partial pressure tritium concentration at each side of the salt/graphite interface can be related as shown in Equation 26. While the flux of tritium from the salt to graphite must be continuous across the surface, the tritium concentration can change significantly because of differences between the Henry's law coefficient for T_2 in Flibe and the Sievert's law coefficient for tritium solubility in graphite. A graphical representation of the tritium concentration profiles in the salt and graphite pebbles is shown in Figure 3-1 which also explains the concentration relationship used for Equation 26.

© 2020 Kairos Power LLC

$$j_{Core,T_2} = k_{T2,Core}\left(T_{2,Core} - T_{2,Surf}\right) \quad \text{Equation 24}$$

$$c_T = K_S\sqrt{p_{T_2}} \;\rightarrow\; p_{T_2} = (c_T/K_S)^2 \quad \text{Equation 25}$$

$$T_{2,Surf}/K_{H,T_2} = \left(T_{d,g}(R_{pebble})/K_{S,g}\right)^2 \quad \text{Equation 26}$$

Each axial node consists of a pebble group with the same tritium retention characteristics and tritium concentration profiles. The total amount of tritium transferred into graphite at each node is the flux as calculated in Equation 24 times the total surface area of pebbles in each node, A_{node}. Similarly, each pebble inside the node is assumed to be exposed to the same salt concentration of T_2 at the pebble surfaces. When calculating the concentration gradient in the salt, the only input provided is the T_2 concentration at the beginning of the node. The change in T_2 concentration with respect to axial height is shown in Equation 27, where G'(z) is the linear tritium production rate in the core and $\Delta A/\Delta Z$ is the amount of pebble surface area per height in the core. When z is in units of axial nodes, $\Delta A/\Delta Z$ is the surface area of pebbles per node, or A_{node}.

$$\frac{dT_2(z)}{dz} = \left(G'(z) - j_{Core,T_2}(\Delta A/\Delta Z)\right)/\dot{V} \quad \text{Equation 27}$$

After substituting in Equation 23 for T_2 flux, replacing the term $k_{Core,T2}\,A_{node}/\dot{V}$ with λ for simplicity, rearranging, and integrating over z, Equation 27 becomes:

$$\int\left(\exp(\lambda z)\frac{dT_2(z)}{dz} + \exp(\lambda z)\left(\lambda T_2(z)\right)\right)dz = \int \exp(\lambda z)\left(G'(z)/\dot{V} + \lambda T_{2,Surf}(z)\right)dz \quad \text{Equation 28}$$

Considering the term on the right side, G'(z) and $T_{2,Surf}$ are defined to be constant throughout the node. The tritium generation rate per node is a defined quantity and is uniform throughout the core in the baseline case. A portion of the total tritium generation per node is converted to T_2 and referred to as $G_{T2,node}$. In true reactor conditions, the individual pebbles in the node could be exposed to a different salt surface T_2 concentration. However, the calculation is defined such that all pebbles in each node share the same $T_{2,Surf}$. A nonlinear solver searches for the most appropriate $T_{2,Surf}$ to use as the average for the node. Integrating Equation 28 then results in Equation 29 for the salt T_2 concentration throughout the node.

$$\mathrm{T_2(z)} = \frac{\mathrm{G_{T_2,node}}}{\dot{\mathrm{V}}\lambda} + \mathrm{T_{2,Surf}} + \mathrm{C}\cdot\exp(-\lambda \mathrm{z}) \quad \text{Equation 29}$$

The constant from integration, C, is fixed by solving the equation at the beginning of the node, where z=0 and the T_2 concentration is known (T_2^N). Solving for the z=0 boundary condition results in Equation 30.

© 2020 Kairos Power LLC

$$T_2(z)=T_2^N\exp(-\lambda z)+\left(\frac{G_{T_2,node}}{\dot{V}\lambda}+T_{2,Surf}\right)\left(1-\exp(-\lambda z)\right) \quad \text{Equation 30}$$

Lastly, the average T_2 concentration across the node is determined by integrating z from node zero to node one and dividing by one node. The mesh notation, concentration averages, and tritium sources and losses for the core nodes are shown in Figure 3-2.

$$T_{2,Avg}-T_{2,Surf}=\left(\frac{G_{T_2,node}}{\dot{V}\lambda^2}-\frac{\left(T_2^N-T_{2,Surf}\right)}{\lambda}\right)\exp(-\lambda)+\frac{\left(T_2^N-T_{2,Surf}+\frac{G_{T_2,node}}{\dot{V}}\right)}{\lambda}-\frac{G_{T_2,node}}{\dot{V}\lambda^2} \quad \text{Equation 31}$$

Calculating the average tritium concentration between the concentration nodes in the core results in a more accurate flux of tritium into the graphite pebbles at each axial location. Once arriving at the graphite surface, tritium transport within the pebbles is simulated with a series of transport and trapping equations. In this treatment, tritium is separated into weakly trapped tritium which is able to diffuse in the graphite bulk and strongly trapped tritium which is no longer mobile (Reference 22). Weak trapping sites can be physically interpreted as dangling carbon bonds at graphite crystallite edges, while strong traps are interstitial loop sites or point defects within crystallites (Reference 23). For both weak and strong trapping sites, the retention mechanism is believed to be dissociative and therefore tritium entering the graphite as T_2 will be retained as atomic tritium (Reference 24).

The transport equation for the weakly trapped tritium is shown in Equation 32 where T_d indicates the diffusing tritium in graphite and $D_{T,g}$ is the diffusion coefficient in graphite. Equation 32 can be interpreted as Fick's second law of diffusion with the addition of a trapping term, which converts the diffusing tritium to trapped tritium as denoted by T_t. The trapped tritium rate of change is solved with Equation 33, where C_{T0} is the total concentration of strong traps in the material, Σ_d is the desorption rate constant and Σ_t is the trapping rate constant. As the strong trapping sites within the graphite fill up during the simulation, the $(C_{T0}-T_t)/C_{T0}$ term approaches zero and the rate of trapping decreases. This term is normalized by C_{T0} in order to keep both rate constants Σ_d and Σ_t in units of s^{-1}. The boundary condition applied at the beginning of each time step is shown in Equation 34 which sets the tritium flux at the graphite surface as twice the flux of T_2 from the salt. Inside the pebble, the flux of atomic tritium is calculated using Fick's law with a first-order radial derivative of the first and second outermost values of diffusing tritium, $T_{d,g}{}^0$ and $T_{d,g}{}^{0\text{-}1}$, and the outer mesh spacing, ΔR_o. The trapped tritium is updated at the end of each time step, therefore Equation 34 is only calculated with the gradient of diffusing tritium.

$$\frac{\partial T_d(x,t)}{\partial t}=\nabla\cdot\left(D_{T,g}\,\nabla T_d(x,t)\right)-\frac{\partial T_t(x,t)}{\partial t} \quad \text{Equation 32}$$

$$\frac{\partial T_t(x,t)}{\partial t}=\Sigma_t\,T_d(x,t)\left(C_{T_0}-T_t(x,t)\right)/C_{T_0}-\Sigma_d T_t(x,t) \quad \text{Equation 33}$$

$$2\cdot j_{Core,T_2}=D_{T,g}/\Delta R_o\left(T_{d,g}^{o}-T_{d,g}^{o-1}\right) \quad \text{Equation 34}$$

As shown inFigure 3-2 and Equation 26, the tritium concentration at the graphite surface relates to the T_2 concentration at the interface in the salt phase. The T_2 surface concentration is used to determine the concentration gradient in the salt and ultimately the flux of tritium into the graphite. However, the interconnection between these variables requires that the equations be solved simultaneously. Four variables are calculated by a nonlinear solver at each axial node in the core: T_2 flux to core pebbles ($j_{Core,T2}$), outer surface tritium concentration in graphite ($T_{d,g}(R_{pebble})$), salt surface T_2 concentration ($T_{2,Surf}$), and average T_2 salt concentration in the node ($T_{2,Avg}$). These variables are determined through minimizing the 4-element matrix shown in Equation 35. Once all variables are calculated, the T_2 concentration at the next node in the core can be found with Equation 36. This procedure repeats for each axial node until the T_2 concentration at the top of the core is calculated.

$$\begin{bmatrix} Calculation\ of\ salt\ T_2\ flux: \\ Conservation\ of\ tritium\ flux: \\ Henry's\ and\ Sievert's\ law\ equilibrium: \\ Calculation\ of\ average\ T_2\ concentration: \end{bmatrix} \begin{matrix} \text{Equation 24} \\ \text{Equation 34} \\ \text{Equation 26} \\ \text{Equation 31} \end{matrix} \qquad \text{Equation 35}$$

$$T_2^{N+1} = \left(T_2^N \dot{V} + G_{T_2,node} - j_{Core,T_2} A_{node}\right)/\dot{V} \qquad \text{Equation 36}$$

For a core of static graphite pebbles, tritium retention will eventually drop to zero as the diffusing and trapped tritium builds up and the salt/graphite boundary condition limits the T_2 flux. The calculation removes tritium through circulation and desorption of the fuel pebbles. In this case, the equilibrium tritium retention rate in the core will be equal to the removal rate in the pebble circulation system. The amount of desorbed tritium depends on the design temperature and holding time each pebble experiences in the recirculation system.

An example calculation is shown below to demonstrate the procedure for calculating removal assuming complete desorption of tritium.

Since graphite fuel pebbles will float in the KP-FHR core, the pebbles would be removed from the top of the core, partially desorbed, and re-inserted into the core bottom. The amount of tritium removal from the top of the core is calculated at each time step as shown in Equation 37, which is the volume integral of the average tritium concentration of the top node pebbles times the pebble recirculation rate. The recirculation rate is the total number of pebbles, $N_{pebbles}$, divided by the pebble residence time in the core, τ.

$$Removal\ \left[\frac{mol}{s}\right] = \frac{N_{pebbles}}{\tau} \int \left({T_{d,g}}^{N_{Core}}(r) + {T_{t,g}}^{N_{Core}}(r)\right) dV \qquad \text{Equation 37}$$

For the rest of the nodes except the top of the core, the circulation of pebbles is simulated by subtracting a portion of the tritium concentration profile from each node and adding it to the next adjacent node, as illustrated in Equation 38 and Equation 39, where Δt is the time step of the model.

Since the number of pebbles in each axial node is $N_{pebbles}/(N_{Core}-1)$ and the number of pebbles leaving a node in each time step is $N_{pebbles}\Delta t/\tau$, the fraction of pebbles leaving the node is $(N_{Core}-1)\Delta t/\tau$. Therefore, the $(N_{Core}-1)\Delta t/\tau$ term is used to calculate the fraction of circulating tritium in each time step as shown in Equation 38 and Equation 39. For complete desorption of pebbles, these equations would be repeated for the strongly trapped tritium, $T_{t,g}$.

$$T_{d,g}{}^{N}(r) = T_{d,g}{}^{N}(r) - (\mathrm{N_{Core}} - 1)(\Delta t/\tau)T_{d,g}{}^{N}(r) \quad \text{Equation 38}$$

$$T_{d,g}{}^{N+1}(r) = T_{d,g}{}^{N+1}(r) + (\mathrm{N_{Core}} - 1)(\Delta t/\tau)T_{d,g}{}^{N}(r) \quad \text{Equation 39}$$

© 2020 Kairos Power LLC

Table 3-1 Functional Containment of TRISO Outer Coating Layers With Qualitative Impact on Fission Product Release

State of the Coating Layer			Impact on Fission Product Release
IPyC	**SiC**	**OPyC**	
Intact	Intact	Intact	Marginal release of Ce, Cs, Eu, Sr
Intact	Intact	Compromised	Marginal release of Ce, Cs, Eu, Sr
Intact	Compromised	Intact	Increased fission product release; Significant Cs release
Intact	Compromised	Compromised	Increased fission product release; Significant Cs release
Compromised	Intact	Intact	Marginal release of Ce, Cs, Eu, Sr
Compromised	Intact	Compromised	Marginal release of Ce, Cs, Eu, Sr
Compromised	Compromised	Intact	Increased fission product release; Significant Cs release
Compromised	Compromised	Compromised	Increased fission product release; Significant Cs release

© 2020 Kairos Power LLC

Table 3-2 Periodic Table of Chemical Groups, Valence Electron Orbital Shell, and Elements

Formal Chemical Group	Common Name Chemical Group	Sub-group Common Name	Valence Electron Orbital Shell	Elements
1	Alkali Metals	---	s-block	Li, Na, K, Rb, Cs, Fr
2	Alkali Earth Metals	---	s-block	Be, Mg, Ca, Sr, Ba, Ra
3-12	Transition Metals	---	d-block	Sc, Y, Fe, Co, Ni, Zn, Cd
4-7	---	Refractory Metals	d-block	Ti, Zr, Hf, V, Nb, Ta, Cr, Mo, W, Mn, Tc, Re
8-12	---	Noble Metals	d-block	Ru, Os, Rh, Ir, Pd, Pt, Cu, Ag, Au, Hg
---	Lanthanides	---	f-block	La, Ce, Pr, Nd, Pm, Sm, Eu, Gd, Tb, Dy, Ho, Er, Tm, Yb, Lu
---	Actinides	---	f-block	Ac, Th, Pa, U, Np, Pu, Am, Cm, Bk Cf
13-17	Post-Transition Metals	---	p-block	Al, Ga, In, Tl, Ge, Sn, Pb, Sb, Bi, Po, At
13-16	Metalloids	---	p-block	B, Si, Ge, As, Sb, Te
14-16	Non-metals	---	p-block	H, C, N, P, O, S, Se
16	Chalcogen	---	p-block	O, S, Se, Te, Po
17	Halogen	---	p-block	F, Cl, Br, I, At
18	Noble Gases	---	p-block	He, Ne, Ar, Kr, Xe, Rn

© 2020 Kairos Power LLC

[[

]]

Table 3-4 AGR In-Service Failure Fractions

In-Service Failure	95% Confidence Fraction
Irradiation – TRISO Failure	$\leq 2.3 \times 10^{-5}$
Irradiation – SiC Failure[(a)]	$\leq 3.6 \times 10^{-5}$
1600°C Safety Testing – TRISO Failure	$\leq 6.6 \times 10^{-5}$
1600°C Safety Testing – SiC Failure[(a)]	$\leq 1.7 \times 10^{-4}$

(a) Historically there is no specification on SiC failure fraction; SiC failure fraction is higher than overall TRISO failure fraction. However, "TRISO failure" implies all three layers, so a portion of the SiC failures are included.

© 2020 Kairos Power LLC

Table 3-5 Diffusion Coefficients for Selected Radionuclides

	D_1 (m^2/s)	Q_1 (kJ/mol)	D_2 (m^2/s)	Q_2 (kJ/mol)
Cesium				
Kernel	$5.6x10^{-8}$	209	$5.2x10^{-4}$	362
Buffer & Buffer-IPyC Gap	10^{-8}	0	---	---
PyC	$6.3x10^{-8}$	222	---	---
SiC	$5.5x10^{-14} \times e^{1.1\phi/5}$ where ϕ is the fast neutron fluence ($x10^{25}$ n/m^2, $E_0 > 0.18$ MeV	125	$1.6x10^{-2}$	514
Matrix	$3.6x10^{-4}$	189	---	---
Strontium				
Kernel	$2.2x10^{-3}$	488	---	---
Buffer & Buffer-IPyC Gap	10^{-8}	0	---	---
PyC	$2.3x10^{-6}$	197	---	---
SiC	$1.2x10^{-9}$	205	$1.8x10^{6}$	791
Matrix	$1.0x10^{-2}$	303	---	---
Silver				
Kernel	$6.7x10^{-9}$	165	---	---
Buffer & Buffer-IPyC Gap	10^{-8}	0	---	---
PyC	$5.3x10^{-9}$	154	---	---
SiC	$3.6x10^{-9}$	215	---	---
Matrix	1.6	258	---	---
Krypton (Iodine, Xenon)				
Kernel (Normal Operation)	$1.3x10^{-12}$	126	---	---
Kernel (Accident)	$8.8x10^{-15}$	54	$6.0x10^{-1}$	480
Buffer & Buffer-IPyC Gap	10^{-8}	0	---	---
PyC	$2.9x10^{-8}$	291	$2.0x10^{5}$	923
SiC ($T > 1625.9$ K)	$3.7x10^{1}$	657	---	---
SiC ($T \leq 1625.9$ K)	$8.6x10^{-10}$	326	---	---
Matrix	$6.0x10^{-6}$	0	---	---

© 2020 Kairos Power LLC

Figure 3-1 Representation for T_2 Mass Transfer From Flibe to Graphite Pebble.

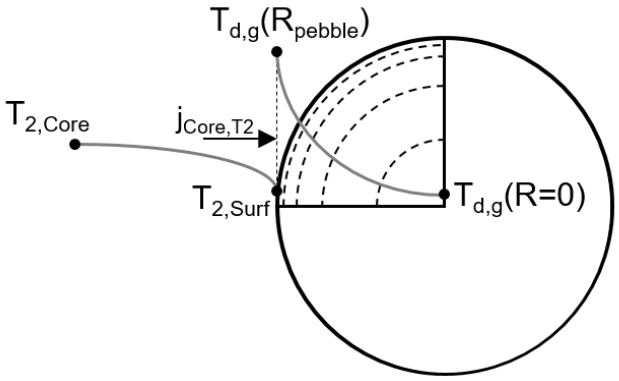

Figure 3-2 Notation for Tritium Gains and Losses Between Nodes

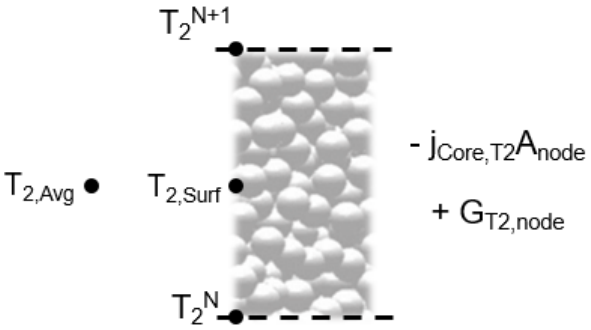

4 EVALUATING FLIBE RETENTION OF RADIONCULIDES

4.1 IMPORTANT SOURCE TERM PHENOMENA IDENTIFIED FOR FLIBE

There are two sets of phenomena that are relevant to the source term methodology for fission product retention in Flibe: phenomena associated with events involving an intact reactor coolant boundary; and phenomena associated with events involving a compromised reactor coolant boundary (a leak or rupture of external parts of the coolant boundary).

4.1.1 Phenomena for Flibe with Intact Reactor Coolant Boundary

The following phenomena from the source term PIRT described in Section 2.4 are coolant-related source term phenomena associated with an intact reactor coolant boundary that are identified in Table 2-2 as having a high or medium importance to safety:

- [[

]]

An additional phenomenon identified outside of the PIRT process was [[

]]

4.1.2 Phenomena for Flibe with Compromised Reactor Coolant Boundary

The following phenomena from the source term PIRT described in Section 2.4 are coolant-related source term phenomena associated with a compromised reactor coolant boundary that are identified in Table 2-3 as having a high or medium importance to safety:

- [[

]]

- [[

]]

4.2 SOURCES OF RADIONUCLIDES IN FLIBE

The MAR in Flibe include radionuclides born in the Flibe as well as radionuclides that are transferred to the Flibe from other media (e.g., fuel). The circulating activity of the Flibe is expected to be controlled by operating limits for the KP-FHR as discussed in Section 2.3.4. The operational limits on circulating activity will be provided in future licensing application submittals. The circulating activity operational limits will be consistent with the initial conditions assumed in design basis accident source term evaluations for the KP-FHR that require a quantification of MAR in the Flibe.

The radionuclides that are born within the Flibe are formed via nuclear reactions with the Flibe and impurities that are subjected to the radiation field in the reactor core. Radionuclides born in the Flibe include:

- Tritium (neutron reactions with ^{6}Li, ^{7}Li, ^{9}Be, and ^{19}F in the Flibe)
- Fission products, activation products and transmutation products from:
  - Flibe impurities such as natural uranium and thorium
  - Dispersed uranium migrated from the pebbles into the Flibe

Radionuclides that transfer into the Flibe come from other media in contact with the coolant, including the fuel and structural materials. Radionuclides transferred into the Flibe include:

- Fission product diffusion into the Flibe from the fuel,
- Tritium gas release from graphite structures and pebbles at high temperature, and,

© 2020 Kairos Power LLC

- Corrosion products absorbed in the coolant that can become activated in the reactor core.

The five high-level categories of radionuclides in the Flibe are:

- oxides,
- noble metals (further subdivided into low- and high-volatility noble metals),
- gases (i.e., tritium and noble gases),
- salt-soluble compounds.

The design of the KP-FHR is expected to include a chemistry control system that will include design features to remove a fraction of the suspended phase separated radionuclide elements, including oxides and noble metals, from the primary loop (consistent with the design information discussed in Section 2.3.4). The remaining phase separated materials will be suspended in the flowing Flibe. The removal features are assumed to process only a small fraction of the total primary system flow to remove phase separated radionuclides while the remaining vast majority of the coolant flow continues to the intermediate heat exchanger (IHX). This removal pathway is assumed to remove the phase separated radionuclides that flow through the cleanup system. Natural deposition of these materials will also contribute to the overall system removal rate to a smaller extent.

Other MAR are expected to come out of the Flibe and be transferred into the cover gas at steady state conditions. The high-volatility noble metals, such as cadmium, may also be vaporized from the pool surface. These processes assure that low concentrations of noble metal fission products will be present in the Flibe at the initiation of the transient. The noble gases and tritium are expected to saturate in the Flibe, therefore under equilibrium conditions they will be removed from the Flibe MAR inventory at the rate they are generated.

All other radionuclides will form salt-soluble compounds and be predominantly retained in the reactor coolant under steady state conditions.

4.3 RADIONUCLIDE TRANSPORT IN FLIBE

4.3.1 Radionuclides Transport Groups in Flibe

Grouping Radionuclides by Redox Reactions with Flibe

Radionuclides are sorted by their chemical behavior in the molten Flibe environment. This chemical sorting separates radionuclide elements into representative groups that transport together. This section describes the thermodynamic basis for the grouping of radionuclides in molten Flibe. These grouping processes and their relation to RFs of radionuclide elements in the Flibe barrier are shown schematically in Figure 4-1.

Independent of their origin, radionuclide elements in the Flibe either form insoluble phases that do not chemically interact with the reactor coolant, or form compounds that are soluble in the molten Flibe. Therefore, chemical behavior sorts radionuclides elements into two groups: those that remain phase-separated, and those that dissolve into the molten Flibe.

© 2020 Kairos Power LLC

The RF of radionuclide elements that form salt soluble species is determined by their concentration in the molten Flibe solution and by the vapor pressure of their representative chemical species.

Phase separated radionuclide elements that are within the Flibe coolant exist within the reactor coolant barrier in steady-state despite being phase separated as they are expected to transport with the Flibe via entrainment or other mechanisms. However, after the initiation of a transient, the release of radionuclide groups that are phase-separated from the Flibe, such as gases or solids, is not inhibited by the barrier. Phase separated radionuclide elements have an RF determined by the vapor pressure of their representative pure species with unit chemical activity (defined below).

Radionuclide gases are released as gases after reaching saturation in the Flibe.

The principle pathway for radionuclides to partition into the Flibe solution is through redox reactions to form cations, becoming salt-soluble metal fluorides via Equation 40 below.

$$M + nF^- \rightarrow MF_n + ne^- \qquad \text{Equation 40}$$

where:

M = a pure element in its reduced form

n = the number of electrons per equivalent in the electrochemical reaction.

If Equation 40 occurs spontaneously, a radionuclide metal will react to form a salt-soluble fluoride. In this case, the RF of the Flibe barrier is derived from the vapor pressure of the representative species for the salt soluble group on account of the unstable elemental phase, *M*, in the system. Alternatively, if the reaction does not occur spontaneously, the RF of the Flibe barrier is determined by the vapor pressure of the representative noble metal element because the element, *M*, is stable in the metallic form and Equation 40 results in a negligible quantity of the metal fluoride.

Each oxidation reaction is characterized by a Gibbs Free Energy of formation (ΔG) value, which is a measure of the spontaneity of the reaction under a given set of conditions. The ΔG of numerous fluorides is provided in databases of thermodynamic properties of material (See discussion of limitations in Section 8.2). These free energies are related to an electrochemical potential (E^0) via Equation 41.

$$\Delta G = -nFE^0 \qquad \text{Equation 41}$$

where:

F = Faraday's constant (96.485 kJ/V-mole)

E^0 = standard reduction potential of the element.

The redox potential of the system, E, can be related to the activities of potential-controlling species via the Nernst equation shown as Equation 42.

© 2020 Kairos Power LLC

$$E = E^0 - \frac{RT}{nF} ln \frac{a_{red}}{a_{ox}}$$ Equation 42

where:

R = the gas constant (0.008314 kJ/mole).

T = the temperature in Kelvin.

a_{red} = the chemical activity of the reduced species, which is defined as $a_{red} = \gamma_{red}[Red]$ where γ_{red} and $[Red]$ are activity coefficient and concentration of the reduced species, respectively.

a_{ox} = the chemical activity of the oxidized species, which is defined as $a_{ox} = \gamma_{ox}[Ox]$ where γ_{ox} and $[Ox]$ are activity coefficient and concentration of the oxidized species, respectively.

The chemical activity of a species, a_i, is further defined by Equation 43.

$$a_i = \gamma_i[i] = \frac{p_i}{p_i^0}$$ Equation 43

where, γ_i is the activity coefficient, $[i]$ is the mole fraction, p_i is the vapor pressure of the species in solution, and p_i^0 is the vapor pressure of the pure species (also referred to as saturated vapor pressure).
[[

]]

$$K = \frac{a_{ox}}{a_{red}} = e^{\left(\frac{nF(E-E^0)}{RT}\right)}$$ Equation 44

These reduced-state elements are metals or gases. The activity for a solid metal (a_{red}) is defined as unity ($a_{red} = 1$), so in the case of a radionuclide, Equation 44 reduces to:

$$K = a_{ox} = e^{\left(\frac{nF(E-E^0)}{RT}\right)}$$ Equation 45

[[

]]

a_{ox} represents the "equilibrium chemical activity" of the metal fluoride, and is equivalent to the equilibrium constant of the metal fluoride in equilibrium with unit activity of its metal according to Equation 45. The fraction of a radionuclide that will form either metallic (insoluble) or fluoride (salt-soluble) phases is assumed to be related to this equilibrium chemical activity of the radionuclide fluoride.

Metallic phases are insoluble in Flibe but are expected to transport with the reactor coolant via entrainment or other mechanisms. Elements that exhibit equilibrium chemical activities of their fluorides less than 10^{-6} under the most oxidizing conditions considered ($E_{Flibe} = Cr^{2+}|Cr$) are assumed to remain in reduced chemical states under all possible Flibe redox conditions of the KP-FHR. (consistent with design features provided in Section 2.3.4). If these metals are released from the fuel, they are

© 2020 Kairos Power LLC

expected to transport as a suspension of metallic particles before plating out on solid materials. This behavior was observed in the MSRE (Reference 20 and Reference 21). These metals may also be removed from the system through filtration in the chemistry control system. The Flibe barrier RFs for these elements is conservatively governed by the vapor pressure of a high volatility noble metal for the respective radionuclide group. The source term treatment of the radionuclides that will remain as metals is restricted to the vapor pressure of the pure elemental (metallic) phases, since the quantities that will oxidize are negligible. The vapor pressure of pure elements is documented in References 32 and 33. The equilibrium vapor pressure of these noble metal radionuclides are used in Section 4.3.2.4 to evaluate their respective vapor pressures above molten Flibe solutions.

Chemically reactive radionuclides that react with beryllium fluoride to form their respective fluorides and beryllium metal are sorted as salt-soluble radionuclides. These elements exhibit more cathodic potentials than $Be^{2+}|Be$, and as a result, the activities of the oxidized phases are greater than unity over the range of Flibe redox potentials for the KP-FHR. The radionuclides that form salt-soluble fluorides will dissolve into the reactor coolant and take on the physical properties of the melt. These dissolved radionuclides are contained within the Flibe. The Flibe barrier RFs applied to radionuclides that form salt-soluble fluorides are derived from their volatility as components of the Flibe solution. The thermodynamics of evaporation of radionuclide phases from Flibe solutions is presented in 4.3.2.2**.**

Chemical activities of radionuclides in their metal fluoride states are calculated by Equation 45 using the two Flibe redox potentials in Table 4-1 This process, shown schematically in Figure 4-1, organizes radionuclides into three groups: (1) those that remain in their reduced phase (noble metals), (2) those that will oxidize to become metal fluorides (salt-soluble fluorides), and (3) those that will have a distribution between oxidized and reduced forms dependent upon the redox condition of the Flibe (redox-dependent elements). The distinction between noble elements and redox-dependent elements is [[

]] The equilibrium between these phases depends on the redox potential of the Flibe, favoring the salt-insoluble elemental phases under reducing conditions, versus favoring salt-soluble fluorides under oxidizing conditions. Elements that have chemical activity of oxidized species greater than 1 are expected to completely oxidize to form salt-soluble fluorides on contact with Flibe and are sorted as salt-soluble. Radionuclide elements that are determined to be redox dependent are analyzed under bounding chemical conditions in which their inventory is considered all oxidized or all reduced. For example, if a radionuclide fluoride is highly volatile, then the Flibe redox potential is assumed to be oxidizing to maximize the quantity of the radionuclide that forms the mobile phase. This approach is conservative and does not credit the functions of the chemistry control system, as the Flibe redox condition is varied between its bounding oxidizing and reducing conditions in the evaluation.

[[

]]

[[

]]

Grouping of Radionuclide Elements by Exchange Reactions with Flibe

The chemical state of the radionuclides prior to contacting molten Flibe may affect their behavior while in contact with molten Flibe. In the TRISO fuel, fission products more chemically reactive than molybdenum (Mo) are assumed to form oxides and carbides, while elements more noble than Mo are likely to exist in their elemental phases. To account for these effects, the exchange reactions between the active radionuclide oxides and beryllium fluoride, shown as Equation 46, are analyzed. Reactions with LiF are not analyzed because BeO and LiF are more stable than Li_2O and BeF_2. Similarly, BeO is more stable than Be_2C. Therefore, all radionuclides are conservatively treated as oxides, and not carbides.

$$M_xO_y + yBeF_2 \rightarrow xMF_{\left(\frac{2y}{x}\right)} + yBeO \qquad \text{Equation 46}$$

The ΔG and equilibrium constant of radionuclide oxides that react with BeF_2 are evaluated using thermodynamic properties of the relative species. Elements that result in negative free energies in Equation 47 go through exchange reactions with molten Flibe to form salt-soluble fluorides and BeO, while elements that result in positive free energies in Equation 47 will remain as salt-insoluble oxides.

The equilibrium constant, K, is related to ΔG by:

$$\mathrm{K} = e^{\left(\frac{-\Delta G}{RT}\right)} \qquad \text{Equation 47}$$

where, *R* is the universal gas constant.

The equilibrium constant determines the distribution of reactants and products in a given chemical reaction. For example, the amount of uranium oxide that reacts with Flibe at equilibrium according to:

$$UO_2 + 2BeF_2 \rightarrow UF_4 + 2BeO \quad \Delta G = -14.638\ kJ/mole \qquad \text{Equation 48}$$

is described by the following equilibrium equation:

$$\mathrm{K} = e^{\left(\frac{-14.638}{0.00834\times 923}\right)} = 0.15 = \frac{a_{UF4} * {a_{BeO}}^2}{a_{UO2} * {a_{BeF2}}^2}$$ Equation 49

where $a_{species}$ denotes the chemical activities of the indicated reaction species.

Elements that result in positive free energies in Equation 47 are grouped as oxides as they are anticipated to remain as insoluble oxides upon contacting Flibe. [[

]]

Where specific data is not available, bounding assumptions are applied to elements that do not exhibit favorable exchange reactions, and to those elements for which the equilibrium constant determined by Equation 49 does not deviate significantly from unity. The bounding assumptions are verified using dose at the site boundary as the figure of merit. Elements more noble than Mo are expected to exist as metals in the TRISO fuel, so their chemical behavior follows predictions formed via chemical analysis of their pure metallic state (Reference 32).

[[

]]

Summary of Radionuclide Grouping for Transport in Flibe

Table 4-2 presents the radionuclide transport groups for the circulating activity in the Flibe. The methodology used to group the radionuclide elements is shown schematically in Figure 4-1. A thermodynamic study predicts whether each radionuclide will chemically react with the Flibe through various mechanisms as described in this section. This study informs the grouping of radionuclides in Table 4-2

4.3.2 Quantification of Release Fractions for Flibe

Radionuclide escape from the Flibe barrier will occur through either vaporization of the radionuclide chemical species, or aerosolization of the bulk reactor coolant. Vaporization is driven by the relevant thermodynamic processes associated with the radionuclide group of interest, the solution in which they are dissolved, and the properties of the gas phase that they are evaporating into. These processes are covered in the subsections below. The methodology covering aerosolization processes related to the KP-FHR is provided in Section 7.

Evaluation of radionuclide vapor transport out of the reactor coolant involves the chemical equilibria of numerous radionuclides exchanging in both condensed and vapor phases. Radionuclides in the Flibe can be mobilized through a series of potential pathways, and each is treated separately. The

following subsections discuss the chemical behavior of cesium halides in Flibe to illustrate the methodology. Cesium is used for the illustration because it is the representative element for the salt soluble fluoride group of radionuclides described in Table 4-2 The calculations and associated data provided in this illustration of the methodology are not intended to represent design-specific results of the KP-FHR source term analysis.

Following dissolution into the molten Flibe, radionuclides can undergo a variety of liquid-phase chemical reactions. The quantity of a radionuclide that forms a given chemical species determines the chemical activity of that species in the molten solution. For example, the chemical activity of cesium iodide (CsI) will depend upon the relative concentrations of Cs^+ and I^- in the solution, their initial chemical bonding states, and how likely they are to react to form molecular CsI. Section 4.3.2.1 describes methods to assess the chemical activity of radionuclide species in the reactor coolant. These methods take the total number of radionuclide atoms in the reactor system as input and apply thermodynamic free energy minimization models to evaluate the quantity of each radionuclide species that will form. The Flibe source term methodology considers varying absolute and relative concentrations of radionuclide elements as well as varied chemical conditions of the Flibe solvent.

Radionuclide species that dissolve into the Flibe take on physical properties of the molten solution. Section 4.3.2.2 presents thermodynamic models of their dissolution into Flibe. These models adjust the physical properties of radionuclide species to provide an accurate description of their transport behavior in the Flibe solution. Specifically, the thermodynamic properties used to evaluate the equilibrium vapor pressure are reviewed to assess how radionuclide phases escape from the Flibe solution through vaporization. The propensity of radionuclide species to escape the Flibe through evaporation is proportionate to the RF that is applied to that radionuclide group for the Flibe barrier.

The equilibrium vapor pressures of relevant radionuclide species above molten Flibe solutions are evaluated and compared in Section 4.3.2.3. Comparisons of the vapor pressures of radionuclide species are used to select an appropriately conservative species to serve as the representative for the radionuclide group of elements that dissolve into the Flibe. The thermophysical proprieties, including vapor pressure, of the representative species are then used in transport analysis of all elements in that radionuclide group.

In Section 4.3.2.4, the chemical activity determined in Section 4.3.2.1 is combined with the equilibrium vapor pressures assessed determined in Section 4.3.2.2 to determine the vapor pressure of radionuclide species above the molten Flibe solution. This conversion to vapor pressure above the solution applies to radionuclides that do chemically interact with the molten Flibe and radionuclides that do not chemically interact with the molten Flibe. Therefore, the methods presented in Section 4.3.2.4 facilitate the evaluation of the vapor pressure of all radionuclide elements above the reactor coolant independent of their respective RFs in the Flibe barrier.

A generalized rate law quantifies the rate at which radionuclides will transport to the gas space. The kinetic rate law in Section 4.3.2.5 converts vapor pressures into radionuclide release rates to the gas space under a specified set of thermal hydraulic conditions.

© 2020 Kairos Power LLC

4.3.2.1 Liquid Phase Equilibria in Molten Flibe Solutions

Once salt soluble radionuclides are dissolved into the molten Flibe solution, they can undergo a variety of liquid (condensed) phase chemical reactions. The retention of radionuclides by the Flibe barrier is dependent upon the chemical state of the radionuclide at the time of interest. Therefore, it is necessary to evaluate what fraction of a radionuclide is expected to be present in a certain chemical species under specified conditions. Once the composition of radionuclide species is known, the vapor pressure of those species can be applied to determine the RF for that radionuclide element in the Flibe barrier.

For example, cesium that is dissolved in the Flibe can react with other dissolved species in either exchange or redox reactions. Several resulting Cs containing species may exist due to the following generalized reactions:

Exchange: $xCsI + MF_x = xCsF + MI_x$ Equation 50

Redox: Cs Halide + Be = Cs + Be Halide Equation 51

Evaluation of the quantity of a radionuclide species that will be present under a given set of circumstances is attained by computing the Gibbs Free energy of reaction, ΔG, and the equilibrium constant, K, for all possible reactions between the radionuclide of interest and other chemical species. For example, the reaction of dissolved cesium fluoride and strontium iodide, shown as Equation 52, is characterized by an intrinsic ΔG for the reaction.

$$2CsF + SrI_2 \rightarrow SrF_2 + 2CsI \quad \text{Equation 52}$$

$$\Delta G = \Delta G_{SrF2} + 2\Delta G_{CsI} - 2\Delta G_{CsF} - \Delta G_{SrI2} \quad \text{Equation 53}$$

The ΔG of the reaction is then related to the equilibrium constant, K, as shown in Equation 54.

$$\mathrm{K} = e^{\left(\frac{-\Delta G}{RT}\right)} = \frac{a_{SrF2} * {a_{CsI}}^2}{a_{SrI2} * {a_{CsF}}^2} \quad \text{Equation 54}$$

where a_{CsI} denotes the chemical activity of CsI in the molten Flibe solution. The equilibrium constant, K, is used to quantify the fraction of a radionuclide that will exist in a given species. In the current example, K will determine the ratio of Cs atoms that are in the form of CsI and CsF under equilibrium conditions.

Once the equilibrium constants for various reaction pathways are assessed, the inventory of radionuclide atoms available for reacting is applied to evaluate the number of radionuclide molecules that will be present each species. The chemical equilibrium shown as Equation 54 is determined by the number of radionuclide atoms that take place in the reaction. Radionuclide inventories are frequently in the form of isotope inventories while the chemical equilibria in the Flibe solution is governed by elemental concentrations. As a result, the input radionuclide inventories are consolidated by combining the atom numbers for all isotopes of each element before conducting chemical analysis.

© 2020 Kairos Power LLC

The methodology shown as Equation 52, Equation 53, and Equation 54 is used to evaluate the effects of reactive vaporization that could occur if the Flibe contacts chemical reactants. The most common example of a chemical reactant that could mobilize radionuclide phases through reactive vaporization is water. An example of the effects of water on radionuclide chemistry in a Flibe solution is the reaction of dissolved zirconium fluoride with water which is shown in Equation 55.

$$ZrF_4 + 2H_2O \rightarrow ZrO_2 + 4HF \quad \text{Equation 55}$$

Reactions such as Equation 55 could occur during an AOO Flibe spill event in which the reactor coolant contacts moisture in the atmosphere. These reactions tend to make radionuclide oxides, such as ZrO_2. The radionuclide MAR that reacted in this manner is grouped as an oxide phase in accordance with Table 4-2 and treated by the vapor pressure of that phase. It is assumed that reactions of reactor coolant with large quantities of chemical reactants that would result in the Flibe deviating from the redox potentials listed in Table 4-1 are considered beyond the KP-FHR design basis (consistent with design features provided in Section 2.3.4).

Independent of the source or the way in which a radionuclide phase is formed, the total quantity of each chemical species is then divided by the inventory of Flibe to assess the concentration of the radionuclide phase as a mole fraction. The activity of the radionuclide phase is obtained by multiplying its mole fraction by the activity coefficient for that radionuclide phase in the Flibe solution according to Equation 56.

$$a_{CsI} = \gamma_{CsI}[CsI] \quad \text{Equation 56}$$

Activity coefficients are determined experimentally and adjust mole fractions to the dimensionless value of activity which is a given species' effective concentration.

4.3.2.2 Equilibrium Vapor Pressure of Pure Radionuclide Species Over Flibe Solutions

The thermodynamics of vaporization out of a molten Flibe solvent are applied to evaluate the equilibrium vapor pressure of a radionuclide species. The vapor pressure of a pure compound is calculated from the equilibrium constant for the liquid-to-gas phase transition, K_i, which is calculated from the Gibbs free energy of the liquid-to-gas phase transformation. In the case of CsF:

$$CsF(liq) = CsF(g) \quad \text{Equation 57}$$

$$\Delta G = \Delta G_{CsF(g)} - \Delta G_{CsF(liq)} \quad \text{Equation 58}$$

$$K_i = e^{\left(\frac{-\Delta G}{RT}\right)} = \frac{p_{CsF(g)}}{a_{CsF(liq)}} \quad \text{Equation 59}$$

where, $p_{CsF(g)}$ is the vapor pressure of CsF in atmospheres, and a_{CsF} is the chemical activity of CsF liquid in the molten Flibe. The chemical activity is equal to unity for a pure phase and is the product of the mol fraction and activity coefficient when dissolved in a Flibe solution.

Adjustments to thermodynamic data of pure compounds are necessary to model the properties of their solubilized phases in a molten solvent at temperatures below the freezing point of the pure species. For example, CsF has a melting point of 682°C, but is solubilized as a fluid when dissolved in molten Flibe at reactor operating conditions of 650°C. In order to accurately predict the behavior of solubilized radionuclide phases under these conditions, the enthalpy of fusion must be added back to the enthalpy and the heat capacity is used to then extrapolate liquid phase data down to the temperature of interest. The gas phase thermodynamic data must be adjusted to reflect the thermodynamic behavior of the gas phase in equilibrium with the solubilized liquid phases at these lower temperatures. An analytical method for making the thermodynamic adjustments to model dissolution in Flibe was developed based on reference (Reference 29). Figure 4-2 shows the vapor pressure equilibrium constant using an analytical method as well as the calculation (using the Factsage thermodynamic database, Reference 34) adjusting for supercooled liquid thermodynamics (Section 8.2, Limitation #2). Factsage performs this adjustment automatically, as illustrated in Figure 4-2.

The experimental data points in Figure 4-2 are from measurements of CsF vapor over solid-phase CsF (Reference 30) and are therefore expected to under-predict the vapor pressure over the CsF liquid. Superimposed on the calculated data is data from Reference 35 showing the physical measurements of CsF vapor pressure over solid CsF in the indicated temperature range. The experimental data for CsF sublimation in the lower temperature range exhibits lower vapor pressure than the calculated values over the liquid phase. However, there is general experimental agreement with the theoretical results from the Factsage calculations.

4.3.2.3 Grouping Radionuclide Vapor Behavior

An appropriate radionuclide species is selected to provide representative vapor properties for the salt soluble fluoride radionuclide groups in Table 4-2 A species is chosen to model radionuclide vapor transport out of the Flibe for the salt soluble radionuclide group by comparing the vapor pressures of the likely species that could form.

Figure 4-3 shows the vapor pressure equilibrium constants of the alkali and alkaline earth fluorides and iodides, as well as for the alkali and alkaline earth metals as calculated using the method described in Section 4.3.2.2 shows vapor pressure vs. temperature calculated according to Equation 60.

$$K_i(torr) = 760e^{\left(\frac{-\Delta G}{RT}\right)} \qquad \text{Equation 60}$$

where, ΔG is the Gibbs free energy for the liquid-to-vapor phase transition in kilojoules per mole, R is the gas constant given as 0.0083145 kJ/K/mole, and T is the temperature in Kelvin. The factor of 760 is necessary to convert atmospheres to torr. Figure 4-2 shows $\log_{10}$(K) vs. temperature and is in units of log-torr, whereas Figure 4-3 shows K vs. temperature and is in units of torr.

As shown in Figure 4-3, Rb, Cs, and BeI_2 have high vapor pressures at or below the operating temperatures of the KP-FHR. Therefore, if these phases form during normal operations, they would

accumulate negligible MAR in the Flibe barrier. This material is transported to the cover gas. The cover gas system is expected to include purification capabilities (consistent with the design features discussed in Section 2.3.4). Therefore, it is assumed that these species do not contribute to MAR exceeding the de minimis thresholds discussed in Section 2.3.3.

As shown in Figure 4-3, of the species considered in this example, CsF has the highest vapor pressure of the radionuclide phases that have insignificant vapor pressure at reactor operating temperatures. Therefore, all radionuclides that are grouped as salt soluble fluorides are conservatively modeled to transport with the vapor properties of CsF. This conservatism applies to anions such as iodine, as CsI exhibits a lower vapor pressure than CsF. Therefore, transporting iodine with the salt soluble fluorides is considered conservative.

4.3.2.4 Vapor Pressure of Radionuclide Phases Over Flibe Solutions

The chemical activity determined using the methods described in Section 4.3.2.1, and the equilibrium vapor pressure determined in Section 4.3.2.2 and Section 4.3.2.3, are used to determine the vapor pressure of the radionuclide species over Flibe. Under the assumed dilute solution limit, the vapor pressure of phase *i*, p_i, is determined using Equation 61.

$$p_i = a_i K_i \qquad \text{Equation 61}$$

where, K_i is the temperature dependent liquid-to-vapor equilibrium constant and a_i is the activity of phase i in the solution. Deviations from ideal behavior, arising from chemical interactions between dissolved phases and the Flibe solvent, are accounted for in Equation 61 by the use of an activity coefficient to reduce the uncertainty associated with the evaluation.

A consequence of Equation 61 is that the vapor pressure over a diluted solute is much lower than the vapor pressure over a compound in its pure form. For example, CsF has an equilibrium vapor pressure of approximately 0.26 atm at 1,100^{o}C. If CsF is present in the reactor coolant at an activity of 1 ppm, assuming ideal solution behavior with a chemical activity coefficient of one, its partial pressure in a cover gas at atmospheric pressure would be 2.6x10^{-7} atm.

Equation 61 applies also to radionuclide groups that do not chemically interact with the Flibe reactor coolant, such as the oxides and noble metal radionuclides. These radionuclide species will exhibit vapor pressures and chemical activities associated with their pure component species because they have a chemical activity of unity by definition. Uranium dioxide is the representative oxide species due to its relative abundance when compared to all other oxide phases. Cadmium is the representative metallic phase of the high volatility noble metal group as is done in MELCOR (Reference 30). Palladium was chosen as the representative element for the low volatility noble metal group based on evaluated vapor pressure at reactor operating conditions.

4.3.2.5 General Vaporization Rate Law

A general rate law for vapor mass transfer, provided as Equation 62, is used to evaluate the rate of radionuclide release under a given set of thermal hydraulic conditions.

$$w_i = \frac{h_i p_i A}{RT} \qquad \text{Equation 62}$$

© 2020 Kairos Power LLC

where, w_i is the molar flow rate of phase *i* in moles per second, h_i is the mass transfer coefficient of species *i,* p_i is the temperature dependent vapor pressure of radionuclide species *i* and *A* is the area of the Flibe pool, R is the universal constant in appropriate units, and T is temperature.

In the source term analyses, mass transfer correlations will be used in accordance with scenario specific assumptions to obtain an applicable mass transfer coefficient.

© 2020 Kairos Power LLC

Table 4-1 Bounding Conditions of Reactor Coolant Redox Potential, E_{salt}, at 650 °C.

[[

]]

Table 4-2 Radionuclide Groups for Transport Analysis in Flibe

[[

]]

Figure 4-1 Schematic Depiction of Grouping of Radionuclides in Flibe Barrier[a]

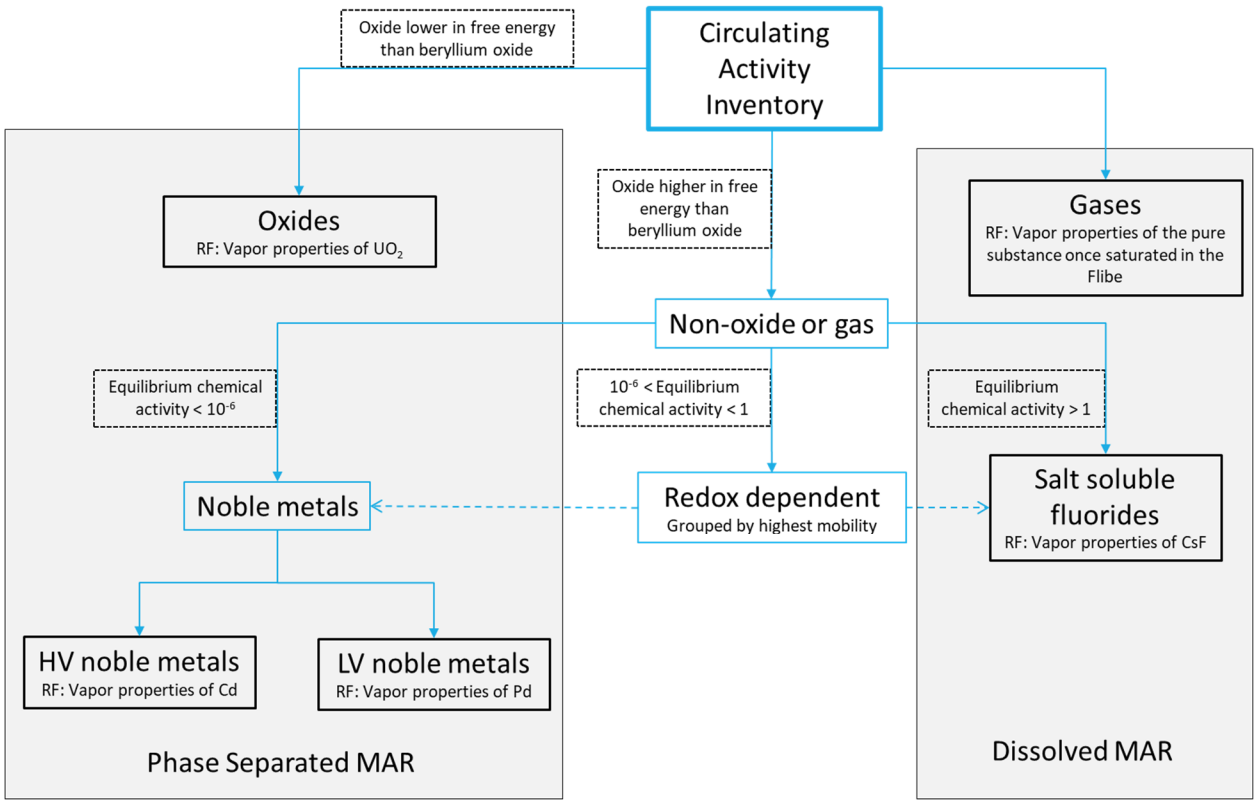

[a]HV indicates high vapor pressure, and LV indicates low vapor pressure.

Figure 4-2 Log Vapor Pressure Equilibrium Constants

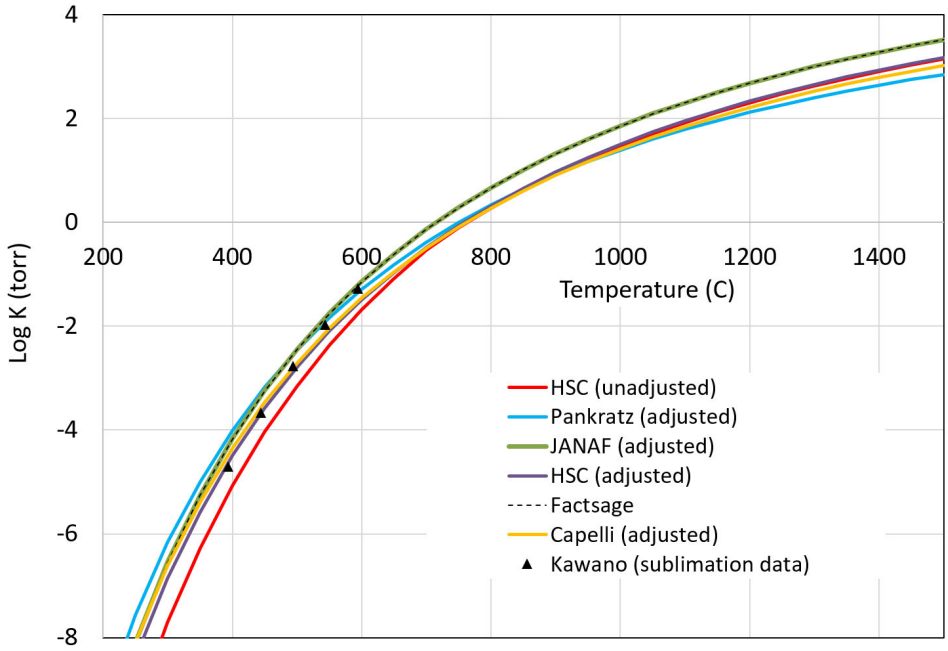

Figure 4-3 Vapor Pressure Equilibrium Constants (K) for the Indicated Liquid-to-Gas Phase Change Reactions

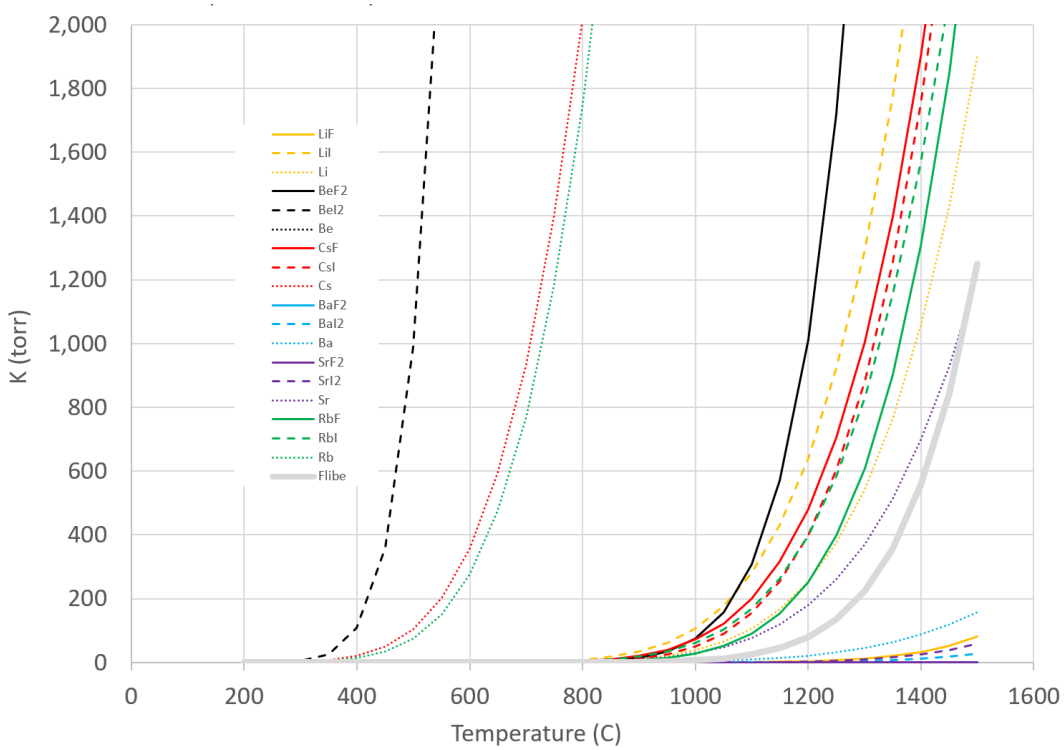

5 EVALUATING RADIONUCLIDE RETENTION IN GRAPHITE STRUCTURES

The graphite reflector of the KP-FHR has tritium retention properties that are accounted for in the KP-FHR mechanistic source term methodology. Although other activation products and fission products may be absorbed by the graphite reflector structures, they are assumed to be negligible (see de minimis pathway release assumptions in Section 2.3.4).

5.1 RADIONUCLIDE RETENTION PHENOMENA IDENTIFIED FOR GRAPHITE STRUCTURES

The phenomena relevant to the retention of radionuclide in graphite structures are separated into two sets: phenomena associated with events involving an intact reactor coolant boundary; phenomena associated with events involving a compromised reactor coolant boundary.

5.1.1 Phenomenon Associated with Events Involving an Intact Reactor Coolant Boundary

Table 2-4 identified the following phenomenon relevant to graphite structures-related source term methodology under conditions associated with an intact reactor coolant boundary as having a high importance to safety:

- [[

]]

5.1.2 Phenomenon Associated with Events Involving a Compromised Reactor Coolant Boundary.

Table 2-5 identified the following phenomenon as relevant to graphite structures-related source term methodology under conditions associated with a compromised reactor coolant boundary as having a high importance to safety:

- [[

]]

5.2 SOURCES OF RADIONUCLIDES IN GRAPHITE STRUCTURES

The radionuclide production in the graphite structures is assumed to be negligible consistent with the de minimis pathway release thresholds in Section 2.3.4. However, the tritium generated in the Flibe will be in direct contact the graphite reflector. The source term methodology for tritium production is described in Section 3.2.5.

5.3 RADIONUCLIDE TRANSPORT IN GRAPHITE STRUCTURES

Tritium transport is modeled using a set of time-dependent one-dimensional representations of the KP-FHR design.

© 2020 Kairos Power LLC

5.3.1 Tritium Speciation

In the absence of other hydrogen isotopes, tritium will exist in Flibe as TF or T_2. TF and T_2 have different diffusivities and solubilities in Flibe and have a different set of transport paths in the reactor system. For example, T_2 can permeate through metals whereas TF will not (Reference 36), but both TF and T_2 can evolve to a gas phase above the salt (Reference 37).

The speciation of tritium between TF and T_2 is determined by assuming the salt is in a chemical equilibrium at a given redox potential. The redox condition is specified using a fluorine potential, $\Delta\overline{G_{F_2}}$, which is related to the TF:T_2 ratio according to Equation 63 (Reference 39)

$$\Delta\overline{G_{F_2}} = 2RTln\left(p_{HF}/\sqrt{p_{H_2}}\right) + 2\Delta G^0_{HF} \qquad \text{Equation 63}$$

where, R is the universal gas constant, T is the temperature in Kelvin, and ΔG^0_{HF} is the standard free energy of formation of HF gas, which is approximately equal to that of TF. Equation 63 uses the partial pressures of HF and H_2 in the salt (p_{HF} and p_{H2}), which are converted to concentrations. The solubility of HF and H_2 in Flibe is observed to follow Henry's law, where the partial pressure has a linear relationship with the concentration of the species in Flibe (Reference 40 and Reference 41). Henry's law relationships for HF and H_2 are shown in Equation 64 and Equation 65, respectively, where $K_{H,HF}$ and $K_{H,H2}$ are the corresponding Henry's law solubility constants.

$$c_{HF} = K_{H,HF}p_{HF} \qquad \text{Equation 64}$$

$$c_{H_2} = K_{H,H_2}p_{H_2} \qquad \text{Equation 65}$$

The redox potential is set during reactor operation. During operation of the MSRE, it was determined that maintaining a 100:1 ratio of UF_4 to UF_3 in the fuel salt would result in satisfactory reducing conditions to limit corrosion of structural alloys (Reference 42). The fluorine potential corresponding to this chemical condition is -700.5 kJ/mol F_2 at 650°C (Reference 38). For Flibe salts without uranium, a practical lower limit for fluorine potential is when Flibe is fully reduced and in chemical equilibrium with beryllium metal, which occurs at -902.5 kJ/mol F_2 (Reference 39). The upper bound for fluorine potential is set as the most oxidizing step during the purification process, typically where a gas sparge of 1:10 HF:H_2 is used which results in -590 kJ/mol F_2 (Reference 39). Chemical purification steps after the HF:H_2 sparge, such as pure H_2 sparging or beryllium reduction will move the salt to a more reducing state (Reference 43). In practice, redox potential of Flibe is measured electrochemically. The redox potential of the salt in volts can be converted to a fluorine potential according to Equation 66 **(**Reference 43), where F is Faraday's constant, E_{salt} is the observed redox potential of the salt, and E_{F2} is the electrode potential of the reduction of F_2 gas in Flibe (Reference 44).

$$E_{salt} = \Delta\overline{G_{F_2}}/2F \; + E_{F_2} \qquad \text{Equation 66}$$

Chemical speciation of tritium can be calculated by modeling tritium generation in the correct balance of TF and T_2 according to the specified redox potential. When T_2 or TF then leaves the reactor systems, the balance is adjusted each time through the loop to maintain chemical equilibrium.

© 2020 Kairos Power LLC

5.3.2 Tritium Retention and Permeation

In the one-dimensional representation, the downcomer is modeled as an annular flow region with the reflector as the inner diameter and the vessel as the outer layer. The Sherwood number for mass transport in the region is found using Equation 67 through Equation 69. The hydraulic diameter is used to calculate the Reynolds number.

$$Sh = 1.86Re^{1/3}Sc^{1/3}(L/d_{pipe})^{-1/3} \quad \{13 < Re < 2030\}$$ Equation 67

$$Sh = 0.015Re^{0.83}Sc^{0.42} \quad \{2030 < Re < 10^4\}$$ Equation 68

$$Sh = 0.023Re^{0.8}Sc^{0.4} \quad \{Re > 10^4\}$$ Equation 69

The hydraulic diameter of the downcomer annulus is found using Equation 70, where d_{RPV} is the inner diameter of the reactor vessel and d_{DC} is the outer diameter of the core graphite reflector. The mass transfer coefficient for the downcomer is then shown in Equation 71.

$$d_H = d_{RPV} - d_{DC}$$ Equation 70

$$k_{DC,T_2} = Sh_{DC}D_{T2}/d_H$$ Equation 71

A nonlinear solver is used to model retention in the reflector graphite. The total matrix requiring a nonlinear solver is shown in Equation 72. The terms are shown graphically in Figure 7-8.

Equation 72

$$\begin{bmatrix} j_{DC,T_2} = k_{DC,T_2}\left(T_{2,Avg} - T_{2,DC,Surf}\right) \\ 2 \cdot j_{DC,T_2} = D_{T,g}/\Delta R_o\left(T^i_{d,DC} - T^{i-1}_{d,DC}\right) \\ T_{2,DC,Surf}/K_{H,T_2} = \left(T^i_{d,DC}/K_{S,g}\right)^2 \\ j_{RPV,T_2} = k_{DC,T_2}\left(T_{2,Avg} - T_{2,RPV,Surf}\right) \\ 2 \cdot j_{RPV,T_2} = D_{T,316}/\Delta R_i\left(T^i_{RPV} - T^{i-1}_{RPV}\right) \\ T_{2,RPV,Surf}/K_{H,T_2} = \left(T^i_{RPV}/K_{S,316}\right)^2 \\ T_{2,Avg}\lambda_2^2 = \left(T_{2,DC,Surf} + \frac{d_{RPV}}{d_{DC}}T_{2,RPV,Surf}\right)(\lambda_1 \exp(-\lambda_2) + (\lambda_2\lambda_1 - \lambda_1)) + \lambda_2 T_2^N(1 - \exp(-\lambda_2)) \end{bmatrix}$$

$$\lambda_1 = k_{DC,T_2}A_{Reflector,node}/\dot{V} \qquad \lambda_2 = \lambda_1(1 + d_{RPV}/d_{DC})$$

6 OTHER SOURCES OF MAR

Based on the design features of the KP-FHR described in Section 1.2 and Section 2.3.4, MAR is anticipated to be located in areas of the KP-FHR aside from the fuel, Flibe, and graphite reflector described in previous sections of this report. This section details the various media that contain these other sources of MAR and the associated release fractions. The media containing MAR detailed in this section include:

- Graphite dust in the reactor vessel and PHSS
- Vapor and off gas in the PHTS and CCS
- Cold trap and filters in the CCS
- Radionuclides in the IHTS
- Vapor and off gas in the IHTS

Any additional sources of MAR that are not identified in this report that could challenge the dose limits will be accounted for in future licensing submittals.

6.1 IMPORTANT SOURCE TERM PHENOMENA IDENTIFIED FOR OTHER SOURCES OF MAR

The phenomena relevant to other MAR are separated into two sets: phenomena associated with radioactive waste systems, and phenomena associated with the PHSS.

Table 2-6identifies phenomena associated with events involving the radioactive waste systems that have a high or medium importance to safety. The KP-FHR source term methodology addresses these phenomena below:

- [[

]]

Table 2-7 identifies phenomena associated with events involving the PHSS that have a high or medium importance to safety:

- [[

]]

6.2 SOURCES OF RADIONUCLIDES IN THE PHSS, CHEMISTRY CONTROL, AND HEAT TRANSPORT SYSTEMS

As noted above, other areas containing MAR that could be released are the graphite dust in the PHSS as well as the reactor vessel, the PHTS and CCS vapor and off gas, the CCS cold trap and filters, the radionuclides in the IHTS and the vapor and off gas from the IHTS. The nature of these sources of MAR are described in this section.

6.2.1 Graphite Dust

Particulate matter consisting primarily of carbon, referred to as graphite dust, will be generated from erosion and mechanical damage to graphitic materials throughout the KP-FHR. Graphitic materials in the KP-FHR include fuel pebbles and structural graphite components in the reactor core. Source term treatment of graphite dust will be consistent, independent of the precursor material from which it was generated. Graphite dust has a relatively low density and is transported in the form of an aerosol throughout various systems or areas that share common gas systems. Specifically, graphite dust will move between the reactor vessel cover gas spaces and the pebble handling and storage system (PHSS).

6.2.2 Vapor and Off-Gas in PHTS and CCS

The cover gas spaces above Flibe in the reactor vessel and in the chemistry control system (CCS) will contain various radionuclides that are transferred into the gas space from the Flibe barrier. Specific systems that will promote transport of radionuclides to the cover gas include the primary salt pump in the reactor vessel, and the inert gas sparging system in the CCS. Both systems will promote portioning

© 2020 Kairos Power LLC

of radionuclide chemical species in the reactor coolant (dissolved or physically entrained) into forms that are transported with the cover gas. The off-gas systems that intake gases and vapors from Flibe containing systems will consist of a series of filters and chemical traps used to sequester gaseous, vapor, and aerosol radionuclides. Each system is expected to employ a series of filters or traps that will target retention of specific chemical forms of MAR (consistent with the design features described in Section 2.3.4).

6.2.3 Cold Trap and Filters in the CCS

It is anticipated that the KP-FHR design will include chemical control features that contain Flibe filters and/or cold traps to remove materials and purify the Flibe (consistent with the design features described in Section 2.3.4). Filtration of the reactor coolant will serve to remove solid matter such as graphite dust or other foreign materials from the reactor coolant. Specific materials for removal by a cold trap include beryllium oxide, corrosion product fluorides, as well as other MAR that may be dissolved in the reactor coolant. Chemical reactants may be employed in the CCS. Induced chemical reactions would act to form phase separated chemical species such as gases, oxides, or metals. Once phase separated, these materials would be removed from the Flibe barrier by off-gassing, filtration, or cold trapping. Filters and cold traps within the CCS will accumulate MAR inventory as a function of time under steady state operation. Filters and cold traps will be designed to be replaced or decontaminated when they have accumulated a pre-determined acceptable quantity of MAR.

As discussed in Section 1.1, the KP-FHR includes an intermediate heat transport system (IHTS) which uses nitrate salt (60%$NaNO_3$ – 40%KNO_3) as the heat transfer fluid between the Flibe based primary heat transport loop and the steam-based power conversion system. The intermediate heat exchanger (IHX) isolates the nitrate salt from the Flibe and serves as a barrier for radionuclide transport between the systems. The intermediate loop is at a lower pressure than the primary loop by design. As a result, leaks in the IHX will result in the transfer of MAR from the Flibe barrier into the IHTS. Additionally, at steady state, tritium is expected to diffuse through the IHX and accumulate in the IHTS. MAR in the IHTS will be sequestered within the nitrate salt barrier where potential paths to release include vaporization out of the molten salt, or mobilization of the bulk salt through aerosolization.

The off-gas system that intakes gases and vapors from nitrate salt in the IHTS is expected to contain a series of filters and chemical traps used to sequester gaseous, vapor, or aerosol materials. These features will have similar operating principles from those employed in the PHTS however they will differ in design due to the chemical differences between nitrate and Flibe salts. Additionally, the chemical species of given radionuclide elements within the two heat transport systems will be different. The gas handling system in the IHTS will additionally employ a dehumidification system to sequester tritium containing water vapor from the gas. The filters, traps, and dehumidification systems will accumulate MAR inventory as a function of time under steady state operation. Each of these systems will be designed to be replaced or decontaminated when it has accumulated a pre-determined acceptable quantity of MAR.

6.3 MODEL INTERFACES

The source term analysis for these other sources of MAR will utilize the methodology for chemical and evaporation modeling, KP-SAM for thermal-fluids modeling, KP-Bison for MAR transport and fuel

© 2020 Kairos Power LLC

performance modeling, RADTRAD for building transport modeling, and ARCON96 for offsite dispersion modeling.

6.4 RADIONUCLIDES PRESENT IN OTHER SOURCES OF MAR

Other sources of MAR (i.e., those not discussed in Sections 3 – 5) do not produce additional MAR. Radionuclides born in these "other MAR" were assessed in this topical report as were those transferred into the barrier from a previous barrier. Those radionuclides that were transferred or escaped out of "other MAR" under normal operating conditions were also considered. The impact of a degraded barrier is also discussed below.

6.4.1 Radionuclides Born in Other Sources of MAR

MAR born in graphitic materials may include tritium as well as fission products due to the presence of trace uranium. Bounding quantities of fission product MAR that is born in graphitic materials will be calculated using KP-Bison.

Radionuclides born within the PHTS off-gas system will consist of daughter isotopes formed from radioactive decay of gaseous, vapor, or aerosolized radionuclides which escape the Flibe barrier. These daughters will consist of a variety of radionuclides formed through a series of decay chains.

Radionuclides born in the cold trap of the chemistry control system will consist of daughter isotopes formed from radioactive decay of MAR that is dissolved in, or flows with, the reactor coolant. Radionuclides form salt soluble fluorides and are entrained in the Flibe as phase separated particulates. The chemical phase of radionuclides born within the cold trap will be different than the parent radionuclides. The transport behavior of the daughter radionuclides in the Flibe environment of the cold trap or filters will be independent of the chemical form of the parent radionuclide.

Radionuclides born in the nitrate salt of the IHTS will include decay products of any MAR radionuclides that leak through the IHX. As a result, the IHTS will contain trace quantities of radionuclides in the Flibe barrier. The nitrate salt is expected to be exposed to negligible neutron flux, so transmutation of isotopes within the IHTS will be negligible.

Radionuclides born within the off-gas system of the intermediate loop will consist of daughter isotopes formed from radioactive decay of gaseous, vapor, or aerosolized radionuclides that escape the nitrate salt. Volatile radionuclides in the IHTS will be in different chemical forms from the PHTS due to the oxidizing atmosphere of the nitrate salts. However, the KP-FHR design is expected to limit circulating activity in the nitrate salt (consistent with the design features discussed in Section 2.3.4 and the limitations discussed in Section 8.2) and limit the MAR in the nitrate salt to nonsafety-significant quantities.

6.4.2 Radionuclides Transfer

MAR in graphite dust may contain trace amounts of tritium and fission product MAR transferred into the graphite from the Flibe and fuel, respectively. Quantification of MAR transferred to the carbon from the fuel will be done using KP-Bison.

© 2020 Kairos Power LLC

The rate of evaporation of radionuclides from the Flibe barrier at steady state is assumed to be much lower than the rate of argon sweep gas through both the reactor vessel head space and the sparging gas in the CCS. As a result, these radionuclides will be collected in the off-gas cleanup system at the rate at which they escape the Flibe barrier. Therefore, the MAR in the cover gas is assumed to be minimal relative to circulating activity MAR in the reactor and intermediate coolants.

Interfacing systems will promote transporting radionuclides from the Flibe barrier to the cover gas. Dissolved gases in the Flibe barrier will be transferred to the cover gas due to gas sparging of the fluid salt. Additionally, MAR that has phase separated in the form of oxides or noble metals could partition to the gas phase via a series of aerosolization mechanisms associated with gas / salt mixing. This material includes notable quantities of graphite dust containing MAR. Radionuclides in the form of volatile salt soluble fluorides vaporize from the Flibe through congruent or reactive vaporization mechanisms.

The inclusion of cold traps and filters in the CCS will separate MAR from the Flibe through mechanical filtration, chemical reactions, or precipitation. Any form of MAR that transports as a dissolved component, or as an entrained phase, in the Flibe is separated by these features in the CCS and its MAR is transferred to the associated medium. Oxide and low volatility noble metals that flow with the reactor coolant as entrained solids are expected to accumulate in these system features. Radionuclides that form salt soluble fluorides with low solubility limits are also expected to precipitate on the cold trap and are removed from the Flibe. Chemical reactants, if employed in the CCS, are expected to form phase separated chemical species such as oxides or metals. Upon phase separation, this MAR would be transferred from the Flibe to the cold trap or filtration systems in the CCS.

The majority of MAR transferred into the nitrate salt of the IHTS under steady state operations will be from tritium that diffuses through the IHX. Tritium diffuses through the intermediate heat exchanger in the form of T^0 or T_2. Upon contacting the nitrate salt tritium oxidizes and forms tritiated water (HTO or T_2O.) Molten nitrate salts have the potential to dissolve water at elevated temperatures. It is anticipated that there will be a non-zero vapor pressure of tritiated water in the head space gas above the intermediate loop, in addition to some quantity of tritium MAR in the form of dissolved tritiated water in the nitrate salt. The cover gas of the intermediate loop will be continuously dehumidified to maintain a low partial pressure of moisture within the system. The exhaust of the dehumidification system will be sequestered and subjected to appropriate tritium storage and disposal regulations.

The molten nitrate salt will also accumulate MAR retained in the Flibe leaks in the IHX. This MAR includes any radionuclides that transport in the primary heat transport system. IHX tube leaks from the PHTS are an anticipated operational occurrence in the design basis of the plant. The flow of MAR through the IHX is expected to be low due to the dilute nature of MAR in the primary loop. Subsequently, the concentration of MAR that will accumulate within the IHTS will be low due to additional dilution into the large inventory of nitrate salt. Upon contacting the nitrate salt, radionuclide chemical species that were stable in the Flibe of the primary loop, are expected to undergo chemical reactions with the nitrate salt. However, the quantity of non-tritium radionuclides allowed in the nitrate salt will be low enough that the methodology can assume this MAR is released in place of rigorous studies of the chemical reactions between radionuclides and the nitrate salt (operational limits on the allowed activity of the nitrate salt are presented as a limitation in Section 8.2).

© 2020 Kairos Power LLC

Upon reacting with molten nitrate salt, various radionuclide elements could form chemical species that are soluble in the molten nitrate salt. Radionuclide species that are expected to be soluble in the nitrate salt include nitrates, nitrites, fluorides, and potential dilute concentrations of oxides. Once dissolved in the nitrate salt these radionuclide species are expected to have similar transport mechanisms as those described for the retention of salt soluble fluoride MAR in the PHTS.

Chemical reactions between radionuclides transferred from the Flibe barrier to the nitrate salt yield radionuclide species that are insoluble in the IHTS. Specific examples include noble metals or oxides at quantities above their solubility limits in the melt. These materials precipitate or are entrained in the nitrate salt and have similar transport mechanisms as described for oxide and noble metal MAR in the PHTS.

Chemical reactions between radionuclides transferred from the Flibe barrier to the nitrate salt yield volatile radionuclide chemical species. This MAR will have a release fraction (RF) near unity in the nitrate salt and will rapidly partition to the gas space of the IHTS.

Radionuclides in the cover gas of the intermediate heat transport loop will primarily consist of various forms of tritium: T_2, HTO, and T_2O. Tritium transport is evaluated exclusively as a gas in RADTRAD. This is conservative due to the likelihood of tritium being bound in the less mobile HTO, and T_2O forms. Volatile radionuclide species that are formed from chemically reacting MAR transported by the Flibe into the IHTS through leaks in the IHX will additionally accumulate in the cover gas of the IHTS. The vapor pressure of nitrate salt is significant at operating temperatures. As a result, vaporization of MAR contained within the nitrate salt is expected to transport to the IHTS cover gas system more readily than in the primary system.

6.4.3 Radionuclides Escaped or Transferred

Trace quantities of MAR are released from graphite dust as it changes location and physical conditions while transporting within the gas space. Graphite dust is mobile as an aerosol and it moves within the gas space between the PHTS and the PHSS. When moving between these systems the graphite dust will change conditions such as temperature, pressure, and chemical environment. Changes in these conditions promote the release of MAR from the graphite dust to the gas space. Most of the MAR that will be released from the graphite under normal operations will consist of tritium as it exhibits a constant diffusion into and out of graphite.

Radionuclides carried as effluents from the off-gas systems of the PHTS and CCS as well as the IHTS will be monitored in accordance with 10 CFR 20. It is expected that any filters, chemical reagent, resins or sorption media used to sequester radionuclides are designed to be replaceable. These materials will be replaced or decontaminated on a periodic basis to maintain levels of MAR accumulation within them within pre-established limits.

Radionuclide retention in the filters and cold trap expected to be present in the CCS will be in an equilibrium process with MAR continuously moving into and out of the barrier. Under normal operations, trace quantities of MAR are expected to transfer from systems in the CCS into the Flibe barrier due to inefficiencies in the filtration or trapping processes. Additionally, MAR may transfer to the cover gas where it will be sequestered by separate filters and traps expected in that system. Filters and cold traps will be replaced or decontaminated on a periodic basis to maintain quantities of stored

© 2020 Kairos Power LLC

MAR within them to pre-established limits. These maintenance operations will transfer MAR from the CCS, and the material will be disposed of in accordance with appropriate regulations.

MAR in the IHTS is expected to form quantities of volatile radionuclide chemical species that will gradually partition from the molten nitrate salt to the cover gas of the IHTS. Vaporization of these radionuclides into the cover gas handling system, including tritium in the form of tritiated water, will occur under normal operations.

6.4.4 Impact of Degraded Barriers on Retention of Radionuclides

The retention of radionuclides in graphite dust depends upon various physical conditions including temperature and chemical environment. As graphite dust moves throughout the cover gas it will be subjected to changes in these parameters and is expected to release trace quantities of MAR. Specific examples include degassing of tritium as the graphite changes temperature, or through reactive vaporization if exposed to trace quantities of moisture.

Degradation of the cold trap or filtration systems in the CCS will lower the efficiency of MAR removal from the Flibe barrier. Underperformance of these systems would result in gradual increases in the levels of MAR in the PHTS either through less efficient MAR removal, or by releasing MAR into the Flibe. The flow of MAR between these systems will be slow due to the large inventory of reactor coolant.

The nitrate salt barrier acts to dissolve MAR to lower the effective concentration and suppress vapor pressure in an analogous manner as the Flibe barrier in the primary loop. Degradation of the barrier promotes vaporization or aerosolization of MAR contained within the IHTS. These processes transfer MAR to the cover gas of the IHTS. Once MAR is introduced to the intermediate loop, it is modeled with behavior similar to MAR in the primary loop, with modifications made to adjust for the separate chemical forms of given radionuclide phases. MAR in the IHTS will be sequestered within the nitrate salt barrier where potential paths to release include vaporization out of the molten salt, or mobilization of the bulk salt through aerosolization.

6.4.5 Radionuclide Transfer During AOOs or DBEs

The MAR in graphite dust is released by degassing or through reactive vaporization. The models developed for tritium transport into, and out of, graphite will describe releases of other radionuclides

MAR is released or escapes from the cover gas systems by mechanical damage to piping systems that would exceed steady state leak rates of the system. Hermeticity of the gas handling system is specified to maintain acceptable leak rates, but damages or breakages in these systems could release gaseous MAR under an AOO or DBE. Additionally, unintended chemical or temperature transients could compromise the ability of filters or traps to retain MAR. These systems retain MAR through a variety of chemical reactions or physical trapping processes. By exposing these systems to unintended conditions, such as changes in chemical environment or temperature, the MAR becomes mobile and escapes the system. The quantity of MAR that could be released in such a scenario will be limited by the appropriate operating limitations for each system. By replacing media that sequester MAR before safety significant quantities of MAR have been accumulated, failure of the media in AOOs or DBEs cannot result in safety significant releases.

© 2020 Kairos Power LLC

The cold trap and salt filtration systems in the CCS will accumulate MAR flowing with the reactor coolant. Failures in the cold trap or filtrations systems could release stored MAR due to mechanical failures or temperature transients. MAR released from such features within the CCS will recombine with the flow of molten Flibe and be returned to the MAR inventory within the reactor coolant. This MAR will interact with the molten Flibe. In scenarios where the primary piping is compromised, a spill of reactor coolant will result. The MAR that is sequestered in filters and cold traps of the CCS will be in the form of nonvolatile solid phases because mobile or volatile phases will be removed by the gas sparging system before the accident initiates. The quantity of MAR that could be released in either scenario will be limited by the pre-established operational limits. As a result, failure of these media alone will not result in safety significant releases.

The processes for MAR mobilization from nitrate salt in the IHTS will be analogous to MAR transport in the PHTS. Transport via aerosolization and transport via evaporation accounts for variations in the chemical environments between the two systems. The concentration of MAR in the IHTS is orders of magnitude lower than in the PHTS due to dilution in the large inventory of nitrate salt. AOOs and DBEs such as salt spills or temperature transients are covered using similar models as are used for the PHTS.

MAR may be released or escape from the cover gas systems of the IHTS by mechanical damage to piping systems that exceed steady state leak rates of the system. Hermeticity of the gas handling system will be specified to maintain acceptable leak rates, but damages or breakages in these systems will release gaseous MAR under an AOO or DBE. Additionally, unintended chemical or temperature transients could compromise the ability of filter or traps to retain MAR. These systems retain MAR through a variety of chemical reactions or physical trapping processes. By exposing these systems to unintended conditions, such as changes in chemical environment or temperatures, the MAR may become mobile and escape the system. The quantity of MAR that is released in such a scenario is limited by the appropriate pre-established operational limit for each system.

6.4.6 Radionuclides Transferred During DBAs

Quantities of material at risk that will be allowed to accumulate in the other sources of MAR are limited by pre-established operational limits. As previously stated, these operational limits will be set such that no quantity of MAR that could result in a safety significant release will accumulate in these potential sources during operation of the plant. These restrictions ensure that none of the associated media that retain these sources of MAR will be safety related. Therefore, the assumptions and treatment of these systems described in Section 6.4.5 for AOOs and DBEs cover DBAs with sufficient conservatism.

© 2020 Kairos Power LLC

7 EVALUATING RADIONUCLIDE TRANSPORT IN THE GAS SPACE AND ATMOSPHERIC TRANSPORT

This section provides the gas space radionuclide transport methodology, which includes the grouping of radionuclides, characterization of aerosols, reactor building transport modeling in RADTRAD, and atmospheric dispersion modeling in ARCON96.

7.1 IMPORTANT SOURCE TERM PHENOMENA ASSOCIATED WITH GAS SPACE TRANSPORT

The phenomena relevant to the transport of radionuclides in gas space are separated into two sets: phenomena associated with events involving an intact reactor coolant boundary, and phenomena associated with events involving a compromised reactor coolant boundary.

7.1.1 Phenomena for Gas Space with Intact Reactor Coolant Boundary

Table 2-8 identified the following phenomena relevant to gas space-related source term methodology under conditions associated with an intact reactor coolant boundary as having a high or medium importance to safety:

- [[

]]

7.1.2 Phenomena for Gas Space with Compromised Reactor Coolant Boundary

Table 2-9 identified the following phenomena as relevant to gas space-related source term methodology under conditions associated with a compromised reactor coolant boundary as having a high or medium importance to safety:

- [[

]]

- [[

]]

7.2 RADIONUCLIDE GROUPS

Table 7-1 provides the KP-FHR gas transport radionuclide groups modified from the default RADTRAD grouping table (Reference 10). Radionuclides are grouped based on similar expected chemical and transport phenomenology. A representative radionuclide is chosen from the group to evaluate its RF in the gas space; all other radionuclides within the radionuclide group are assumed to have the same RF as the representative radionuclide. If radionuclides are expected to form a compound that behaves differently than the representative radionuclide, those compounds are given their own radionuclide group.

Within the gas space, the movement of radionuclides is modeled as either a gas or as an aerosol. While LWR models may either source different radionuclide groups at different rates or remove radionuclide groups preferentially with scrubbers or sprays, the KP-FHR source term methodology only models gravitational settling of aerosols and radioactive decay within rooms as decontamination processes within the reactor building. This effectively reduces the traditional radionuclide groups to two groups: aerosols and gases.

7.3 CHARACTERIZING AEROSOLS

This section details the mechanical aerosol generation methodology for two scenarios in the KP-FHR design basis: pipe breaks and PHSS transients.

7.3.1 Material at Risk During a Pipe Break

The material at risk for a compromised reactor coolant boundary involving a pipe break is the circulating activity of the fluid contained in the pipe (either Flibe or nitrate salt). This section demonstrates the methodology to calculate an airborne release fraction (ARF) using the assumptions in Table 7-2.

Airborne release fractions are quantified from the salt leaving the pipe and from the salt splashing on a surface. Assigned location of a postulated pipe break is in the most conservative pipe segment in the loop (i.e., the location that produces the highest activity in the gas space). The capability of insulation materials to retain and reduce releases from Flibe leaks is neglected, so the assumptions of mechanical aerosolization will bound actual releases from insulated parts of the coolant boundary.

© 2020 Kairos Power LLC

7.3.1.1 Aerosolization of Salt Leaving the Pipe

The breakup length of the jet, $L_{break}(m)$, in Equation 73 formed from the break flow, assuming that droplets are much smaller than the diameter of the jet (equal to the break diameter, $d_o(m)$), is correlated by References 11 and 12:

$$L_{break} = 5.0 d_0 \left(\frac{\rho_f}{\rho_g}\right)^{0.5} \quad \text{Equation 73}$$

where:

ρ_f = the fluid density (i.e., Flibe or nitrate salt in kg/m^3)

ρ_g = the gas density (e.g., air) (kg/m^3)

This is valid when the Weber number in Equation 74 is greater than approximately 10 (Reference 11 and 12):

$$We_f = \frac{u^2 d_0 \rho_g}{\sigma} > \sim 10 \quad \text{Equation 74}$$

where:

We_f = the Weber number for the jet

σ = the surface tension (N/m), and

u = the initial break flow velocity (m/s) provided in Equation 75:

$$u = C_D \times \left(\frac{2\Delta P}{\rho_f}\right)^{1/2} \quad \text{Equation 75}$$

If the predicted jet breakup length is longer than the expected room size, the ARF calculated in Equation 92 is conservative because a limited jet breakup is predicted to occur for large break accident given the expected size of the compartments. Smaller breaks would imply the potential for complete jet breakup but still bounded by the ARF in Equation 92. The driving pressures are low relative to the range of available data.

7.3.1.2 Aerosol Formation from Jet Breakup

The first step in calculating the aerosol formation from jet breakup is to calculate a representative diameter for the resulting distribution of particles. A formula for the arithmetic mean droplet diameter $\overline{D}$ was derived by Reference 51 as:

Equation 76

$$\overline{D} = 9\pi(16)^{1/3} B \left(\frac{\mu_f^2 \sigma}{\rho_g^2 \rho_f \mu_0^4} \right)^{1/3}$$

[[

]]

The spray distribution can be represented by the Rosin-Rammler size distribution function which takes the from:

$$f_D = 1.0 - exp\left(-\left(\frac{D}{X}\right)^q\right) \quad \text{Equation 82}$$

where:

f_D = the fraction of the total volume of the collection of drops below a given drop diameter D,
X = the size parameter given by:

$$X = \left[\Gamma\left(1 - \frac{1}{q}\right)\right] SMD \quad \text{Equation 83}$$

where, Γ is the gamma function.

Equation 82 can be linearized using Taylor series expansion such that it becomes:

$$f_D = \frac{1}{\left[\Gamma\left(1 - \frac{1}{q}\right)\right]^q}\left(\frac{D}{SMD}\right)^q \quad \text{Equation 84}$$

[[

]]

[[

]]

[[

]]

The fraction of the spray contained in drops below any size, p_D (m), is given by the Rosin- Rammler formula in Equation 92 (Reference 12).

$$ARF_D = f_D = 1.0 - exp\left(-\left(\frac{p_D}{X}\right)^q\right) \quad \text{Equation 92}$$

where,

q = the spread in the droplet size distribution (methodology assumes q is 2.4)

X is defined in Equation 83

When using the assumed value of q = 2.4, X = 1.529 for a driving pressure of 2 barg. The ARF as a function of driving pressure is shown in Figure 7-1 and assumes a particle diameter of 50 µm. This ARF occurs if the jet is allowed to travel to its breakup length.

7.3.1.3 Aerosolization of Salt Splashing on a Surface

Aerosols are generated by spills because the spilled liquid entrains air into the developing pool, and this air causes bubble burst aerosol formation as it leaves the pool. Correlations for continuous spills into already-formed pools are bounding (Reference 12).

For an intact, coherent liquid jet, the velocity at impact, V_j is provided in Equation 93.

$$V_f = (u^2 + 2gH)^{1/2} \quad \text{Equation 93}$$

where:

u = the break flow velocity (m/s) as calculated in Equation 75

g = the gravitational constant (9.8 m/s^2)

H is the fall height (m).

The velocities for a one-meter drop are shown in Figure 7-2.

Equation 94 for the gas entrainment rate by a plunging, coherent liquid jet gives satisfactory agreement with experiments Reference 13 and 12.

$$\frac{Q_g}{Q_f} = 0.04 Fr_j^{0.28} \left(\frac{H}{d_0}\right)^{0.4}$$ Equation 94

where:

Q_g = the volumetric flow rate of entrained gas

Q_f = the volumetric flow rate of spill liquid ($u\pi \frac{d_0^2}{4}$)

d_0 = the break diameter (m)

Fr_j = the jet Froude number defined by Equation 95 (Reference 12)

$$Fr_j = \frac{V_j^2}{g d_0}$$ Equation 95

Equation 94 is based on experiments with $\frac{L_j}{d_0} \leq 100$ and $\frac{Q_g}{Q_f} \geq 0.4$. Equation 94 may have to be extrapolated beyond the available database when applied to actual spill conditions to lower pressure and velocity regimes, which should be conservative as the impact forces causing aerosolization are significantly reduced. The Froude number (Equation 95 and the gas entrainment rate (Equation 94)) are shown in Figure 7-3.

The aerosol generation rate Q_{en} is defined in Equation 96 by the entrainment rate of liquid drops emerging from the bursting bubbles (Reference 12).

$$Q_{en} = E Q_g$$ Equation 96

where, the entrainment coefficient E has a low value of $E = 2 \times 10^{-7}$ (Reference 12) as the recommended bubble burst entrainment coefficient for waste liquid with high concentrations of impurities see Figure 7-4 from Ginsberg (Reference 14). To be conservative, Flibe with impurities is assumed to be best represented by $E = 2.1 \times 10^{-6}$, which bounds the Garner water-$CaCo_3$ data. All bubble burst aerosols are generated in the 1 to 10 µm range (References 15 and 16), so all entrained aerosols predicted by Equation 96 constitute the ARF as Equation 97 (Reference 50 and 16).

$$ARF_{splash} = \frac{Q_{en}}{Q_f}$$ Equation 97

The ARF from spills are negligible compared to the ARF from jet breakup given the assumed one meter drop height as shown in Figure 7-5.

7.3.1.4 Treatment of AOOs, DBEs and DBAs for Splashes

[[

]]

[[

]]

7.3.2 Pipe Break Airborne Release Fraction Approach

Key parameters considered when analyzing a break location are the pressure at the break location (i.e., cover gas pressure plus pump head plus gravitational head minus frictional losses) and the total amount of Flibe available to leak out of the break. The methodology assumes that when a fluid aerosolizes, all dissolved radionuclides aerosolize at an equivalent fraction due to very low liquid-phase mass diffusion rates.

[[

]]

7.3.3 Material at Risk in the Pebble Handling and Storage System

7.3.3.1 TRISO fuel

MAR in the TRISO fuel will be quantified using KP-Bison for an equilibrium cycle PHSS loading.

7.3.3.2 Plated Aerosols

7.3.3.2.1 Graphite Dust

The MAR associated with graphite dust is determined by quantifying the radionuclide loading associated with the dust and the graphite dust generation rate.

[[

]]

MAR activities per unit dust volume can be calculated by Equation 98.

$$MAR_{GD} = \frac{MAR_{Matrix}}{M_{Matrix}} M_{GD} \qquad \text{Equation 98}$$

where:

MAR_{GD} = the MAR for all graphite dust in the PHSS

MAR_{Matrix} = the calculated MAR in the matrix material

M_{Matrix} = the mass of the matrix material containing MAR_{Matrix}

M_{GD} = the mass of the graphite dust being generated as calculated by Equation 99.

$$M_{GD} = R_{GD}T \quad \text{Equation 99}$$

where:

R_{GD}[2] = the graphite dust settling rate in kg/year[3]

T = the operating timeframe for the PHSS in year

7.3.3.2.2 Flibe Dust

Flibe is expected to freeze into relatively large fragments (i.e. greater than the 50µm fallout particle diameter) in the PHSS and is not expected to mobilize given the combination of driving force for resuspension and the aerosol fallout criteria. This MAR is assumed to have the same mass normalized activity levels as the reactor coolant. This is consistent with assumptions typically used in aerosol transport codes such as MELCOR (Reference 17). This value will be used as the critical diameter for aerosol formation correlations. When calculating the airborne release fraction from correlations for sprays and spills, the bounding respirable particle diameters (<10µm) are applied to aerosol generation rate correlations (Reference 49).

7.3.3.3 Cover Gas

The cover gas MAR will be quantified using the methods discussed in Section 4.3. Flibe aerosols generated in the cover gas region are included in the cover gas MAR.

7.3.4 Airborne Releases for Material at Risk in the Pebble Handling and Storage System

7.3.4.1 Diffusion

MAR in the PHSS could be released from fuel pebbles if the pebbles experience a temperature transient severe enough to cause diffusion of the radionuclides through the pebble. Pebbles could experience transients in the handling or storage portions of the PHSS:

- Temperature transient in pebble handling - Pebbles will not reach failure temperature due to events (e.g., spills, loss of forced circulation) that occur in the PHSS (consistent with the design features described in Section 2.3.4).

- Temperature transient in pebble storage - The pebble storage tanks have the potential of losing forced circulation for a given period of time. Under these circumstances, the fuel temperatures will be calculated and radionuclides subsequently diffused. No holdup will be credited for radionuclides released to the storage tank.

7.3.4.2 Cover Gas Leakage

The KP-FHR operates at near ambient pressure. However, in a cover gas leakage event, the MAR from the cover gas and settled graphite dust are modeled as being released into the reactor building.

© 2020 Kairos Power LLC

[[

]]

7.3.4.3 Mechanical Damage

For mechanical stresses, such as crushing and pebble impacts, ARF products are based on loss of functional containment surrounding pulverized spent fuel fragments taken from the worst-case release fractions listed in NUREG/CR-6410, and listed in Table 7-3. These values are conservative for TRISO particles because the pebble and fuel matrix hold relatively little MAR and the TRISO coatings would minimize stress on most of the fuel kernels due to both the particles small spherical size and the high strength of the SiC layer in either an impact or crushing event involving the pebble.

The PHSS would stop operation upon detection of ongoing mechanical damage to the fuel pebble, consistent with design features described in Section 2.3.4.

[[

]]

7.4 BUILDING TRANSPORT MODELS

The KP-FHR source term methodology includes the RADTRAD code to model building transport. There are no changes to the RADTRAD governing equations. The description of the building transport models in this section includes how the gas is modeled for:

- Non-Risk-Significant AOOs and DBEs
- Risk-Significant AOOs and DBEs
- DBAs

If no distinction is provided, the model applies to all AOOs, DBEs, and DBAs.

7.4.1 RADTRAD Model Structure

RADTRAD is a simplified compartmental radioactive material transport code that is used to determine EAB dose estimates for the KP-FHR without modifying the code structure and only relying on models that are not LWR-specific. The following subsections will describe how a RADTRAD model is constructed.

7.4.1.1 Single Radionuclide Release

The KP-FHR source term methodology includes the RADTRAD model of a single source of radionuclides that are transferred into a single volume like the reactor building. The radionuclides are subject to a holding time in the building as described in Section 7.5.2 during which time radioactive decay (Section 7.4.2.2) and aerosol settling (Section 7.4.2.1) are modeled. $\frac{\chi}{Q}$ values mapping release from the "holdup" room (e.g., "two hour" DBA passive leakage assumption in the reactor building) to the environment.

A Symbolic Nuclear Analysis Package (SNAP) schematic of a single radionuclide source RADTRAD model is shown in Figure 7-6. This model structure is applicable to AOO, DBE, and DBA analyses.

7.4.1.2 Multiple Radionuclide Releases

Radionuclide sources for certain event sequences, such as vapor release from the primary system, dynamically change magnitude over the course of the transient. These releases can be modeled as a series of discrete, constant release rate sources that flow into the reactor building to conservatively represent the releases to the gas space. Each discrete source is passed into a "no-holdup" volume before combining the content of these volumes in the reactor building.

No aerosol deposition (see Section 4.1.2.1) is allowed in the "no-holdup" volume.

A SNAP schematic of a multiple radionuclide source RADTRAD model is shown in Figure 7-7. This model structure is applicable to AOO, DBE, and DBA analyses.

7.4.2 Release Models

7.4.2.1 Henry Correlation for Aerosol Deposition

The Henry correlation for aerosol deposition is the only modeled physical removal mechanism in the gas space. It does not explicitly model gravitational settling rates differently for different particle sizes. It correlates the removal rate to the aerosol density. The Henry correlation is provided in Equation 100 (Reference 10):

$$\lambda = C_1\left(\frac{h_{ref}}{h}\right)\left(\frac{\rho_p}{\rho_{p,ref}}\right)(\rho_A)^k \qquad \text{Equation 100}$$

where:

λ = the gravitational settling rate constant (1/hr)

h_{ref} = 5.0m, as determined from the ABCOVE test AB5

h = the user provided fall height in meters

ρ_P = the user-provided particle density in kg/m^3

$\rho_{p,ref}$ = the theoretical sodium oxide particle density of 2270 kg/m^3, as determined from the ABCOVE test AB5

ρ_A = the aerosol density in the volume, calculated by RADTRAD using Equation 101

$$\rho_A = \frac{\sum M_A}{V} \qquad \text{Equation 101}$$

where:

M_a = the mass of the aerosols in the volume calculated by RADTRAD

V = the user defined volume (the KP-FHR building volume must be large enough to conservatively bound the size of the beryllium enclosure).

The coefficients applied to the data are:

C_1= 0.022 and k=0.6 when $\rho_A \geq 6 \times 10^{-5}$ kg/m^3

C_1= 0.0016 and k=0.33 when $\rho_A < 6 \times 10^{-5}$ kg/m^3

The Henry correlation conservatively models aerosol deposition when applied to Flibe, carbon, and nitrate aerosols. The Henry correlation is fit to sodium combustion aerosol depositions measurements from ABCOVE AB5 tests (Reference 56) and is included in RADTRAD for generic aerosol gravitational deposition. A large fraction of the aerosols settled onto the floor of the AB5 experimental vessel. The aerosol density experienced in AB5 was bounded between 10^{-3} g/m^3 and 170g/m^3. When Flibe aerosols generated from vaporization in fusion reactors were measured, the particle diameters were recorded to range from 0.3 to 3 µm after 0.25s, which are within the lower range of sodium combustion particle sizes measured in AB5 and consistent with the default 1µm particle diameter for the Henry correlation (References 46 and 48) While only studied under a short timeframe for pulsed-fusion applications, agglomeration of these Flibe aerosols from smaller to larger particles and preferential settling of larger aerosols were observed between 0.001s and 0.25s demonstrating that the formation of larger aerosol size distributions should be expected if the distribution were allowed to continue to agglomerate and settle.

The implementation of the Henry correlation in RADTRAD only includes radioactive masses when calculating aerosol densities. The result of excluding non-radioactive aerosol masses will be an under-

© 2020 Kairos Power LLC

prediction of aerosol settling in the reactor building. RADTRAD cannot be used to track non-radioactive materials because the input and output files only tracks materials in terms of activities as opposed to masses or atoms.

The Henry correlation is only applied to aerosol settling in the reactor building where temperatures provide assurance that vapors will have condensed to aerosols. Gas transport in volumes where temperatures cannot be assumed to be low enough to condense aerosols (e.g., the cover gas region) do not use the Henry correlation, thus transporting vapors like gases.

The λ generated from the Henry correlation reduces the activity of the i^{th} isotope, A_i, in the gas space through Equation 102.

$$\frac{dA_i(t)}{dt} = -\lambda A_i(t) \qquad \text{Equation 102}$$

7.4.2.2 Radioactive Decay

Decay of radioactive materials is calculated by RADTRAD (Reference 10) using decay data from ICRP-38 (Reference 45). Consistent with RG 1.145, only radionuclides in ICRP-38 are carried into the RADTRAD analysis and thus no radionuclide decay constants are user-defined.

RADTRAD models radionuclide decay from the initiation of the transient. No portion of the KP-FHR source term methodology other than gas space transport incorporates radionuclide decay thus preventing double counting of the radionuclide decay's impact on the releases. This is consistent with LWR source term methodologies which hold radionuclide decay until the dose calculation component of the source term evaluation (Reference 7). Errors resulting from decay-based radionuclide group transitions will not impact the radioactive mass of a given radionuclide group by more than four percent within a thirty-day analysis window.

7.5 BUILDING TRANSPORT INPUTS

7.5.1 Activities of Radionuclide Sources

Activities are sourced into the gas space from salt vaporization, salt aerosolization, or direct release from the fuel handling system using the "activities per MW" RADTRAD input. The total number of MW is set to 1.0 to avoid unintentional scaling. RADTRAD treats all gases as gas and everything else as aerosols using the models described in Section 7.4 for the radionuclide groups described in Section 7.2.

If the Henry correlation is not used in a volume, aerosols will transport as gases. The Henry correlation will not be used in high temperature volumes, such as the cover gas, thus effectively modeling aerosol radionuclide transport as vapors in high temperature regions.

The timing of the release and the release duration into the reactor building is determined by the sequence boundary conditions. If the release cannot be modeled as a single, constant radionuclide release to the reactor building, the modeling structure in Section 7.4.1.1 represents the release.

There is no difference between how radionuclides are sourced for AOOs and DBEs versus DBAs.

© 2020 Kairos Power LLC

7.5.2 Volumetric Flow Rates

Volumetric flow rates can be impacted by heating, ventilation, and air conditioning (HVAC) systems as well as a temperature gradient between the beryllium confinement rooms and the rest of the auxiliary building. For buildings that are not designed to be "leak-tight", wind loadings on the exterior of the building can cause a "wind-tunnel" effect which can affect the gas leakage out of a given room. AOOs and DBEs will model room flow rates differently than DBAs.

For scenarios that model no holdup in a volume, the source term analysis models the "no effective holdup" as a leakage rate of 6.9 x 10^5 % volume per day (Reference 46).

7.5.2.1 Volumetric Flow Rates for AOOs and DBEs

[[

]]

7.5.2.2 Volumetric Flow Rates for DBAs

Volumetric flow rates for DBA calculations will be prescribed deterministically to ensure a conservative result. The reactor building is assumed to be a nonsafety-related structure, so additional holdup beyond a passive leakage rate in the building is not credited in DBAs. The beryllium confinement building's passive leakage rate is set to a value equivalent to releasing all radionuclides in the building within a two-hour window. This passive leakage rate is consistent with NRC guidance in Regulatory Guide 1.183 for analyzing an event during fuel handling operations in an LWR fuel building or in containment when containment is open. The DBA volumetric flow rate will assume a 2-hour holdup time consistent with guidance in RG 1.183, Appendix B.

The RADTRAD user's manual describes a method for translating the 2-hour holdup time in RG 1.183 to a constant leakage rate (Reference 46). The volume normalized form of the leakage rate (i.e., in percent volume per day as opposed to cubic feet per minute) is provided in Equation 103:

$$R(t) = e^{-Q_v t} \qquad \text{Equation 103}$$

where,

R(t) = the time-dependent retention concentration of the material in the volume atmosphere

Q_V = the fractional volumetric flow rate per hour

t = the time it takes to achieve that retention fraction.

© 2020 Kairos Power LLC

[[

]]

7.5.3 Aerosol Formation Heights

Aerosol formation heights are typically determined by the source of the aerosol creation. The Henry correlation ratios the problem-specific aerosol formation to the sodium spray source in the AB5 experiment which subsequently generated the sodium oxide aerosols. The higher the aerosol source in a room, the longer aerosols take to settle in that volume.

7.5.3.1 Aerosol Formation Heights for AOOs and DBEs

[[

]]

7.5.3.2 Aerosol Formation Heights - DBAs

[[

]]

7.5.4 Aerosol Particle Density

The particle density is set to:

- [[

]]

These values will be used for all AOOs, DBEs, and DBAs.

7.5.5 Atmospheric Dispersion Ratios

$\frac{\chi}{Q}$ values are determined by the ARCON96 code. The ARCON96 models are described in Section 7.7.

7.6 BUILDING TRANSPORT OUTPUTS

7.6.1 Worst Two-Hour Dose

DBA analyses require the worst two-hour doses to evaluate the source term against regulatory limits. RADTRAD computes the cumulative doses over a two-hour rolling window, reports the time period for the worst two-hour window, and provides the total effective dose equivalent (TEDE) over that time period (Reference 46).

7.6.2 Cumulative 30-day dose

KP-FHR source term analyses require the cumulative thirty-day doses for the KP-FHR LBEs. RADTRAD reports a summary of the cumulative TEDE doses over the simulation time. All RADTRAD simulations are run for a minimum of 30 days. If the TEDE dose is still rising after thirty days, the RADTRAD simulation is extended until any increase in TEDE dose is less than half a percent per day. The entire dose history is reported and the worst thirty-day TEDE will be reported as the AOO, DBE, and DBA thirty-day doses.

7.6.3 Release Fractions

The RF of the gas space is calculated using Equation 105.

$$RF_{GS} = \frac{D_{LBE\ Holdup}}{D_{No\ Holdup}} \qquad \text{Equation 105}$$

where:

RF_{GS} = the release fraction for the gas space

$D_{LBE\ Holdup}$ = the dose over the relevant time period assuming whatever LBE building holdup conditions are used

$D_{No\ Holdup}$ = the dose over the relevant time period assuming no holdup

7.7 ATMOSPHERIC DISPERSION MODELS

The KP-FHR source term methodology includes the governing equations used by ARCON96 as presented in the manual (Reference 9) for near-field dispersion analysis. All LBEs satisfy the applicable supporting requirements in the non-LWR PRA standard (Reference 47) or must justify why they are not applicable.

7.7.1 Selecting the Conservative Release Distance

ARCON96 calculates directionally dependent, time averaged $\frac{\chi}{Q}$s from the side of building from which radioactive material is being released to the specified dose receptor (i.e., the EAB). [[

]]

7.7.2 Calculation of the Time Averaged Percentile $\frac{\chi}{Q}$ Values

ARCON96 provides time averaged directional $\frac{\chi}{Q}$s at the 95th percentile. The 95th percentile directionally independent $\frac{\chi}{Q}$s are computed by setting the sector window to 360 degrees. The 99.5th percentile directionally dependent $\frac{\chi}{Q}$s are calculated from the complementary cumulative distribution functions provided in the standard outputs from ARCON96.

ARCON96 provides these complementary cumulative distribution functions in terms of the total number of one-hour periods that would produce a $\frac{\chi}{Q}$ greater than a given value. Dividing this frequency distribution by the total number of one-hour inputs produces the probability that the $\frac{\chi}{Q}$ would be greater than a given value. From this set of complementary cumulative distribution functions, the value for $\frac{\chi}{Q}$ is greater than 99.5 percent of the data, and can be determined for each time period (e.g., 0-1 hour, 0-2 hours, . . . , 0-720 hours).

© 2020 Kairos Power LLC

The $\frac{\chi}{Q}$ for a given time interval that does not start from zero can be calculated using the methodology in the ARCON96 manual (Reference 9), only using the ith percentile values instead of the 95th percentile values as shown in Equation 106.

$$\frac{\chi}{Q}^{i^{th}\%tile}_{t_1 \to t_2} = \frac{t_2 \frac{\chi}{Q}^{i^{th}\%tile}_{t_2} - t_1 \frac{\chi}{Q}^{i^{th}\%tile}_{t_1}}{t_2 - t_1} \qquad \text{Equation 106}$$

where:

$\frac{\chi}{Q}^{i^{th}\%tile}_{t_1}$ = the ith percentile $\frac{\chi}{Q}$ pulled from the complementary cumulative distribution functions averaged between zero and t_1

$\frac{\chi}{Q}^{i^{th}\%tile}_{t_2}$ = the ith percentile $\frac{\chi}{Q}$ pulled from the complementary cumulative distribution functions averaged between zero and t_2

$\frac{\chi}{Q}^{i^{th}\%tile}_{t_1 \to t_2}$ = the ith percentile $\frac{\chi}{Q}$ averaged between t_1 and t_2

[[

]]

7.7.3 Selecting the Conservative Release Wind Direction

For each release location, all 16 wind directions will be analyzed consistent with RG 1.145. For DBAs and non-risk-significant AOOs and DBEs, the most conservative wind direction is used to determine dose at the receptor using the 99.5th percentile $\frac{\chi}{Q}$ values. For risk-significant AOOs and DBEs, all 16 sectors are sampled uniformly to determine the distribution of site boundary dose.

7.8 ATMOSPHERIC DISPERSION INPUTS

This section describes ARCON96 input parameters and their treatment for LBEs.

7.8.1 Release Inputs

7.8.1.1 Release Height

For AOOs, DBEs, and DBAs where the release is assumed to occur via normal building leakage, the release height is set to zero meters. For AOOs, DBEs, and DBAs where the release is redirected by the HVAC system, the height of the release is set to the off-gas stack height. The corresponding stack radius, flow rates, and vertical velocities is set by system parameters of the off-gas system. Elevated

release sequences are less conservative than ground level release event sequences and thus ground level releases are bounding for all release types.

7.8.1.2 Building Area

[[

]]

7.8.2 Receptor Data

7.8.2.1 Direction to Source

The direction to source is the direction from the source to the receptor in degrees. This direction is the center of each 22.5 degree segment.

7.8.2.2 Distance to Intake

The distance to the intake (i.e., receptor) is the distance to the EAB for AOOs, DBEs, and DBAs. The release locations will be defined as a set of building walls closest to the EAB and thus the distance of the release location to the EAB, d, will be less than the total EAB distance, thus decreasing diffusion.

7.8.2.3 Intake Height

The height to the intake (i.e., receptor) is the height of the intake above ground level at the EAB for AOOs, DBEs, and DBAs. It is set to a ground level release of 0.0m for conservatism.

7.8.2.4 Terrain Elevation Difference

The terrain elevation difference is the difference in elevation between the reactor building and the EAB. This difference will be negative (e.g. the EAB fence-line should be at a lower elevation than the reactor building) with a magnitude that will be site specific. The magnitude of this value is either determined by the site or should bound a range of sites.

7.8.3 Meteorological Data

Meteorological data are input to ARCON96 using meteorological data files (Reference 9) and consistent with the guidance in RG 1.23. All meteorological data must have one record per hour.

7.8.3.1 Wind Direction Sector Width

The default sector width of the circumference of 22.5 degree arc is where the receptor is located (see Equation 107).

$$W_{s,max} = 2\pi d \frac{22.5}{360} \qquad \text{Equation 107}$$

where:

$W_{s,max}$ = the maximum sector width

d = the distance to the receptor from the release site within a default 90-degree window.

© 2020 Kairos Power LLC

7.8.3.2 Wind Direction Window

This parameter states the wind direction for the analysis. Wind directions are entered in degrees. A wind from the north is entered as 360 degrees and a wind from the south is entered as 180 degrees. To get a complete picture of the dose to possible receptors, ARCON96 must be executed 16 times (i.e., the number of degrees in a circle = 360 divided by the wind direction sector width = 22.5).

7.8.3.3 Minimum Wind Speed

The minimum wind speed used for all calculations is 5.0 (i.e., 0.5 m/s) and is the boundary below which winds are considered "calm" (Reference 9). Calm winds conservatively place the receptor directly downwind of the release point in ARCON96.

7.8.3.4 Surface Roughness

Surface roughness is set to a default 0.2m unless it is shown that it is more conservative to set a site-specific value.

7.8.3.5 Averaging Sector Width Constant

Averaging sector width constant is set to a recommenced value of 4.3 and is related to the appropriateness of the sector width value. This value is set to default unless it is shown that it is more conservative to set a site-specific value.

7.8.3.6 Initial Horizontal Diffusion

The initial horizontal diffusion coefficient is used to reduce conservatisms by defining the source over a virtual area. For DBAs and non-risk significant AOOs and DBEs, the initial horizontal diffusion coefficient, σ_y, is set to zero.

For risk significant AOOs and DBEs, σ_y is calculated by determining the radius of a virtual circle over which the release occurs and dividing that radius, r, by 2.15 to ensure that 90 percent of the plume is contained with the circle as shown in Equation 108.

$$\sigma_y = \frac{r}{2.15} \qquad \text{Equation 108}$$

7.8.3.7 Initial Vertical Diffusion

The initial vertical diffusion coefficient is used to reduce conservatisms by defining the source over a virtual area. [[

]]

7.9 DISPERSION OUTPUTS

7.9.1 Pre-calculated 95th percentile

ARCON96 reports 95th percentile Q values for five time intervals:

1. Zero to two hours
2. Two to eight hours
3. Eight to twenty-four hours
4. One day to four days
5. Four days to thirty days

[[

]]

7.9.2 Complimentary Cumulative Distribution Functions

By default, ARCON96 reports the complementary cumulative distributions of counts of weather data that produce a $\frac{\chi}{Q}$ greater than a given value averaged from zero to: 1, 2, 4, 8, 12, 24, 48, 96, 168, 360, and 720 hours. A plot of the raw data using the first sample problem provided by ARCON96 is shown in Figure 7-9.

By dividing these counts by the total number of weather trials provided to ARCON96, the complementary cumulative distributions are transformed from counts to percentiles, as shown in Figure 7-10. These curves are then used to calculate the time averaged $\frac{\chi}{Q}$ values needed for the RADTRAD analysis (see Section 7.7.2). The horizontal lines on Figure 7-10 denote the 95th and the 99.5th percentiles, respectively.

© 2020 Kairos Power LLC

Table 7-1 KP-FHR Radionuclide Groups and Representative Elements and Compounds for Gas Space Transport

[[

]]

Table 7-2 Pipe Break Assumptions in Aerosol Characterization Methodology Demonstration

Assumption	Properties
The leaked salt from the hot leg is at 650°C:	Density = 1963 kg/m^3, ρ = 2413 − 0.488T(K) [kg/m^3]
	Viscosity = 6.78x10^{-3} kg/m-s, $\mu = 1.16 \times 10^{-4} e^{3755/T(K)}$ [Pa-s = kg/m-s]
	Surface tension = 0.182 N/m, $\Upsilon = 260 - 0.12T(^oC)$ [dynes/cm] = 182 dynes/cm = 0.182N/m
Confinement gas properties at 0 barg and 57°C (330.15 K) and has the following properties:	Density = 1.07 kg/m^3
	Viscosity = 2.0x10^{-5} kg/m-s
Break properties	Loss Coefficient, C_D = 0.61
	Pipe diameter = 14 inches (full diameter break)
	Pipe at leak location is suspended 1 m off the ground
	Internal pressure at pipe break provides constant driving pressure of 2 bar gauge
Cover Gas	Slightly above atmospheric pressure

© 2020 Kairos Power LLC

Table 7-3 Summary of the 95th Percentile ARF from NUREG/CR-6410

Material Type	ARF
Noble Gases	7E-2
Tritium	1E-2
Iodine	2.5E-3
Cesium	2E-3
Fuel Fines	8E-7

© 2020 Kairos Power LLC

Table 7-4 Determination of B

ΔP (Pa)	A (m^2)	$Q_{D,PNNL}/D^{2.4}$	$Q_D \times B/D^{2.4}$	$B^{2.4}$	B
2.62E+06	3.14E-06	8.54E+04	2.72E+04	3.19E-01	0.62
2.62E+06	1.00E-05	2.14E+05	8.67E+04	4.05E-01	0.69
2.62E+06	2.00E-05	3.71E+05	1.73E+05	4.68E-01	0.73
2.62E+06	7.60E-05	1.07E+06	6.59E+05	6.17E-01	0.82
1.38E+06	3.14E-06	2.11E+04	7.07E+03	3.36E-01	0.63
1.38E+06	1.00E-05	5.28E+04	2.25E+04	4.27E-01	0.7
1.38E+06	2.00E-05	9.14E+04	4.50E+04	4.92E-01	0.74
1.38E+06	7.60E-05	2.64E+05	1.71E+05	6.49E-01	0.84
6.90E+05	3.14E-06	4.65E+03	1.65E+03	3.55E-01	0.65
6.90E+05	1.00E-05	1.16E+04	5.25E+03	4.51E-01	0.72
6.90E+05	2.00E-05	2.02E+04	1.05E+04	5.21E-01	0.76
6.90E+05	7.60E-05	5.82E+04	3.99E+04	6.86E-01	0.85

© 2020 Kairos Power LLC

Figure 7-1 Airborne Release Fraction and Sauter Mean Diameter as a Function of Pipe Pressure

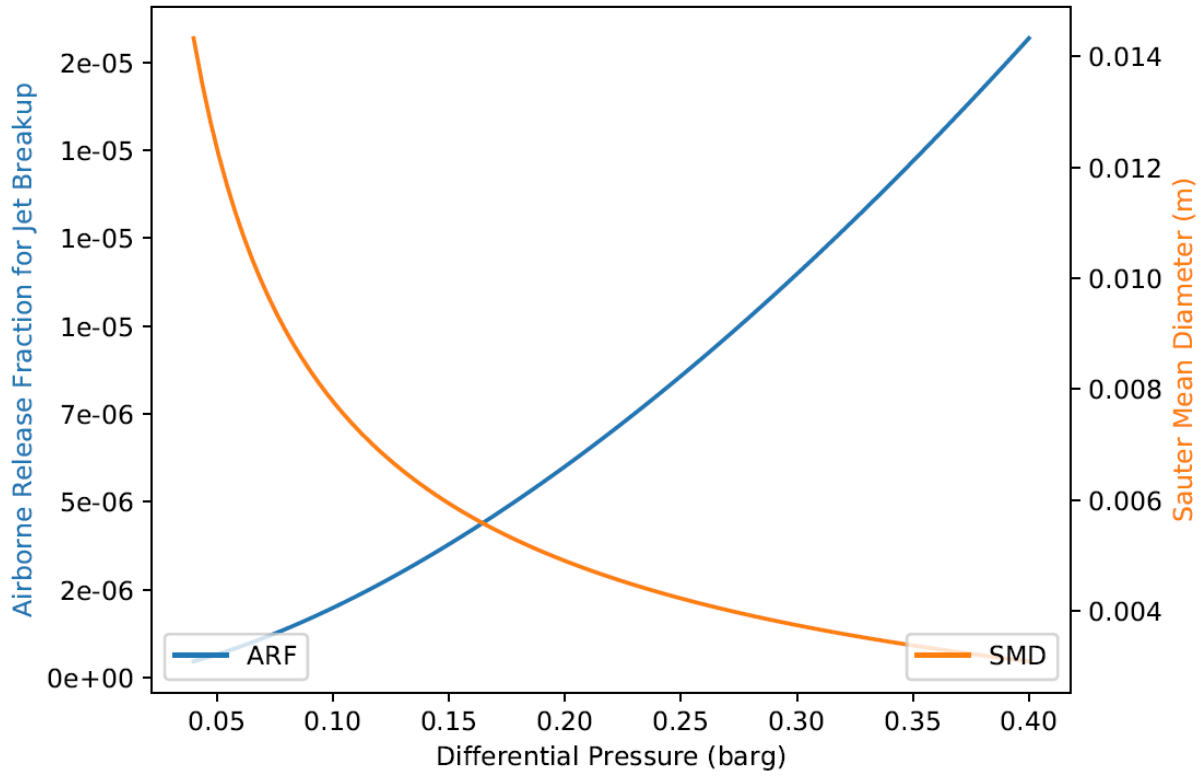

Figure 7-2 Initial and Impact Velocity of the Salt Given a One Meter Drop as a Function of Pressure

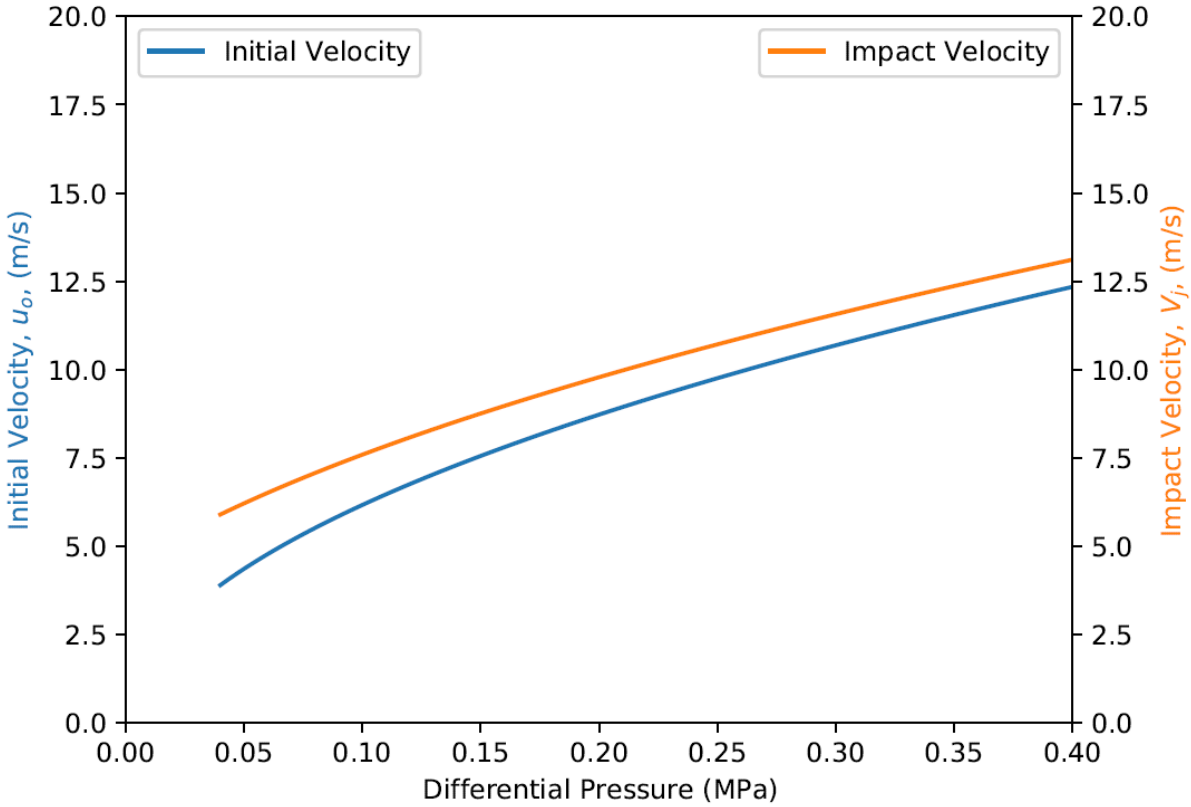

Figure 7-3 The Froude Number and the Gas Entrainment Rate as a Function of Pressure

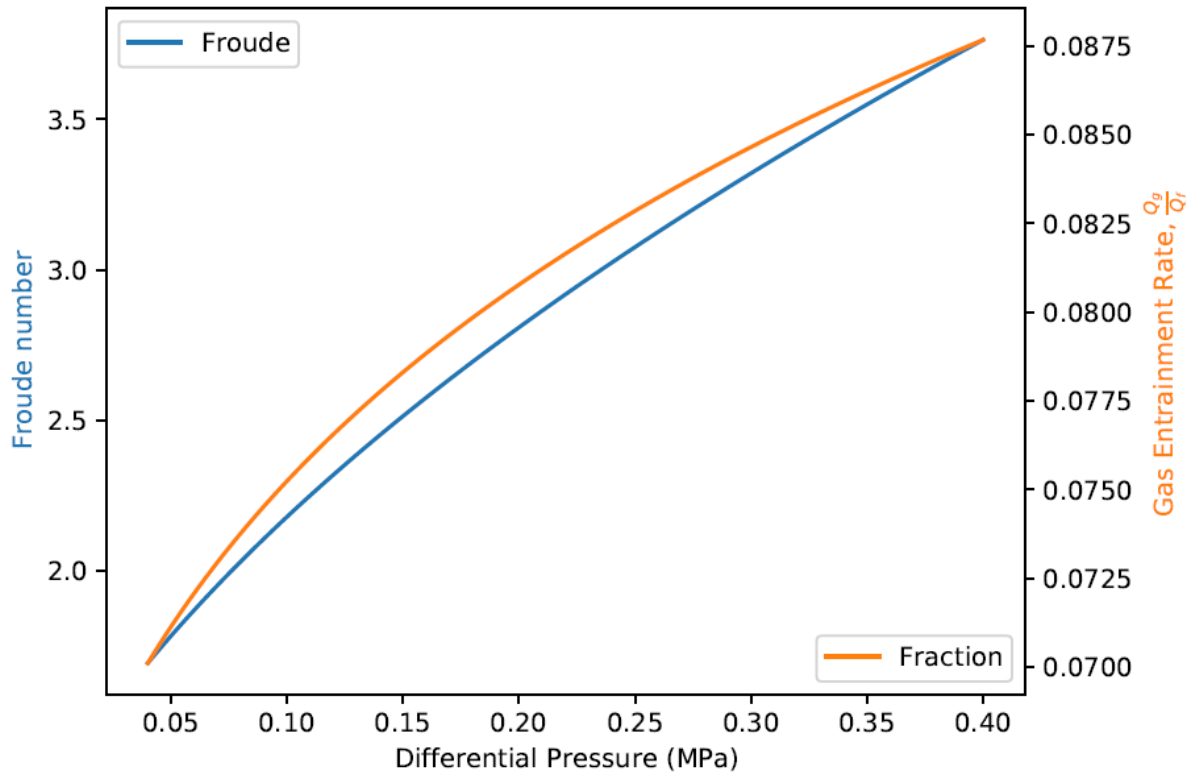

© 2020 Kairos Power LLC

Figure 7-4 Entrainment Coefficient for Bubble Burst Aerosols from Ginsberg

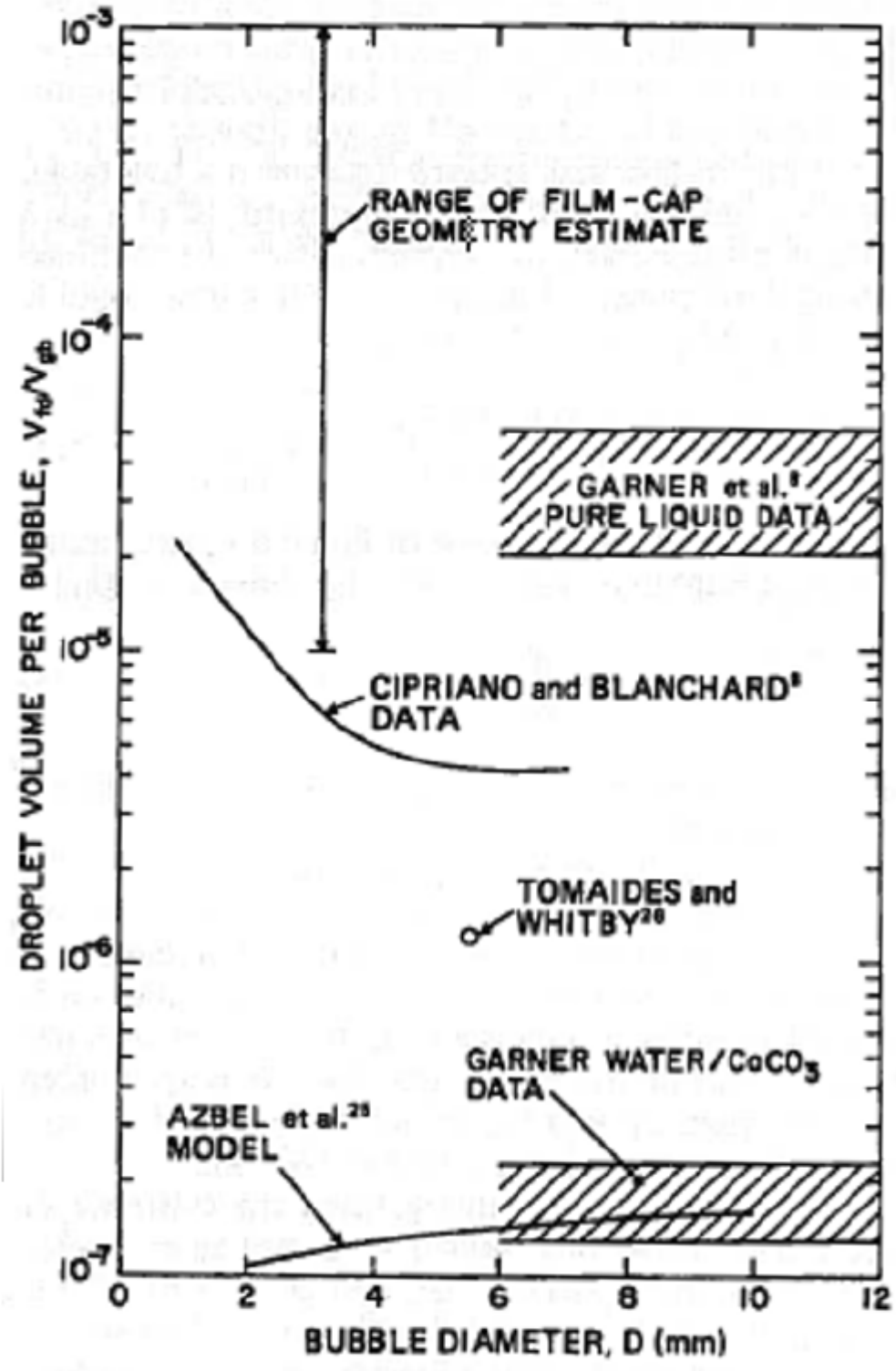

Figure 7-5 Airborne Release Fractions for a One Meter Drop Height as a Function of Pressure

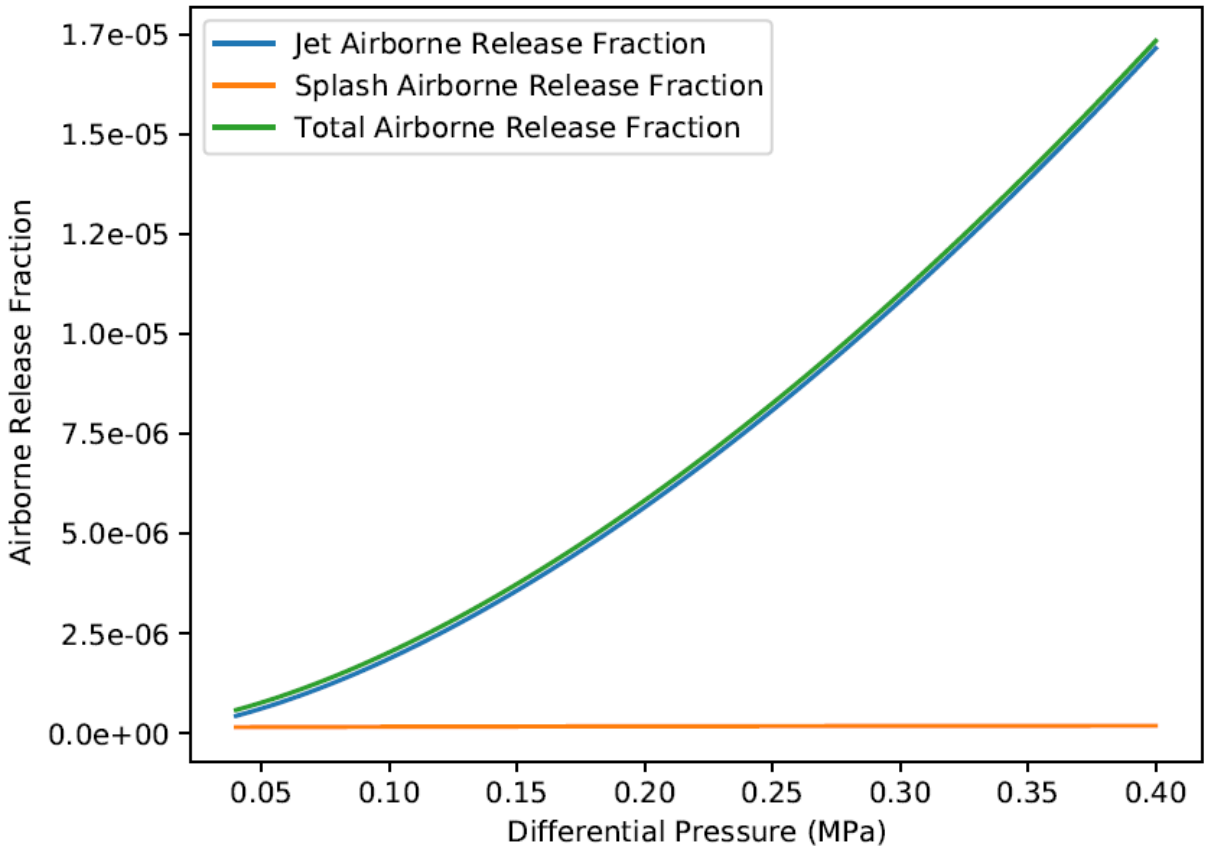

© 2020 Kairos Power LLC

Figure 7-6 A SNAP graphical schematic of a single source RADTRAD model

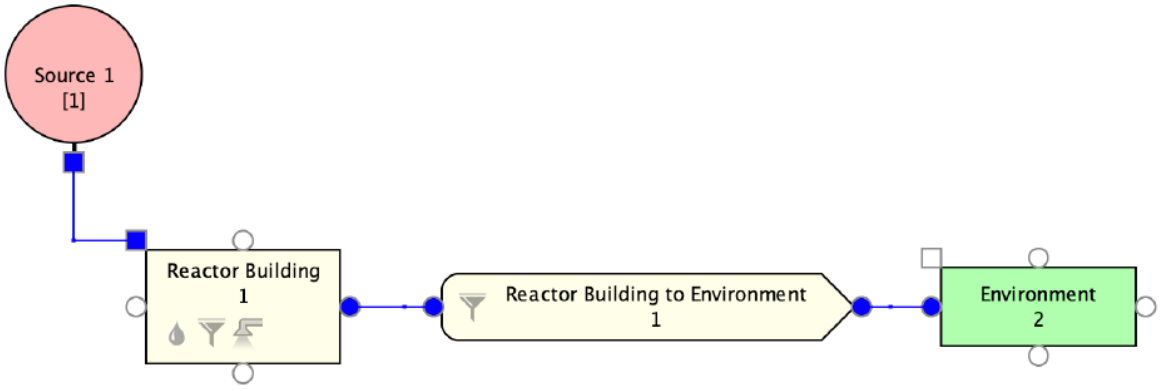

Figure 7-7 A SNAP Graphical Schematic of a Multiple Source RADTRAD model

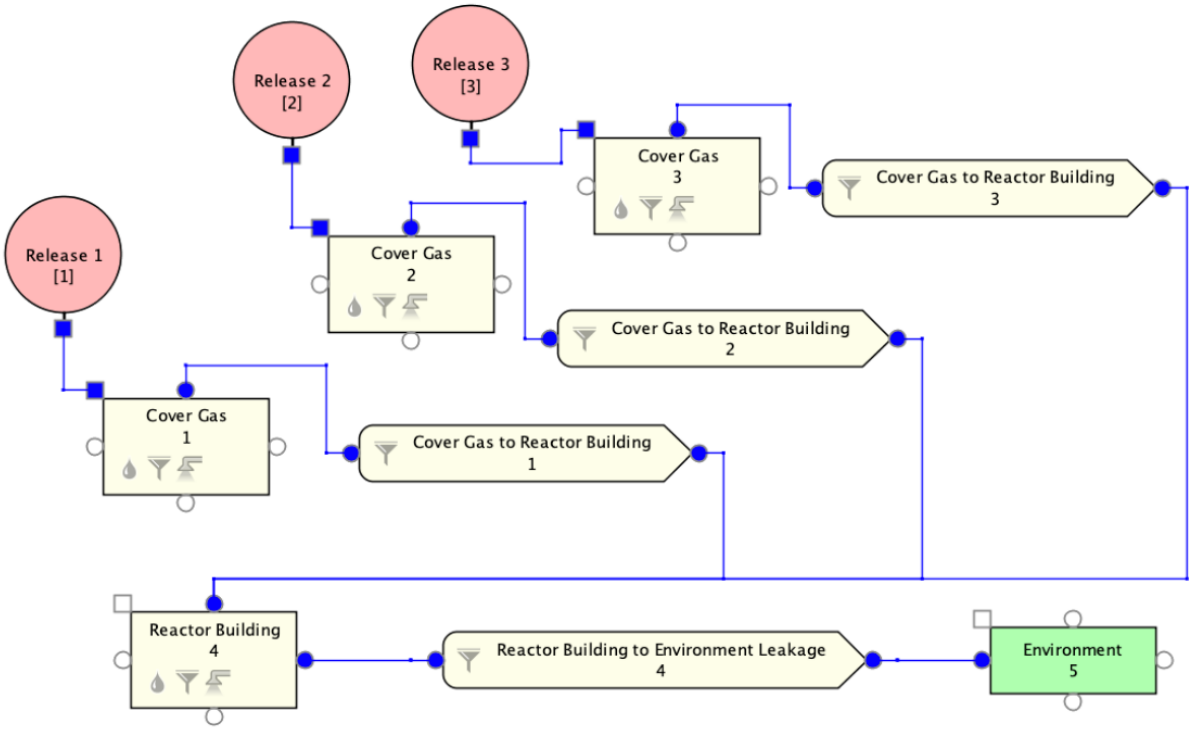

Figure 7-8 Notation for Tritium Flows in One Node of the Downcomer Region

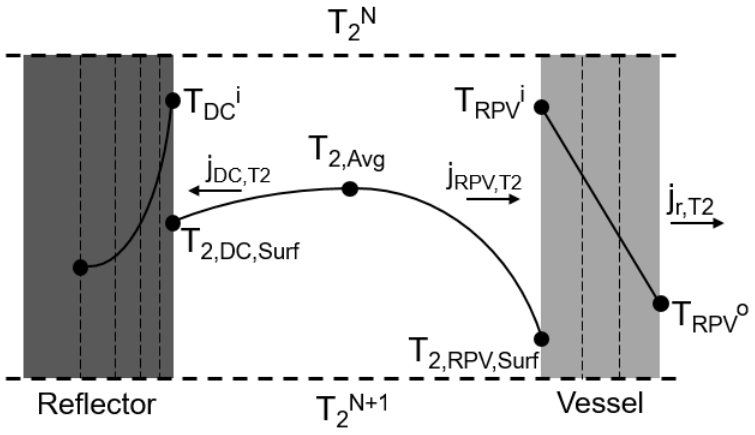

Figure 7-9 Raw Complementary Cumulative Distribution Produced by the SAMPLE problem in ARCON96

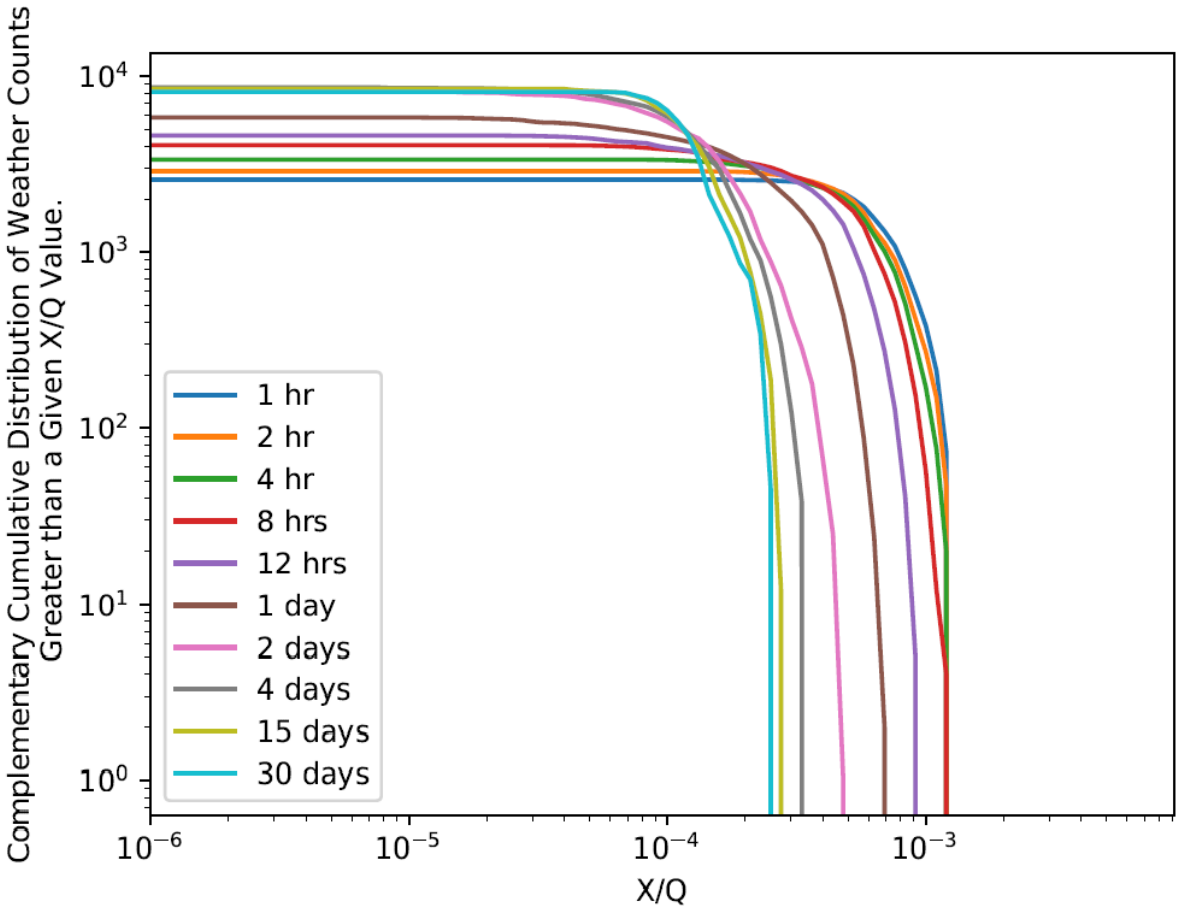

Figure 7-10 Complementary Cumulative Distribution Produced by SAMPLE Problem in ARCON95 With Counts Converted to Percentiles

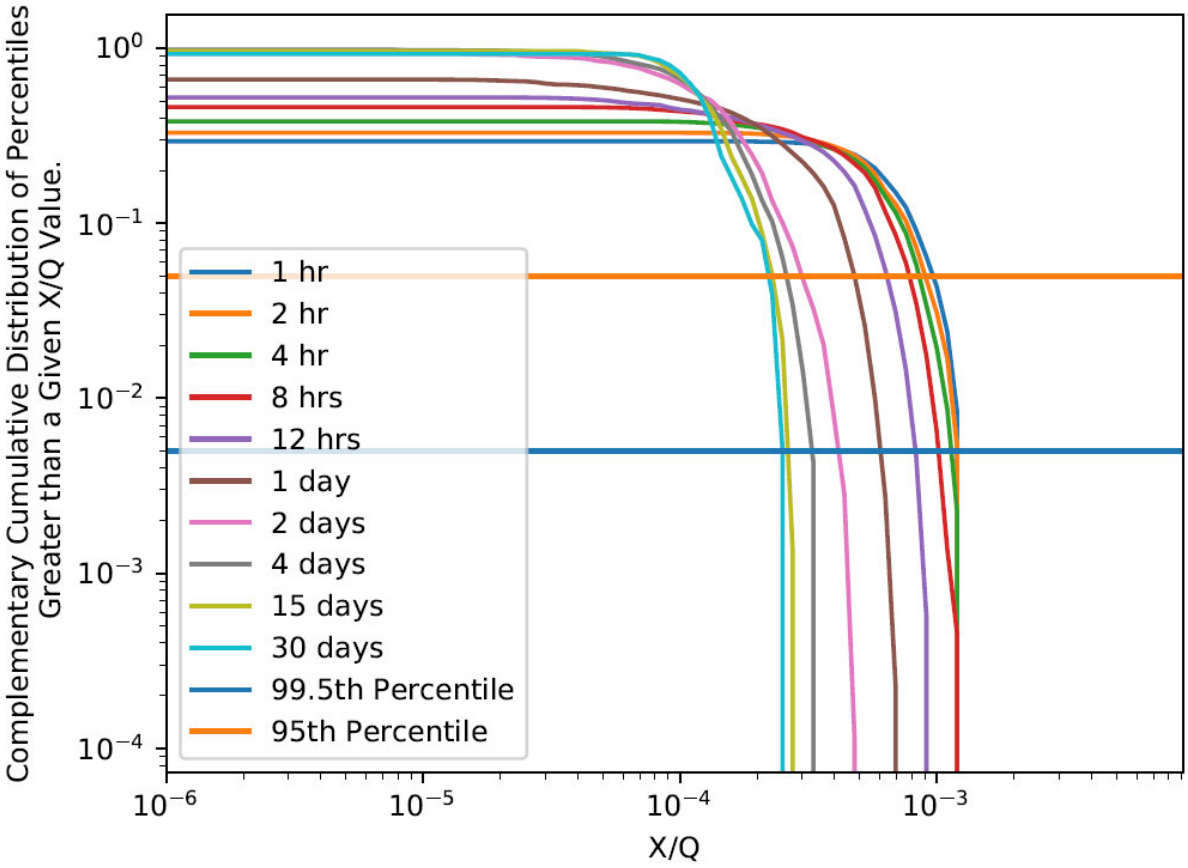

8 CONCLUSIONS AND LIMITATIONS

8.1 CONCLUSIONS

This report documents the mechanistic source term methodology to calculate off-normal radiological source terms and consequences for AOOs, DBEs, and DBAs for the KP-FHR. Kairos Power is requesting NRC approval of this methodology (subject to the limitations in Section 8.2 below) for use by licensing applicants of a KP-FHR as an appropriate means to calculate: consequences of AOOs and DBEs for evaluation of frequency-consequence targets and quantitative health objectives (QHOs); and source terms to evaluate DBA consequences to ensure that the KP-FHR meets the dose limits in 10 CFR 50.34. Such analyses are required by 10 CFR 50.34(a)(1)(D), 10 CFR 50.34(b)(1), 10 CFR 52.47(a)(2)(iv), 10 CFR 52.79(a)(1)(vi), 10 CFR 52.137(a)(2)(iv), 10 CFR 52.157(d). The evaluation of beyond design basis events is outside the scope of this topical report.

8.2 LIMITATIONS

This section describes limitations on the use of the source term methodology presented in this topical report. Each limitation must be addressed in safety analysis reports associated with licensing application submittals which use this methodology or justification provided for the item remaining open.

1. Approval of KP-Bison for use in fuel performance analysis as captured in Reference 4.
2. Confirmation of thermodynamic databases supporting chemical analysis of key radionuclides.
3. Validation of tritium transport modeling methodology.
4. Confirmation of minimal ingress of Flibe into pebble matrix carbon under normal and accident conditions, such that incremental damage to TRISO particles due to chemical interaction does not occur as captured in Reference 8.
5. Establishment of operating limitations on maximum circulating activity and concentrations relative to solubility limits in the reactor coolant, intermediate coolant, cover gas, and radwaste systems that are consistent with the initial condition assumptions in the safety analysis report.
6. Quantification of the transport of tritium in nitrate salt and between nitrate salt and the cover gas
7. The phenomena associated with radionuclide retention discussed in this report is restricted to molten Flibe. The retention of radionuclides in solid Flibe is beyond the scope of the current analysis.
8. The methodology presented in this report is based on design features of a KP-FHR provided in Section 1.2.2 and Section 2.3.4. Deviations from these design features will be justified by an applicant in safety analysis reports associated with license application submittals.

© 2020 Kairos Power LLC

9 REFERENCES

1. Kairos Power LLC, “Design Overview of the Kairos Power Fluoride Salt Cooled, High Temperature Reactor (KP-FHR),” KP-TR-001, Revision 1
2. Kairos Power LLC, “Testing and Development Program Overview for the Kairos Power Fluoride Salt Cooled, High Temperature Reactor”, KP-TR-002.
3. Leppänen, J., et al. (2015) "The Serpent Monte Carlo code: Status, development and applications in 2013." Ann. Nucl. Energy, 82 (2015) 142-150.
4. Kairos Power LLC, “KP-FHR Fuel Performance Methodology,” Topical Report, KP-TR-010-P.
5. ANL/NE-17/4, SAM Theory Manual, Argonne National Laboratory, March 2017
6. J. D. Hales, R. L. Williamson, S. R. Novascone, D. M. Perez, B. W. Spencer and G. Pastore, "Multidimensional multiphysics simulation of TRISO particle fuel," Journal of Nuclear Materials, vol. 443, pp. 531-543, 2013.
7. “Radionuclide Inventory and Decay Heat Quantification Methodology for Severe Accident Simulations,” Sandia National Laboratories, SAND2014-17667, September 2014.
8. Kairos Power LLC, “Fuel Qualification Methodology for the Kairos Power Fluoride Salt-Cooled High Temperature Reactor (KP-FHR)”, KP-TR-011.
9. “ARCON96 Code System to Calculate Atmospheric Relative Concentrations in Building Wakes,” Pacific Northwest National Laboratory, NUREG/CR-6331; PNNL-10521, May 1997.
10. W. Arcieri, D. Mlynarczyk, and L. Larsen, “SNAP/RADTRAD 4.0: Description of Models and Methods,” U.S. NRC, NUREG/CR-7220, June 2016.
11. M. Epstein and H. Fauske, “Applications of the turbulent entrainment assumption to immiscible gas-liquid and liquid-liquid systems,” Chemical Engineering Research and Design, vol. 79, no. 4, pp. 453–462, 2001.
12. M. Epstein and M. Plys, “Prediction of aerosol source terms for DOE site facility applications,” Proc. EFCOG Safety Analysis Working Group, April-May 2006.
13. A. K. Bi´ n, “Gas entrainment by plunging liquid jets,” Chemical Engineering Science, vol. 48, no. 21, pp. 3585–3630, 1993.
14. T. Ginsberg, “Aerosol Generation by Liquid Breakup Resulting from Sparging of Molten Pools of Corium by Gases Released During Core/Concrete Interactions,” Nuclear Science and Engineering, Taylor & Francis, vol. 89, no. 1, pp. 36–48, 1985.
15. F. Garner, S. Ellis, and J. Lacey, “The Size Distribution and Entrainment of Droplets,” Trans. Instit. Chem. Engrs., vol. 32, pp. 222–229, 1954.
16. R. J. Cipriano and D. C. Blanchard, “Bubble and aerosol spectra produced by a laboratory ‘breaking wave’,” Journal of Geophysical Research: Oceans, vol. 86, no. C9, pp. 8085–8092, 1981.
17. “MELCOR Computer Code Manuals Vol. 1 and 2: Reference Manual Version 2.2.9541 2017,” Sandia National Laboratories, SAND2017-0876 O, January 2017.
18. M. Kissane, F. Zhang, and M. Reeks, “Dust in HTRs: Its nature and improving prediction of its resuspension,” Nuclear Engineering and Design, vol. 251, pp. 301–305, 2012.

© 2020 Kairos Power LLC

19. “Uranium Oxycarbide (UCO) Tristructural Isotropic (TRISO) Coated Particle Fuel Performance” Topical Report EPRI-AR-1(NP), May 2019.
20. S. Whitaker, "Forced Convection Heat Transfer Correlations for Flow in Pipes, Past Flat Plates, Single Cylinders, Single Spheres, and for Flow in Packed Beds and Tube Bundles," AIChE Journal, vol. 18, no. 2, pp. 361-371, 1972.
21. K. Dolan, G. Zheng, D. Carpenter, S. Huang and L.-w. Hu, "Tritium content and chemical form in nuclear graphite from molten fluoride salt irradiations," Fusion Science and Technology, vol. (submitted), 2019.
22. H. Atsumi, "Hydrogen bulk retention in graphite and kinetics of diffusion," Journal of Nuclear Material, Vols. 307-311, pp. 1466-1470, 2002
23. H. Atsumi, T. Tanabe and T. Shikama, "Hydrogen behavior in carbon and graphite before and after neutron irradiation - Trapping, diffusion and the simulation of bulk retention," Journal of Nuclear Materials, vol. 417, pp. 633-636, 2011.
24. S. Lam, K. Dolan, W. Liu, R. Ballinger and C. Forsberg, "Weak and strong hydrogen interactions on porous carbon materials in high-temperature systems," Journal of Nuclear Materials, vol. 519, pp. 173-181, 2019.
25. “Fuel Performance and Fission Product Behavior in Gas Cooled Reactors,” International Atomic Energy Agency, TECDOC-978, November 1997.
26. H. Atsumi, S. Tokura and M. Miyake, "Absorption and Desorption of Deuterium on Graphite at Elevated Temperatures," Journal of Nuclear Materials, Vols. 155-157, pp. 241-245, 1988.
27. Y. Shirasu, S. Yamanaka and M. Miyake, "Thermodynamic analysis of hydrogen solubility in graphite," Journal of Nuclear Materials, vol. 200, pp. 218-222, 1993.
28. Haubenreich PN, Engel JR. Experience with the Molten-Salt Reactor Experiment. Nuclear Applications and Technology. 1970;8(2):118-36.
29. Bagri, Prashant, and Michael F. Simpson. "Determination of activity coefficient of lanthanum chloride in molten LiCl-KCl eutectic salt as a function of cesium chloride and lanthanum chloride concentrations using electromotive force measurements." Journal of Nuclear Materials 482 (2016): 248-256.
30. Kedl RJ. The Migration of a Class of Fission Products (Noble Metals) in the Molten Salt Reactor Experiment ORNL 3884. Oak Ridge National Laboratory; 1972. ORNL 3884.
31. Mathews AL, Baes CF. Oxide chemistry and thermodynamics of molten lithium fluoride-beryllium fluoride solutions. Inorganic Chemistry. 1968;7(2):373-82.
32. Honig RE. Vapor Pressure Data for the Solid and Liquid Elements. RCA Review. 1962; XXIII(4):567.
33. Lide DR. CRC Handbook of Chemistry and Physics: CRC Press; 2004.
34. Moritz to Baben B, Belisle, Cao, Chartrand, et.al. Factsage. 7.3 ed. Montreal, Quebec2019.
35. Determination of the vapor pressures of cesium fluoride and cesium chloride by means of surface ionization. Bull Chem Soc Jpn. 1984;57:581-2.

© 2020 Kairos Power LLC

36. A. Suzuki, T. Terai and S. Tanaka, "Tritium release behavior from Li2BeF4 molten salt by permeation through structural materials," Fusion Engineering and Design, Vols. 51-52, pp. 863-868, 2000.
37. A. Suzuki, T. Terai and S. Tanaka, "Change of tritium species in Li2BeF4 molten salt breeder under neutron irradiation at elevated temperature," Journal of Nuclear Materials, Vols. 258-263, pp. 519-524, 1998.
38. J. Stempien, "Tritium Transport, Corrosion, and Fuel Performance Modeling in the Fluoride-Salt-Cooled High-Temperature Reactor," Thesis: Ph. D, Massachusetts Institute of Technology, 12 May 2015. [Online]. Available: https://dspace.mit.edu/handle/1721.1/103727.
39. D. Olander, "Redox Condition in Molten Fluoride Salts Definition and Control," Journal of Nuclear Materials, no. 300, pp. 270-272, 2002.
40. P. E. Field and J. H. Shaffer, "The solubilities of hydrogen fluoride and deuterium fluoride in molten fluorides," The Journal of Physical Chemistry, vol. 71, pp. 3218-3222, 1967.
41. A. P. Malinauskas and D. M. Richardson, "The Solubilities of Hydrogen, Deuterium, and Helium in Molten Li2BeF4," Industrial & Engineering Chemistry Fundamentals, vol. 13, pp. 242-245, 1974.
42. R. E. Thoma, "Chemical Aspects of MSRE Operations," Oak Ridge National Laboratory, Oak Ridge, TN, 1971.
43. B. Kelleher, K. Dolan, M. Anderson and K. Sridharan, "Observed Redox Potential Range of Li2BeF4 Using a Dynamic Reference Electrode," Nuclear Technology, vol. 195, pp. 239-252, 2016.
44. C. F. Baes, "Symposium on Reprocessing of Nuclear Fuels," Nuclear Metallurgy, vol. 15, p. 617, 1969.
45. “Radionuclide Transformations – Energy and Intensity of Emissions,” ICRP Publication Ann. ICRP 11-13, 1983.
46. “Alion RADTRAD 3.10: User’s Manual,” Alion Science; Technology, ALION-UMG-RADTRAD-2408-02, Feb. 2007.
47. “Probabilistic Risk Assessment Standard for Advanced Non-LWR Nuclear Power Plants (DRAFT),” ANS/ASME, RA-A-1.4, Dec. 2020.
48. “A model for estimating the release rate of aerosol droplets from pressurized liquid leaks,”; Westinghouse Hanford Co. Report, WHC-SD-GN-TI-30003, 1992.
49. “U.S. Department of Energy Pressurized Spray Release Technical Report,” U.S. Department of Energy, AU-30-RPT-02, April 2019.
50. F. Garner, S. Ellis, and J. Lacey, “The Size Distribution and Entrainment of Droplets,” Trans. Instit. Chem. Engrs., vol. 32, pp. 222–229, 1954.
51. E. Mayer, “Theory of liquid atomization in high velocity gas streams,” ARS Journal, vol. 31. Pp.1783-1785, 1961.
52. “Large-Scale Spray Releases: Additional Aerosol Test Results,” Pacific Northwest National Laboratory, PNNL-22415, WTP-RPT-221 Rev. 0, August 2013.
53. GCRA, “Preliminary Safety Information Document for the Standard MHTGR,” Gas-Cooled Reactor Associates, Report HTGR-86-024, January 1986.

© 2020 Kairos Power LLC

54. “Clinch River Nuclear Site Early Site Permit Application, Part 2, Site Safety Analysis Report, Revision 2,” Tennessee Valley Authority, January 2019.
55. Mathews, A. L., and Charles F. Baes Jr. "Oxide chemistry and thermodynamics of molten lithium fluoride-beryllium fluoride solutions.” Inorganic Chemistry 7.2 (1968): 373-382.
56. R. K. Hilliard, J. D. McCormack, and A. K. Postma, “Results and code predictions for ABCOVE aerosol code validation - Test AB5,” Nov. 1983.

© 2020 Kairos Power LLC

APPENDIX A. SAMPLE SOURCE TERM CALCULATION: ANTICIPATED OPERATIONAL OCCURRENCE

A.1 SAMPLE CALCULATION

This anticipated operational occurrence sample calculation is for a large Flibe leak and is provided to illustrate the KP-FHR source term methodology presented in this topical report. The design details included in this Appendix are not intended to reflect final KP-FHR design details, and Kairos Power is not requesting NRC approval of the results of this calculation. This sample calculation is provided to illustrate the KP-FHR source term methodology presented in this topical report.

A.2 EVENT DESCRIPTION

The initiating event is a large pipe break in the hot-leg of the primary coolant loop, allowing a Flibe to leak out. The control rod and/or shutdown blades insert into the core to stop additional fission energy and the primary pumps trip causing primary system flow to coast down with the flow inertia of the system. The reactor vessel isolates, and the normal decay heat removal system starts to remove excess energy from the fuel pebbles, graphite structures, and reactor vessel.

The fuel and Flibe are then assessed for releases to a gas space such as the reactor building. Once in the building, aerosols may gravitationally settle onto surfaces and both gases and aerosols will leak out of the building to the environment. The system is designed to accommodate such an event while preventing excessive Flibe level loss in the vessel, and significant air ingress from the reactor building back into the vessel to preclude the displacement of argon cover gas beyond operating limits.

This sample problem is intended to illustrate methods presented in this topical report. However, the design information used in the calculation are not final KP-FHR design inputs, and certain areas of the methodology were simplified with conservative assumptions. These assumptions include:

- A higher activity in the Flibe based on a continuous accumulation of radionuclides over an assumed 20-year Flibe design life.
- Conservative heavy metal contamination transport assumptions in the fuel
- Tritium transport is not explicitly modeled according to the methodology presented in this topical report. The tritium contribution is conservatively modeled as an instantaneous “puff” release.

The following design inputs are assumed for the sample calculation in addition to the design features assumed in the methodology:

- The cover gas pressure is approximately 0.03 MPa gauge.
- The primary pump pressure head is 0.2 MPa during normal operation
- The HVAC system is tripped (i.e., conservatively assumed failed) at the event initiation.
- Pipes at break location are assumed to be suspended 5 meters above ground and 3 meters below the primary pumps.
- It is assumed that the KP-FHR has no tritium permeation barrier coatings (i.e. permeation reduction factor equals 1.0). The salt activity is determined by using:
    - the steady state tritium concentration of 6.12×10^{-6} mol-T/m^3 or 0.177 Ci-T/m^3
    - the assumed quantity of salt in the primary system of 105,400 kg

© 2020 Kairos Power LLC

- the density of salt at 900K (ρ = 2413 − 0.488T (K)) of 1973.8 kg/m^3

The tritium MAR distributed throughout the primary system is shown in Table A-1. It is assumed that the tritium concentrations have reached steady state saturation conditions by 4.75 years and that these numbers can be applied to a 20-year core. However, structural graphite tritium inventories are still slowly growing in time at 4.75 years and these numbers assume no shutdown or maintenance time which would allow for desorption of structural tritium.

- The mass of the Flibe in the reactor is assumed to be 105,403 kg with a 15,000 kg leak from the hot leg. The flow loss coefficient is C_D = 0.61 and the pipe diameter is 14 inches. The leaked salt from the hot leg is assumed to be 923.15 K with a density of 1963 kg/m^3, viscosity of 6.78x10^{-3} kg/m-s and a surface tension of 0.182 N/m. Confinement gas properties at 0 barg and 57^{o}C (330.15 K) provide the standard properties of air: a density of 1.07 kg/m^3 and a viscosity of 2.0x10^{-5} kg/m-s.
- The system is designed such that it can accommodate a large salt spill while maintaining system temperatures such that the release of tritium from structures can be approximated from steady state degassing rates (i.e., 340 Ci/day). This rate, which exclude tritium transport through the intermediate heat exchangers (IHXs) due to the pipe break and corresponding pump trips, which quickly isolate most of the tritium from the IHX, is conservatively represented by: a pebble recirculation removal rate of 150 Ci/day, a hot leg release rate of 80 Ci/day, a reactor pressure vessel release rate of 60 Ci/day and a cold leg release rate of 50 Ci/day.

A.3 SOURCE TERM EVALUATION

The MAR for this sample event are identified using the methods presented in this topical report. The barriers identified that release MAR during this event sequence are the structures such as graphite and steel, Flibe coolant, and gas space (i.e., buildings and off-site dispersion). TRISO fuel contributes to steady state MAR that contributes to the MAR within the coolant. This section provides the quantification of MAR in each barrier, the attenuation factor evaluations, the atmospheric dispersion calculation, and the resulting dose at the EAB.

A.3.1 Evaluation of Releases from the Fuel

Most of the non-tritium radionuclides in the Flibe are diffused into the Flibe over the operating life of the core. Hence, understanding what constituents are assumed to leak into the Flibe is key to understanding Flibe MAR. The TRISO particles are the primary retention mechanism for fission products in the KP-FHR as detailed in this topical report. The MAR in the TRISO particle is held up by the fuel kernel and its three protective barriers. These layers have varying manufacturing and in-service defect fractions that impact their radionuclide retention functions during steady state operations.

The left-hand portion of Figure 2-1 in the topical report graphically depicts the primary cohorts of TRISO particles. These cohorts will determine the amount of MAR contained in fuel pebbles as opposed to being bound up in the Flibe. Fission products from exposed kernels in-service failures and failed SiC layer TRISO particle types are released into the Flibe coolant prior to the transient. The inventory is based on the parameters defined in Table A-5.

© 2020 Kairos Power LLC

A.3.2 Evaluation of Releases from Flibe

Flibe MAR consists of circulating activity originating from irradiation of uranium and thorium impurities in the coolant, a slow accumulation of the pebbles' heavy metal contamination and fission products, and activation products in the coolant. Radionuclides in the Flibe take four primary forms: salt soluble fluorides, noble metals, oxides and dissolved gases.

It is assumed that MAR will transition from the spilled Flibe into the gas space proportional to MAR that exists in the hot-leg pipe. In order to determine the cumulative ARF for the pipe break accident, the quantities must be determined for the pressure history of the break location due to pump coast-down, the instantaneous quantities for mass flow rate out of the break, ARF for the leaking Flibe, aerosol formation rates as well as integral quantities for the mass flow rate out of the break, ARF for the leaking Flibe and aerosol formation rates.

For this sample calculation, a pre-determined amount of Flibe is assumed to be available to leak. Once the leak reaches that integral quantity of leaked Flibe, the leak is assumed to end.

Aerosolization of the bulk fluid Flibe mobilizes non-gas radionuclides without separating them from the Flibe. Gas radionuclides are separated from the Flibe aerosols and travel as gases. All radionuclide groups are assumed to move into the gas space in the same proportions to the Flibe as they exist in the circulating coolant.

However, the leaked Flibe must be broken into small enough particles to facilitate gas transport. All non-aerosolized Flibe is assumed to pool and freeze in the reactor building. The fraction of spilled Flibe that aerosolized for subsequent gas transport is known as the Airborne Release Fraction (ARF). ARFs will change as a function of break pressure and therefore must be evaluated continuously over the duration of the leak. As such, a time dependent model of break pressure and corresponding flow rates will be required to assess the integral ARF.

Flibe aerosolization occurs through two pathways: aerosol generation from jet breakup of Flibe leaving the pipe and from splashing of the Flibe jet once it impacts a surface. The ARF for jet breakup and splash breakup of Flibe is computed in accordance with the methodology provided in this topical report.

A.3.3 Evaluation of Releases from Structures

Tritium is the only modeled MAR to be held up in the structures such as the pebbles, structural graphite, vessel, hot-leg piping, cold-leg piping, and IHXs. All other radionuclides that can be held up in the structures are assumed to be de minimis. Table A-1 displays the inventories of tritium MAR assumed in this calculation for structures, which is consistent with no permeation reduction coatings.

In steady state, tritium is constantly sorbed and desorbed by various structures producing steady state holdup inventories of tritium MAR. During the transient, the reactor SCRAMs and the production rate of tritium drops to effectively zero. The structures will then desorb their stored tritium into neighboring fluids (e.g., Flibe or gas). This process is limited by the relative concentrations of tritium in the structures and the neighboring fluids.

© 2020 Kairos Power LLC

While the normal decay heat removal system is working, system temperatures are kept at or below operational limits for Reactor Vessel Auxiliary Cooling System (RVACS) actuation and tritium desorption rates can be bounded by extrapolating steady state transfer rates. During a pipe break, the associated primary pump trip will effectively cut off the IHXs from being effective tritium removal pathways because primary flow through these heat exchangers are shut off. By not crediting tritium removal through the IHX, tritium is assumed to desorb from the system's structures at approximately 340 Ci/day. All tritium desorbed from the structures are conservatively assumed to directly transfer into the reactor building.

A.3.4 Evaluation of Gas Space Releases and Atmospheric Transport

The gas space is the only barrier that accepts MAR from other barriers. Radionuclide transport into the gas space can occur through congruent vaporization of the Flibe pool, congruent and reactive vaporization of the spilled Flibe pool, mechanical aerosolization of Flibe, and desorption of tritium from the graphite structures, fuel pebbles, vessels, pipes, and IHXs.

Radionuclide release is assessed for the various gas space barriers with building release models and atmospheric dispersion models. RADTRAD is used to calculate release in the reactor building.

The key inputs to RADTRAD are radionuclide activities being sourced into rooms in the reactor building, gas transport rates from room to room and $\frac{\chi}{Q}$ values to convert release from the building to doses at the site boundary or other areas of interest. The key outputs of RADTRAD are the worst two-hour dose (for DBAs), and thirty-day dose (for Licensing Basis Events (LBEs) that are AOOs or DBEs). Radionuclides coming out of the Flibe and structural materials will be sourced immediately into the reactor building.

The reactor building is assumed to have a leakage rate of one percent per day radionuclides can attenuate by gravitational settling of aerosols and radioactive decay of all radionuclides.

Transport within the gas space is divided into a building transport model and an atmospheric dispersion model. The building model requires four inputs aside from the Flibe releases and $\frac{\chi}{Q}$ calculated for this sequence to calculate the building releases. The model requires gas flow rates, room volume, the Henry Correlation and the aerosol release height. The reactor building is assumed to be 1000 m^3. A leak rate and flow rate consistent with the methodology will be used and the Henry correlation will use the density of Flibe and aerosol release height consistent with the methodology and the assumptions made in Section A.2.

The mass of Flibe aerosol generated from the break is calculated in Equation A2. Figure A-1 shows the time history of liquid and aerosol Flibe entering the reactor building; only the aerosol Flibe enters the gas space. When the mass of Flibe leaking out of the break reaches 15,000 kg is calculated in Equation A1:

$$M_f = \int_{t=0}^{t_{crit}} u(t) \frac{\pi D^2}{4} \rho_f dt = 15{,}000 \qquad \text{Equation A1}$$

where:

$M_f(t)$ = the mass of Flibe leaking out of the break (kg)

$u(t)$ = the break flow velocity (m/s)

D = the pipe diameter (m)

ρ_f = the fluid density (kg/m^3)

t = time (s)

The break flow velocity $u(t)$ is calculated using Equation 75 of this topical report.

The integrated aerosol generated is a function of M_f and ARF(t):

$$M_a = \int_{t=0}^{t_{crit}} M_f(t) \times ARF(t)\, dt \qquad \text{Equation A2}$$

where:

M_a = the mass of total aerosol generated in kg

ARF(t) = the ARF at time t; is the sum of ARF from jet breakup and splash aerosolization

The cumulative ARF is calculated by dividing the total aerosol mass generated by the total liquid Flibe mass leaked. Using the RF and ARF values calculated above, Table A-2 summarizes the computation of the input to the gas space MAR.

The radionuclides that contributed doses above 2.5x10^{-5} rem are shown for both AOO conditions in Table A-3 Radionuclides for AOO Leakage Conditions that Produce a Thirty Day TEDE Above 2.5E-05 rem and no holdup conditions in Table A-4 Radionuclides for No Holdup Leakage Conditions that Produce a 30 Day TEDE Above 2.5E-05 rem. These results will be used to calculate the gas and aerosol release fractions. In these lists, the only gas that contributes dose above 2.5x10^{-5} rem is tritium, all other radionuclides will transport as aerosols.

The release fraction for the AOO structural desorption of tritium is calculated using the 30-day tritium dose for AOO building leakage (10.1 mrem), the 30-day tritium dose for no holdup building leakage (76.5 mrem) and the release fraction for the gas space ($\frac{10.1\ mrem}{76.5\ mrem} = 0.132$). The release fraction for the AOO aerosols resulting from a salt spill of 15,000 kg of hot leg Flibe is calculated using the 30-day aerosol dose for AOO building leakage (0.37 mrem), the 30-day aerosol dose for no holdup building leakage (32 mrem) and the release fraction for the gas space ($\frac{0.37\ mrem}{32\ mrem} = 0.012$).

A.4 CONCLUSIONS:

Table A-6 presents the 30-day RF for various radionuclide groups for individual barriers and multiplied across all barriers. The 30-day dose for this scenario as calculated by this evaluation is 10.5 mrem. This dose is dominated by a conservative, non-mechanistic release of tritium from sorbed

© 2020 Kairos Power LLC

structures such as graphite, reactor vessel, piping, and the IHX. Aerosols from the spill contributed only 0.36 mrem of dose dominated by Pu-238 which is produced by transmuting a combination of dispersed uranium released by the pebble matrix which is given no credit for radionuclide holdup and uranium impurities inherent in the Flibe upon initial salt loading.

In order for this accident sequence to be considered non-risk significant, the frequency of occurrence for this pipe break should be shown to be less than 9.6×10^{-2} events per reactor year.

© 2020 Kairos Power LLC

Table A-1 Tritium Distribution in Primary System with no Permeation Barrier Coatings at 4.75 Years

Component	Salt	Pebble	Reflector	Reactor Vessel	Hot and Cold Leg Piping	Intermediate Heat Exchanger
Inventory (Ci)	9	4743	1181	320	60	55

© 2020 Kairos Power LLC

Table A-2 Summary of the Activity Transmission from Flibe to Gas Space

Total Flibe (kg)	Release Fraction for Spilled Flibe	Time for Spill to Complete (s)	Total Aerosol Mass Released (kg)	Total Aerosol Airborne Release Factor
1.05403E+05	1.42E-01	1.18E+01	5.11E-02	3.4E-06

© 2020 Kairos Power LLC

Table A-3 Radionuclides for AOO Leakage Conditions that Produce a Thirty Day TEDE Above 2.5E-05 rem

Radionuclides	EAB Dose (rem)
Total	1.047E-02
H-03	1.010E-02
Pu-238	1.300E-04
Cm-244	1.000E-04
Cm-242	9.000E-05
Pu-241	6.000E-05

© 2020 Kairos Power LLC

Table A-4 Radionuclides for No Holdup Leakage Conditions that Produce a 30 Day TEDE Above 2.5E-05 rem

Radionuclides	EAB Dose (rem)
Total	1.0847E-01
H-3	7.6500E-02
Pu-238	9.8000E-03
Cm-244	7.3600E-03
Cm-242	6.7500E-03
Pu-241	4.4700E-03
Am-241	1.5600E-03
Sr-90	8.2000E-04
Pu-239	3.9000E-04
Pu-240	3.2000E-04
Ce-144	1.4000E-04
Am-242m	1.1000E-04
Am-243	8.0000E-05
Cm-243	7.0000E-05
Cs-134	4.0000E-05
Am-242	3.0000E-05
Eu-154	3.0000E-05

© 2020 Kairos Power LLC

Table A-5 Source Term Inventory Calculation Parameters

Inventory	Year (yr)	Fraction of HMC Released	Fraction of Fission Product Released	U Impurities (ppm)	Th Impurities (ppm)
6th Pass	20	1E-05	1.96E-04	2	1

© 2020 Kairos Power LLC

Table A-6 Summary of Release Fraction Values for Various Radionuclide Groups Across Various Barriers

RN Group	Structures/Pebbles	Flibe	Building	Total
Gas (tritium)	1.0	1.0E+00	1.32E-01	1.32E-01
Gas (other)	de minimis	3.4E-06	2.53E-02	8.63E-08
All Other Groups	de minimis	3.4E-06	1.16E-02	3.94E-08

© 2020 Kairos Power LLC

Figure A-1 Mass of Aerosol Generated from the Leak as a Function of Time

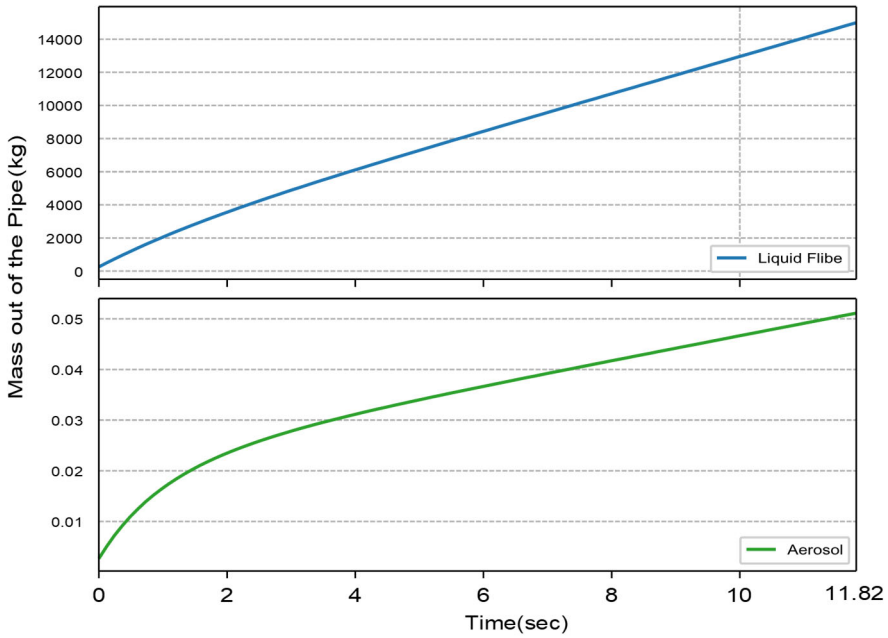

APPENDIX B. SAMPLE SOURCE TERM CALCULATION: DESIGN BASIS ACCIDENT

B.1 SAMPLE CALCULATION

This appendix provides a sample design basis accident consequence analysis assuming a loss of all AC power and normal decay heat removal with subsequent RVACS operation. This sample calculation is provided to illustrate the KP-FHR source term methodology presented in this topical report. The design details included in this Appendix are not intended to reflect final KP-FHR design details, and Kairos Power is not requesting NRC approval of the results of this calculation.

B.2 EVENT DESCRIPTION

The initiating event is a station blackout (loss of all AC power) which disables normal decay heat removal capability. The operation of the nonsafety-related control rods is not credited. The shutdown blades insert into the reactor to stop additional fission energy and the RVACS valves automatically fail open to remove decay heat from the vessel via radiative heat transfer to water panels positioned along the side of the vessel. The fuel, Flibe, and structures are then assessed for releases to the gas space. Radionuclides that enter the cover gas region are transported with no holdup to the reactor building. Once in the reactor building, some aerosols may gravitationally settle and both gases and aerosols will leak out of the reactor building to the environment using the conservative DBA leakage assumptions. Radionuclides and cover gas leak from the system, but there is negligible counter-current flow that leads to significant air intrusion into the system.

This sample problem is intended to illustrate methods presented in this topical report. However, the design information used in the calculation are not final KP-FHR design inputs, and certain areas of the methodology were simplified with conservative assumptions. These assumptions include:

- A higher activity in the Flibe based on a continuous accumulation of radionuclides over an assumed 20-year Flibe design life.
- Conservative heavy metal contamination transport assumptions in the fuel
- Tritium transport is not explicitly modeled according to the methodology presented in this topical report. The tritium contribution is conservatively modeled as an instantaneous “puff” release.
- Reactor buildings and filters that will provide additional aerosol scrubbing are not accounted for in this calculation.

The following design inputs are assumed for the sample calculation in addition to the design features assumed in the methodology:

- Consistent with the DBA leakage assumption of the methodology, the HVAC system is assumed to trip at the beginning of the DBA.
- It is assumed that the KP-FHR has no tritium permeation barrier coatings (i.e. permeation reduction factor equals 1.0). The salt activity is determined by using:
    - the steady state tritium concentration of 6.12×10^{-6} mol-T/m^3 or 0.177 Ci-T/m^3
    - the assumed quantity of salt in the primary system of 105,400 kg

© 2020 Kairos Power LLC

- the density of salt at 900K ($\rho = 2413 - 0.488T$ (K)) of 1973.8 kg/m^3

The tritium MAR distributed throughout the primary system is shown in Table B-1. It is assumed that the tritium concentrations have reached steady state saturation conditions by 4.75 years and that these numbers can be applied to a 20-year core. However, structural graphite tritium inventories are still slowly growing in time at 4.75 years and these numbers assume no shutdown or maintenance time which would allow for desorption of structural tritium.

- There are 105,400 kg of Flibe in the system available for evaporation during the transient and that the radionuclides dissolved uniformly into the entire inventory of the reactor coolant.
- Cover gas pressure is 0.03 MPag (1.3 atm).
- Radionuclides evaporate through the vertical piping that penetrates the vessel head and the Flibe free surface. These pipes are three pebble extraction pipes of 10 in (0.254 m) diameter, and three pebble insertion pipes of 2 in (0.0508 m) diameter.
- The length of pipe between the Flibe free surface and the top of the vessel head in which radionuclides escape is assumed to be 1 ft (0.3m).
- Reference diffusivity of Ar is 2 x 10^{-5} m^2/s.
- Cover gas space volume is 5.5 m^3 and the reactor building volume is 1,000 m^3.

B.3 SOURCE TERM EVALAUTION

The MAR for this sample event are identified using the methods presented in this topical report. The MAR is located in the fuel, Flibe, and structural materials. This section provides the quantification of MAR in each barrier, the attenuation factor evaluations, the atmospheric dispersion calculation, and the resulting dose at the EAB.

B.3.1 Evaluation of Releases from the Fuel

An evaluation of the release fraction of non-tritium MAR in the fuel results in negligible quantities of radionuclides being released from intact fuel particles. The majority of the release from the fuel results from manufacturing defects of the fuel (failed TRISO layers or dispersed heavy metal). This non-tritium MAR contained in the fuel attenuates through the TRISO layers in steady state operation to either the Flibe coolant barrier or the gas space barrier. A calculation using SERPENT2 accounts for the MAR that has been transferred to the circulating activity in the Flibe and gas space. A thermal fluids analysis of the SBO demonstrates that the fuel will not reach temperatures that result in additional fuel failures. Therefore, no additional non-tritium fuel MAR is released after the initiation of the transient.

The tritium release from the fuel pebbles is determined to be de minimis, and therefore treated conservatively consistent with the de minimis guidance in the methodology. The amount of tritium in the fuel pebble is described in the assumptions in Section 9.2, and it is assumed to be “puff released” with an attenuation factor of 1.0.

B.3.2 Evaluation of Releases from Structures

Consistent with the treatment of tritium in the fuel, the entire steady state tritium inventory held up by structural materials is conservatively assumed to be released over a one-second duration. The attenuation factor of the structures MAR is set to 1.0.

© 2020 Kairos Power LLC

B.3.3 Evaluation of Releases from Flibe

A SERPENT2 calculation provides the total non-tritium MAR circulating in the Flibe (The Flibe inventory includes Flibe in the core, hot leg, cold leg, downcomer and intermediate heat exchanger) using the inputs in Table B-2. This non-tritium MAR in the Flibe is released to the gas space via vaporization, consistent with the methodology described in this topical report. The RF of radionuclide groupings that are not gases in Flibe for each duration analyzed are summarized in Table B-3. The cumulative AF for the other radionuclide groupings in Flibe are calculated consistent with the methodology of this topical report and the results are summarized in Table B-4. The radionuclides are released over seven durations:

- Five 6-hr releases (Durations 1 to 5)
- One 18-hr release (Duration 6)
- One 132-hr period to capture the remaining release (Duration 7)

The release for Duration 1 is the accumulated release at the end of Duration 1. For the remaining durations, the release is the accumulate release at the end of that duration, subtracted by the releases in prior duration(s). The releases over the duration of the transient for the radionuclide groups are shown in Figure B-1through Figure B-3.

The amount of tritium MAR in the Flibe is provided in Section 9.2 and assumed to be puff-released (an attenuation factor of 1.0) into the gas space. Any tritium that is assumed to puff release from other barriers (i.e. fuel and structures) is conservatively assumed to pass directly through the Flibe to the gas space. All inventory of gases in circulating activity and tritium are released over the first second.

B.3.4 Evaluation of Gas Space Releases and Atmospheric Transport

The gas space release evaluation includes radionuclide transport through the building and atmospheric dispersion.

The following inputs were used for the building transport model:

- Gas volumetric flow rates:
  - [[

]]
- Room Volume: The cover gas space volume is assumed to be 5.5 m^3. The reactor building is assumed to be 1,000 m^3.
- The Henry correlation uses the density of Flibe of 2195 kg/m^3. Density input in RADTRAD is in g/cm^3.
- The aerosol release height is set to the minimum value to 0.25 m above the vessel head.

For the atmospheric dispersion model in RADTRAD, the calculation uses bounding $\frac{\chi}{Q}$ values from the Clinch River Early Site Permit (Reference 54) for the EAB at 335 m from the reactor building and LPZ at 1 mile from the reactor building.

DBA acceptance criteria are based on ensuring that the worst two-hour rolling average dose at the EAB during the transient does not exceed 25 rem. Therefore, the entire transient is analyzed so that RADTRAD can perform the rolling average dose calculation.

The thirty-day dose evolution at the EAB for the RVACS transient is shown in Figure B-4 for the isotopes shown in Table B-5.

Another DBA acceptance criterion is that the thirty-day dose the LPZ does not exceed 25 rem. The thirty-day LPZ dose evolution is shown in Table B-5

The radionuclides that contributed thirty-day EAB doses above 2.5 x 10^{-5} rem are shown in Table B-5. Tritium is the dominant dose driver compared to other radionuclides.

B.4 CONCLUSIONS

Evaluations of DBAs must assure that both the worst two-hour dose at the EAB and the thirty-day LPZ dose are maintained below a TEDE of 25 rem. The worst two-hour EAB dose is experienced in the first two hours (i.e., 0-2 hours) of the SBO sample calculation with a TEDE dose of 0.71 rem. The thirty-day LPZ dose is calculated to be 0.045 rem. Both of these doses are below the 25 rem acceptance criteria for DBAs.

TEDE doses, dose rates, and timings were dominated by the assumed tritium desorption from structures (e.g., pebbles, structural graphite, vessel, piping, IHXs). RVACS operation during this event prevented fuel and Flibe temperatures from releasing significant quantities of stored MAR to the site boundary.

This sample calculation exercises the methodology presented in this topical report. However, some simplifying design assumptions resulted in overly conservative results. The conservative treatment of tritium release artificially inflates both the worst 2-hour EAB dose and the 30-day LPZ dose. Not all of the desorbed tritium would reach the reactor building to be leaked out of the environment due to engineered cleanup systems. The tritium that would reach the reactor building would likely do so at a slower rate, pushing the tritium that does make it to the EAB and LPZ out in time either past the 30-day window or, at-least, into smaller $\frac{\chi}{Q}$ time-averaged intervals which would effectively lower the dose of the leaked tritium. An unquantified fraction of the tritium would also exist as T_2O (i.e., aerosol) instead of T_2 (i.e., gas) which would allow for un-modeled deposition of tritium. Additionally, radionuclides in the Flibe gases group have limited but non-zero solubility in Flibe. The retention and RF of these radionuclides at their solubility limits within the Flibe barrier would likely slow the release of gas radionuclides and would lower the dose due to the release being in the smaller $\frac{\chi}{Q}$ time-averaged intervals.

© 2020 Kairos Power LLC

Table B-1 Tritium Distribution in the Primary System with no Permeation Barrier Coatings at 4.75 years

Component	Salt	Pebbles	Reflector	Reactor Vessel	Hot and Cold Leg Piping	Intermediate Heat Exchanger
Inventory (Ci)	9	4743	1181	320	60	55

© 2020 Kairos Power LLC

Table B-2 Flibe Source Term Inventory Calculation Inputs

Flibe Lifetime (years)	Fraction of Heavy Metal Contamination Released from Fuel	Fraction of Fission Products Released from Fuel	Uranium Impurities of the Flibe (ppm)	Thorium Impurities of the Flibe (ppm)
20	1E-05	1.96E-04	2	1

© 2020 Kairos Power LLC

Table B-3 Release Fractions of Radionuclide Groups in Flibe

Radionuclide Group	Duration 1	Duration 2	Duration 3	Duration 4	Duration 5	Duration 6	Duration 7
Salt Soluble Fluoride	1.08E-08	3.39E-08	4.92E-08	5.07E-08	4.46E-08	8.19E-08	1.22E-07
Elements Dependent on Redox	1.08E-08	3.39E-08	4.92E-08	5.07E-08	4.46E-08	8.19E-08	1.22E-07
Low Volatility Noble Metal	5.98E-19	5.96E-18	1.34E-17	1.43E-17	1.06E-17	1.13E-17	2.59E-18
Oxides	1.29E-27	3.72E-26	1.25E-25	1.39E-25	8.58E-26	5.63E-26	3.50E-27

© 2020 Kairos Power LLC

Table B-4 Cumulative Attenuation Factor of Flibe Radionuclide Groups

Radionuclide Group	Release Fraction
Salt Soluble Fluoride	3.93E-07
Element Dependent on Redox	3.93E-07
Nobel Metals	5.87E-17
Oxide	4.48 E-25
Nobel Gases and Tritium	1.0

© 2020 Kairos Power LLC

Table B-5 EAB TEDE Dose Results

Radionuclide	EAB Dose (rem)
Total	7.16E-01
H-3	7.05E-01
Xe-138	2.85E-03
Cs-138	2.34E-03
Pu-238	1.54E-03
Cm-244	1.15E-03
Cm-242	1.05E-03
Pu-241	7.01E-04
Kr-88	2.67E-04
Am-241	2.45E-04
Xe-135m	1.69E-04
Sr-90	1.28E-04
Kr-87	1.10E-04
Pu-239	6.20E-05
Rb-88	5.50E-05
Pu-240	5.10E-05

© 2020 Kairos Power LLC

Figure B-1 Cumulative Release of Salt Soluble Fluoride and Elements Dependent on Redox from Flibe

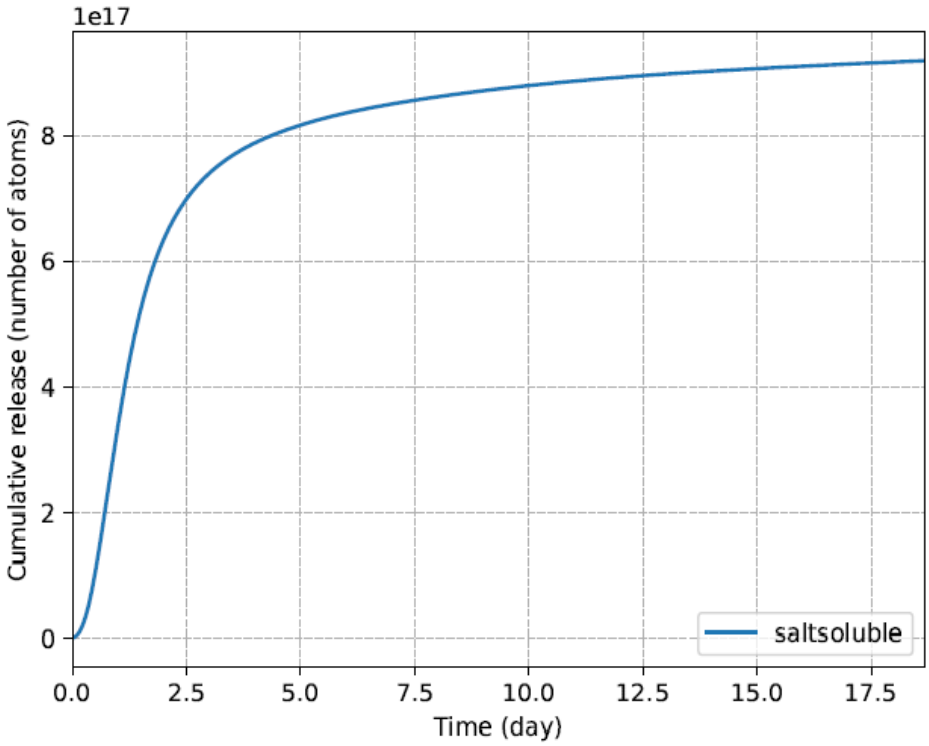

Figure B-2 Cumulative Release of Noble Metals from Flibe

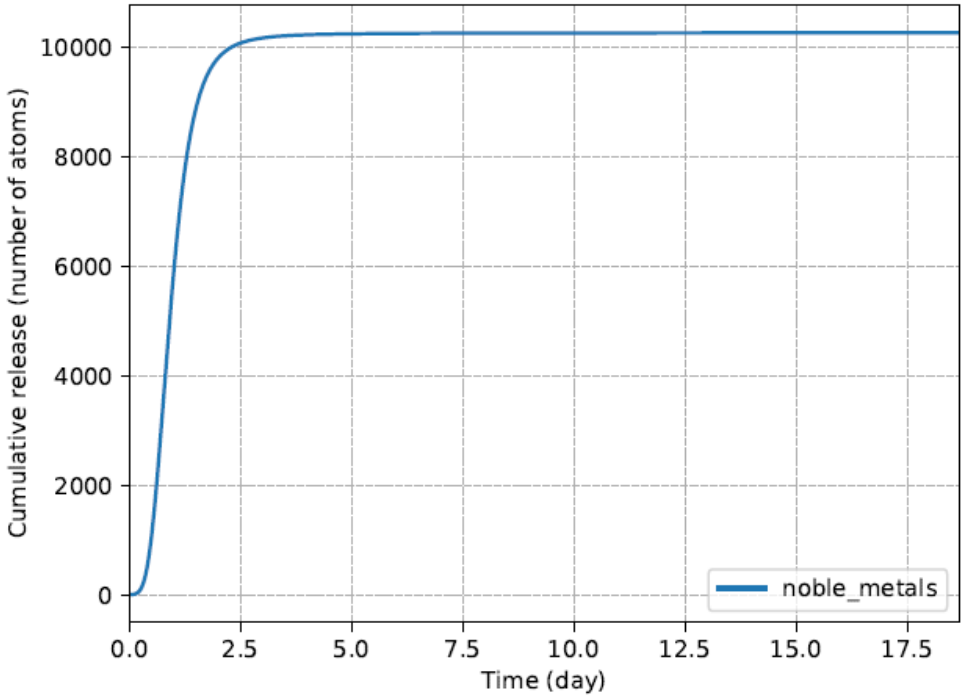

© 2020 Kairos Power LLC

Figure B-3 Cumulative Release of Oxides from Flibe

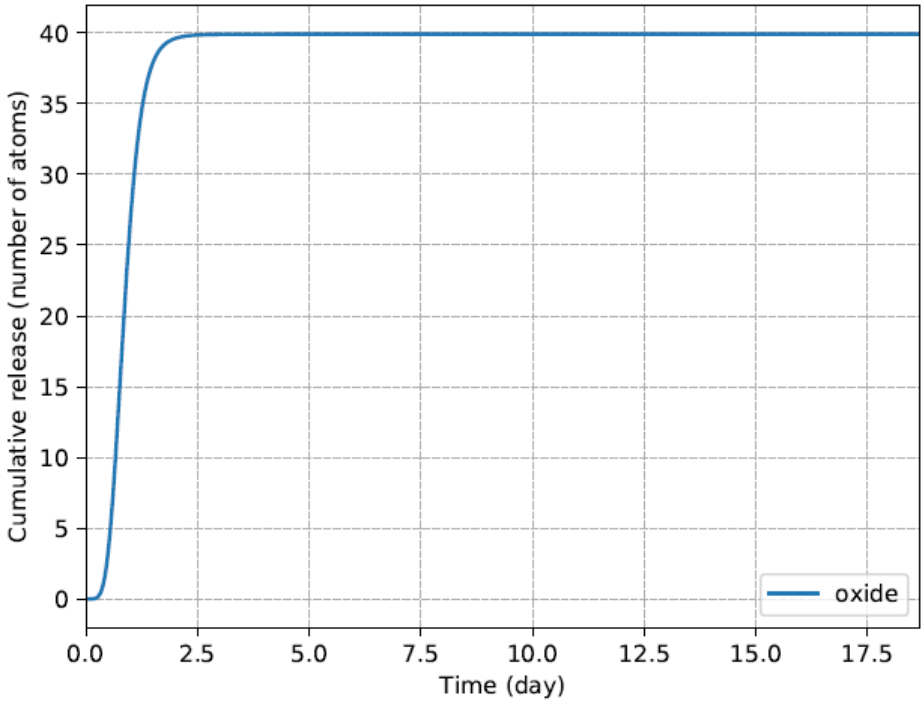

© 2020 Kairos Power LLC

Figure B-4 Thirty Day Doses at the EAB

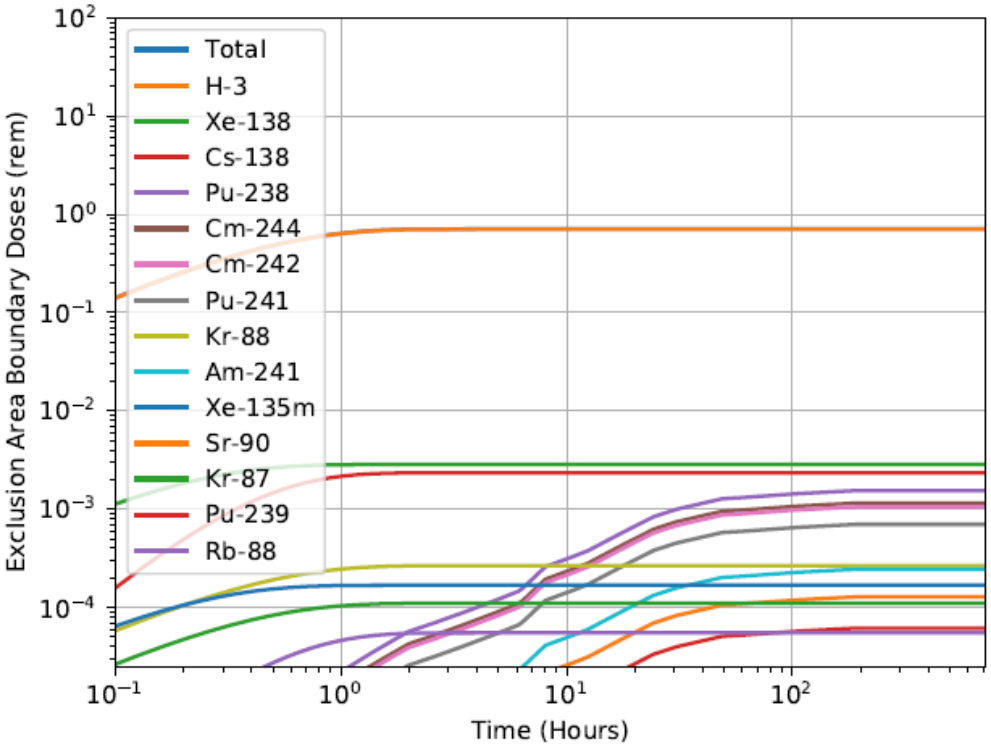

© 2020 Kairos Power LLC

Figure B-5 Thirty Day Doses at the LPZ

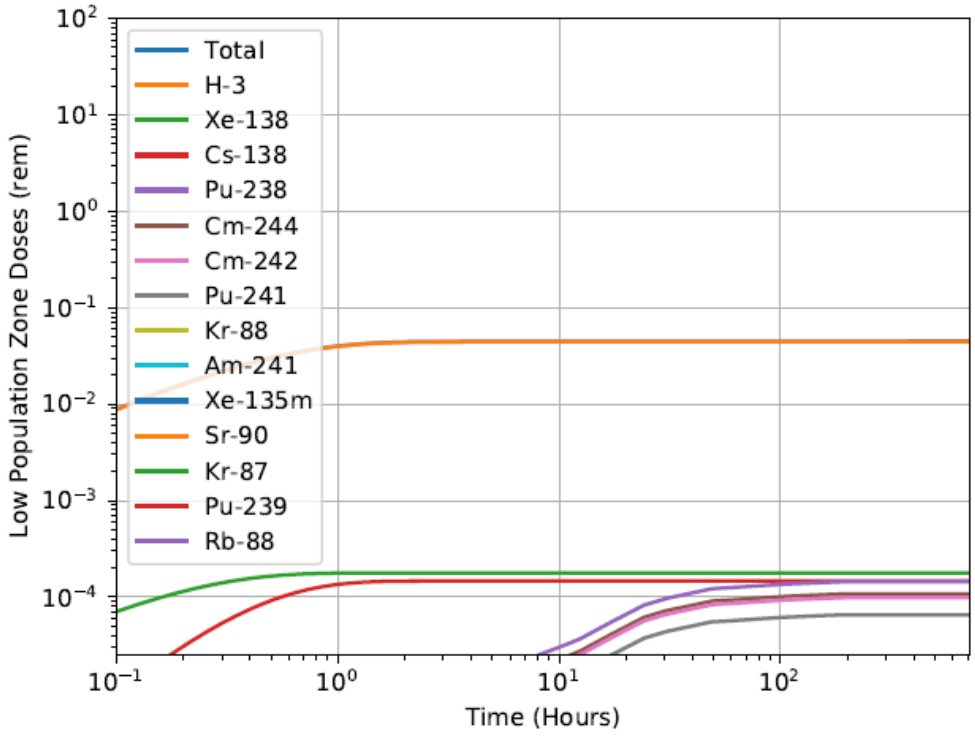

© 2020 Kairos Power LLC

Enclosure 3

Kairos Power LLC Affidavit and Request for Withholding from Public Disclosure (10 CFR 2.390)

I, Peter Hastings, hereby state:

1. I am Vice President, Regulatory Affairs and Quality at Kairos Power LLC ("Kairos"), and as such I have been authorized by Kairos to review information sought to be withheld from public disclosure in connection with the development, testing, licensing, and deployment of the Kairos reactor and its associated structures, systems, and components, and to apply for its withholding from public disclosure on behalf of Kairos.
2. The information sought to be withheld, in its entirety, is contained in Kairos' Enclosure 1 to this letter.
3. I am making this request for withholding, and executing this affidavit in support thereof, pursuant to the provisions of 10 CFR 2.390(b)(1).
4. I have personal knowledge of the criteria and procedures utilized by Kairos in designating information as a trade secret, privileged, or as confidential commercial or financial information. Some examples of information Kairos considers proprietary and eligible for withholding under §2.390(a)(4) include:
    a. Information which discloses process, method, or apparatus, including supporting data and analyses, where prevention of its use by Kairos competitors without license or contract from Kairos constitutes a competitive economic advantage over other companies in the industry;
    b. Information, which if used by a competitor, would reduce his expenditure of resources or improve his competitive position in design, manufacture, shipment, installation, assurance of quality;
    c. Information which reveals cost or price information, production capacities, budget levels, or commercial strategies of Kairos, its customers, its partners, or its suppliers;
    d. Information which reveals aspects of past, present, or future Kairos or customer funded development plans or programs, of potential commercial value to Kairos;
    e. Information which discloses patentable subject matter for which it may be desirable to obtain patent protection; and/or
    f. Information obtained through Kairos actions which could reveal additional insights into reactor system development, testing, qualification processes, and/or regulatory proceedings, and which are not otherwise readily obtainable by a competitor.
5. Information contained in Enclosure 1 to this letter contains details of Kairos' mechanistic source term methodology. This information could provide a competitor with a commercial advantage if the information were to be revealed publicly.

6. Pursuant to the provisions of §2.390(b)(4), the following is furnished for consideration by the Commission in determining whether the information sought to be withheld from public disclosure should be withheld:

   a. The information sought to be withheld from public disclosure is owned and has been held in confidence by Kairos.

   b. The information is of a type customarily held in confidence by Kairos and not customarily disclosed to the public. Kairos has a rational basis for determining the types of information customarily held in confidence by it and, in that connection, utilizes a system to determine when and whether to hold certain types of information in confidence. The application of that system and the substance of that system constitute Kairos policy and provide the rational basis required.

   c. The information is being transmitted to the Commission in confidence and, under the provisions of 10 CFR 2.390, it is to be received in confidence by the Commission.

   d. This information is not readily available in public sources.

   e. Public disclosure of this proprietary information is likely to cause substantial harm to the competitive position of Kairos, because it would enhance the ability of competitors to provide similar products and services by reducing their expenditure of resources using similar project methods, equipment, testing approach, contractors, or licensing approaches. This information is the result of considerable expense to Kairos and has great value in that it will assist Kairos in providing products and services to new, expanding markets not currently served by the company.

   f. The information could reveal or could be used to infer price information, cost information, budget levels, or commercial strategies of Kairos.

   g. Each component of proprietary information pertinent to a particular competitive advantage is potentially as valuable as the total competitive advantage. If competitors acquire components of proprietary information, any one component may be the key to the entire puzzle, thereby depriving Kairos of a competitive advantage.

   h. Unrestricted disclosure would jeopardize the position of Kairos in the world market, and thereby give a market advantage to the competition in those countries.

I declare under penalty of perjury that the foregoing is true and correct.

Executed on: June 30, 2019

Peter Hastings
Vice President, Regulatory Affairs and Quality